U. S. Department
of Transportation
Federal Railroad Administration

THE AERODYNAMIC EFFECTS OF HIGH-SPEED TRAINS ON PEOPLE AND PROPERTY AT STATIONS IN THE NORTHEAST CORRIDOR

Office of Research
and Development
Washington, D.C. 20590

Safety of High-Speed Ground Transportation Systems

DOT/FRA/ORD-99/12
DOT-VNTSC-FRA-99-11

Final Report
November 1999

**This document is available to the public through the National Technical Information Service, Springfield, VA 22161
This document is also available on the FRA web site at www.fra.dot.gov.**

REPORT DOCUMENTATION PAGE

Form Approved
OMB No. 0704-0188

1. AGENCY USE ONLY (Leave blank)	2. REPORT DATE	3. REPORT TYPE AND DATES COVERED
	November 1999	Final Report January 1998 – January 1999

4. TITLE AND SUBTITLE The Aerodynamics Effects of High-Speed Trains on People and Property at Stations in the Northeast Corridor	5. FUNDING NUMBERS RR963/R9061 DTRS57-97-D-00030
6. AUTHOR(S) Sam Liao, Paul Mosier, William Kennedy, and David Andrus	
7. PERFORMING ORGANIZATION NAME(S) AND ADDRESS(ES) Parsons Brinckerhoff Quade and Douglas, Inc.* 75 Arlington St. Boston, MA 02116	8. PERFORMING ORGANIZATION REPORT NUMBER DOT-VNTSC-FRA-99-11
9. SPONSORING/MONITORING AGENCY NAME(S) AND ADDRESS(ES) U.S. Department of Transportation Federal Railroad Administration Office of Research and Development 400 7th St., SW Washington, D.C. 20590	10. SPONSORING/MONITORING AGENCY REPORT NUMBER DOT/FRA/ORD-99/12

11. SUPPLEMENTARY NOTES

*Under contract to: U.S. Department of Transportation
Research and Special Programs Administration
John A. Volpe National Transportation Systems Center
55 Broadway
Cambridge, MA 02142-1093

12a. DISTRIBUTION/AVAILABILITY STATEMENT This document is available to the U.S. public through the National Technical Information Service, Springfield VA 22161 This document is also available on the FRA web site at www.fra.dot.gov.	12b. DISTRIBUTION CODE

13. ABSTRACT (Maximum 200 words)

This report presents the results of a study to evaluate the aerodynamic (air velocity and pressure) effects of the new high-speed trains on the safety and comfort of people, and the impacts on physical facilities, in and around Northeast Corridor stations. This report focuses particularly on the effects at "non-express-stop" stations, i.e., stations where the trains are not scheduled to stop and will thus pass the stations at potentially higher speeds than the current operations.

14. SUBJECT TERMS Northeast Corridor, computational fluid dynamics, Acela trainset, aerodynamics, FLUENT	15. NUMBER OF PAGES 146
	16. PRICE CODE

17. SECURITY CLASSIFICATION OF REPORT	18. SECURITY CLASSIFICATION OF THIS PAGE	19. SECURITY CLASSIFICATION OF ABSTRACT	20. LIMITATION OF ABSTRACT
Unclassified	Unclassified	Unclassified	

PREFACE

Amtrak's high-speed train service using the Acela trainset will be inaugurated in the Northeast Corridor between Boston, Massachusetts, and Washington, DC, by the end of 1999, with maximum allowable train speeds in certain locations of up to 150 miles per hour (mph). Trains will be passing through stations in the Corridor without stopping at higher speeds than the present maximum of 125 mph. This report presents the results of a study to evaluate the aerodynamic (air velocity and pressure) effects of the new high-speed trains on the safety and comfort of people, and the impacts on physical facilities, in and around Northeast Corridor stations. This report focuses particularly on the effects at "non-express-stop" stations, i.e., stations where the trains are not scheduled to stop and will thus pass the stations at potentially higher speeds than the current operations.

A significant amount of information gathered for this study and used as input to the analyses was made available through the efforts and contributions of numerous staff members of various agencies and organizations. Acknowledgment is accorded to the support of and cooperation of the John A. Volpe National Transportation Systems Center (VNTSC); the Federal Railroad Administration (FRA); National Railroad Passenger Corporation (Amtrak); Maryland Rail Commuter (MARC); Delaware Department of Transportation; Southeastern Pennsylvania Transportation Authority (SEPTA); New Jersey Transit (NJT); Metro North Railroad (MNR); State of New York Public Transportation Safety Board; Connecticut Department of Transportation; Rhode Island Department of Transportation; Massachusetts Bay Transportation Authority (MBTA); Massachusetts Department of Public Utilities; District of Columbia Historical Preservation Division; Maryland Historical Trust; Pennsylvania Historical and Museum Commission; New Jersey Historic Preservation Office; New York Department of Parks, Recreation, and Historic Preservation; Connecticut Historical Commission; Rhode Island Historic Preservation Trust; and Massachusetts Historical Commission.

This study was performed by Parsons Brinckerhoff Quade & Douglas Inc. (PB) for the VNTSC, under Contract No. DTRS57-97-D-00030, Task Order No. 17. Funding for this study was provided by the FRA.

METRIC/ENGLISH CONVERSION FACTORS

ENGLISH TO METRIC / METRIC TO ENGLISH

LENGTH (APPROXIMATE)

English to Metric		Metric to English	
1 inch (in)	= 2.5 centimeters (cm)	1 millimeter (mm)	= 0.04 inch (in)
1 foot (ft)	= 30 centimeters (cm)	1 centimeter (cm)	= 0.4 inch (in)
1 yard (yd)	= 0.9 meter (m)	1 meter (m)	= 3.3 feet (ft)
1 mile (mi)	= 1.6 kilometers (km)	1 meter (m)	= 1.1 yards (yd)
		1 kilometer (km)	= 0.6 mile (mi)

AREA (APPROXIMATE)

English to Metric		Metric to English	
1 square inch (sq in, in^2)	= 6.5 square centimeters (cm^2)	1 square centimeter (cm^2)	= 0.16 square inch (sq in, in^2)
1 square foot (sq ft, ft^2)	= 0.09 square meter (m^2)	1 square meter (m^2)	= 1.2 square yards (sq yd, yd^2)
1 square yard (sq yd, yd^2)	= 0.8 square meter (m^2)	1 square kilometer (km^2)	= 0.4 square mile (sq mi, mi^2)
1 square mile (sq mi, mi^2)	= 2.6 square kilometers (km^2)	10,000 square meters (m^2)	= 1 hectare (ha) = 2.5 acres
1 acre = 0.4 hectare (he)	= 4,000 square meters (m^2)		

MASS - WEIGHT (APPROXIMATE)

English to Metric		Metric to English	
1 ounce (oz)	= 28 grams (gm)	1 gram (gm)	= 0.036 ounce (oz)
1 pound (lb)	= 0.45 kilogram (kg)	1 kilogram (kg)	= 2.2 pounds (lb)
1 short ton = 2,000 pounds (lb)	= 0.9 tonne (t)	1 tonne (t)	= 1,000 kilograms (kg)
			= 1.1 short tons

VOLUME (APPROXIMATE)

English to Metric		Metric to English	
1 teaspoon (tsp)	= 5 milliliters (ml)	1 milliliter (ml)	= 0.03 fluid ounce (fl oz)
1 tablespoon (tbsp)	= 15 milliliters (ml)	1 liter (l)	= 2.1 pints (pt)
1 fluid ounce (fl oz)	= 30 milliliters (ml)	1 liter (l)	= 1.06 quarts (qt)
1 cup (c)	= 0.24 liter (l)	1 liter (l)	= 0.26 gallon (gal)
1 pint (pt)	= 0.47 liter (l)		
1 quart (qt)	= 0.96 liter (l)		
1 gallon (gal)	= 3.8 liters (l)		
1 cubic foot (cu ft, ft^3)	= 0.03 cubic meter (m^3)	1 cubic meter (m^3)	= 36 cubic feet (cu ft, ft^3)
1 cubic yard (cu yd, yd^3)	= 0.76 cubic meter (m^3)	1 cubic meter (m^3)	= 1.3 cubic yards (cu yd, yd^3)

TEMPERATURE (EXACT)

English to Metric		Metric to English	
[(x-32)(5/9)] °F	= y °C	[(9/5) y + 32] °C	= x °F

QUICK INCH - CENTIMETER LENGTH CONVERSION

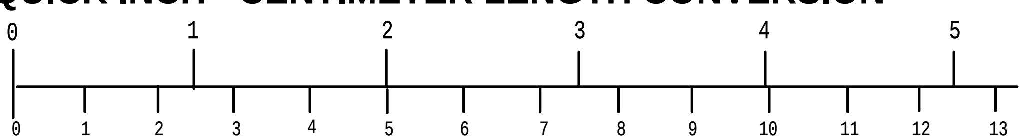

QUICK FAHRENHEIT - CELSIUS TEMPERATURE CONVERSION

°F	-40°	-22°	-4°	14°	32°	50°	68°	86°	104°	122°	140°	158°	176°	194°	212°
°C	-40°	-30°	-20°	-10°	0°	10°	20°	30°	40°	50°	60°	70°	80°	90°	100°

For more exact and or other conversion factors, see NIST Miscellaneous Publication 286, Units of Weights and Measures. Price $2.50 SD Catalog No. C13 10286

Updated 6/17/98

TABLE OF CONTENTS

Section **Page**

TABLE OF CONTENTS (Cont'd)

LIST OF FIGURES

LIST OF FIGURES (Cont'd)

LIST OF FIGURES (Cont'd)

Figure **Page**

LIST OF TABLES

EXECUTIVE SUMMARY

Amtrak's high-speed train service using the Acela trainset will be inaugurated in the Northeast Corridor between Boston, Massachusetts, and Washington, DC, by the end of 1999, with maximum allowable train speeds in certain locations of up to 150 miles per hour (mph). Trains will be passing through stations in the Corridor without stopping at higher speeds than the present maximum of 125 mph. This report presents the results of a study to evaluate the aerodynamic (air velocity and pressure) effects of the new high-speed trains on the safety and comfort of people, and the impacts on physical facilities, in and around Northeast Corridor stations. This report focuses particularly on the effects at "non-express-stop" stations, i.e., stations where the trains are not scheduled to stop and will thus pass the stations at potentially higher speeds than the current operations.

This study included the following components:

- Numerical modeling of aerodynamic effects, using a Computational Fluid Dynamics (CFD) model of the new high-speed Acela trainset and the existing Amfleet trainset.
- Field measurements of the air velocities caused by passage of the existing Amfleet trainset at non-express-stop stations at Princeton Junction, New Jersey, and Newark, Delaware.
- Visual field surveys of 57 selected stations between Boston and Washington to assess some of the conditions (especially as they relate to the idealized numerical models) that may be affected by the Acela operations, and to provide observations that would help to define the potential effects of the Acela trainset.

All of the above components were combined with a review of literature and previous studies to guide and prepare the recommendations in this report. The review of literature provided information on the effects of various wind speeds and pressures on human beings and objects. This was useful in giving a physical sense to the potential effects of the calculated air velocities from the CFD models, and the actual air velocities recorded by the field measurements.

The most significant result of this study is that a new Acela trainset, running at 150 mph past a passenger station, is calculated to have overall aerodynamic effects and impacts ranging from less intense to somewhat more intense than an existing Amfleet trainset, running past a station at 125 mph. It is likely that the percent increase of the Acela's induced air velocities compared to the Amfleet's will be significantly less than the percent increase estimated from the ratio of the corresponding maximum train speed from 125 mph to 150 mph. The reason why the effects are not greater can be partially attributed to the fact that the Acela trainset is much better aerodynamically streamlined than the Amfleet trainset. This would mitigate the otherwise expected disruption and turbulence of the air surrounding the train as it passes. However, the spatial and temporal distribution of the effects would be different for the Acela trainset versus the Amfleet trainset. For example, the Acela would induce lower air velocities at the head of the train as it approaches a station and along the sides while it is passing immediately adjacent to a platform. But the wake effects after the train has passed would extend further laterally on the platform, though the effects would be of a shorter duration than the effects of the Amfleet trainset. Another significant result is the determination that aerodynamic effects are calculated to be less intense at a high-level station platform than at a low-level platform.

The field measurements for the Amfleet trainsets compared well with the Amfleet CFD results. Thus a verification of the CFD analyses was provided, as well as a further confirmation of the calculated relative impacts of the new Acela trainset versus the Amfleet trainset. One observation from the field measurements is that the effects of a back wall close to a low-level platform might cause an increase in aerodynamic effects compared to a platform without such a wall. This effect may also be important for high-level platforms as well.

Data on the stations in the Northeast Corridor were gathered from various agencies in the political jurisdictions in which the Acela trainsets will operate. The visual field surveys of the selected stations provided an inventory of conditions to confirm or identify station and platform characteristics that were either the same or different from the assumptions used in the CFD analyses, and the conditions at the location of the field velocity measurements. The data collected are provided as Appendices to the report, and can be useful to identify the relative potential impacts of the proposed Acela service at specific stations.

The CFD modeling results and instrumentation field measurements are encouraging in terms of indicating that the overall increase of the aerodynamic effects will range from slight to moderate for the operation of the Acela trainset compared to the existing Amfleet trainset. Given that the aerodynamic effects of operating the Amfleet trainsets at the current speeds are acceptable, the Acela trainset should not pose any significant new impacts.

However, it is not certain that all the potential variables affecting Acela trainset impacts at any given particular station have been accounted for. It may also be desired to mitigate existing impacts by instituting improvements to operations or facilities in the longer term. Thus, a prudent approach would be to develop a strategy now, which would be responsive to the possibility of unanticipated adverse impacts becoming noticeable only after the start of the high-speed Acela service. To this end, this report provides recommendations that could be part of that strategy. These include:

- Observations or field measurements of Acela trainsets to be planned as part of testing of the Acela at the Transportation Technology Center in Pueblo, Colorado, and during the Acela field trials in the Northeast Corridor. Additional measurements of existing Amfleet effects may also be considered. This observational approach should further confirm that the aerodynamic impacts of the Acela range from less to moderately greater than those of the existing Amfleet, but could also offer advance warnings of unforeseen adverse aerodynamic impacts.
- An action plan for possible improvements in facilities or operations to mitigate the potentially adverse aerodynamic effects of the Acela trainsets. The plan could either be designed to meet the needs of each specific station that could be affected, or it could be generic, or a combination of both. For example, the plan could account for temporary conditions such as snow hazards, which can be mitigated locally (on each Amtrak Division) through use of Amtrak’s Temporary Speed Restriction Bulletin.

The recommendations are not prescriptive in nature, but rather suggest further steps that could be taken to minimize or mitigate potential effects of high-speed trains operating in the Northeast Corridor

This document is composed of the following sections:

Section 1 – Introduction: Delineates the purpose and scope of the study.

Section 2 – Review of the Literature and Relevant Findings: Presents the results of previous research and publications relevant to the study.

Section 3 – Numerical Modeling of Aerodynamic Effects of High-Speed Trains: Describes the computational fluid dynamics (CFD) model used in the study, and the results for the new high-speed Acela trainset and the existing Amtrak trainset.

Section 4- Field Measurements: Presents the results and conclusions drawn from the air velocity measurements performed at Princeton Junction, NJ and Newark, DE for existing Amfleet trainsets.

Section 5 – Station Surveys: Presents and discusses the results of the visual field surveys performed at stations along the Northeast Corridor.

Section 6 – Summary and Conclusions: Summarizes the results and conclusions of the study.

Section 7 – Recommendations: Presents the recommendations based upon the conclusion of the study.

Appendix A – Description of Computational Fluid Dynamics Model Used in the Study: Describes the computational fluid dynamics (CFD) model and its formulation.

Appendix B – High-Speed Trainset Input Data: Summarizes the data used for input to the CFD analyses for the Acela trainset.

Appendix C – Adjustments of the Coefficient of Friction in the Computational Model: Provides the mathematical equations used for the adjustments of the coefficient of friction used in the CFD model.

Appendix D – Linear Interpolation for Train Velocities Between 110 and 150 Miles Per Hour: Provides the basis for the use of linear interpolation in the CFD model and interpretation of results.

Appendix E – Explanation of Turbulence Fluctuations: Provides the explanation for the calculation f the fluctuating component of the flows in the CFD model.

Appendix F – List of Stations on the Northeast Corridor and Other Information: Lists the provider owner and operator, services, maximum authorized speeds, etc., of stations from Washington, DC to Boston, MA on the Northeast Corridor.

Appendix G – Northeast Corridor Characteristics, By State: Lists various characteristics of stations on the Northeast Corridor, including the number in each State, maintenance, safety systems, and ADA landmark status.

Appendix H – Characteristics of Stations Surveyed: Provides, in tabular form, characteristics of the Northeast Corridor stations, including high or low platform, width of platform, etc.

Appendix I – Station Data from Representative Station Checklist Forms: Provides three examples of a summary data checklist form used in the study.

Appendix J – Field Measurement Reports: Presents three field reports for air velocity measurements for the passage of the existing Amfleet trainset at Princeton Junction, NJ (two sites) and Newark, DE (one site).

1. INTRODUCTION

1.1 Purpose

Amtrak's high-speed train service using the Acela trainset will be inaugurated in the Northeast Corridor between Boston, Massachusetts and Washington, DC (see Figure 1-1) by the end of 1999, with maximum allowable speeds up to 150 mph. These high-speed trains will only stop at the major city stations, and run as express trains through numerous commuter rail stations on the Corridor. Trains will be passing through many intermediate (non-express-stop) stations at higher speeds than the present maximum of 125 mph in the Corridor. With trains traveling at these high speeds, a variety of operational and safety concerns are being evaluated and addressed. There is a concern about aerodynamic (air velocity and pressure) effects from this proposed higher speed operation on people and property at these locations. This study examines the aerodynamic effects that high-speed trains can be expected to have on the safety and comfort of people in and around Northeast Corridor stations, focusing on the anticipated induced airflow effects on station facilities in the Corridor.

1.2. Scope of the Study

This study included the following components:

- Numerical modeling of aerodynamic effects, using a Computational Fluid Dynamics (CFD) model of the new high-speed Acela trainset and the existing Amfleet trainset.
- Field measurements of the air velocities caused by passage of the existing Amfleet trainsets at Princeton Junction, New Jersey and Newark, Delaware.
- Visual field surveys of 57 selected stations between Boston and Washington to assess some of the conditions (especially as they relate to the idealized numerical models) that may be affected by the Acela operations, and to provide observations that would help to define the potential effects of the Acela trainsets.

All of the above components were combined with a review of literature and previous studies to guide and prepare the recommendations in this report. The literature review provided information on the effects of various wind speeds and pressures on human beings and objects. This was useful in giving a physical sense to the potential effects of the calculated air velocities from the CFD Acela and Amfleet trainset models, and the actual air velocities recorded by the field measurements.

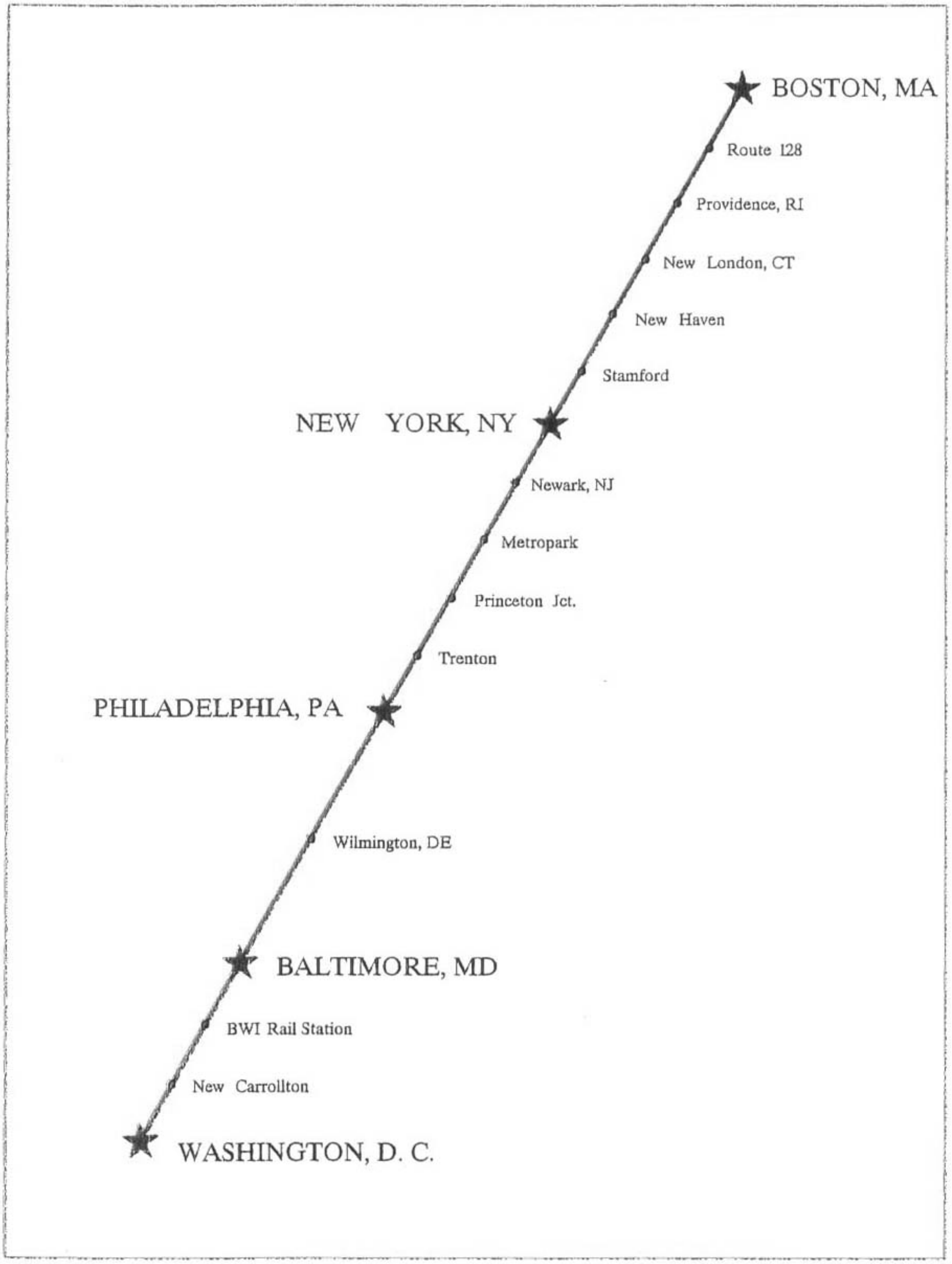

Figure 1-1. Schematic of Amtrak's Northeast Corridor, Showing the Acela Trainset Stops

2. REVIEW OF LITERATURE AND RELEVANT FINDINGS

2.1 Review of Literature

Numerous publications and reports were reviewed to develop background information on the aerodynamic effects of rail vehicles, or utilized to obtain data directly relevant to this study. Included in the review were the volumes of 15 symposia or proceedings on aerodynamics or related subjects, as listed in the Bibliography of this report. Of the papers and reports on aerodynamics presented in the Bibliography, some were focused on the aerodynamic effects on the train rather than on the surrounding environment. Such was the case with respect to the report by Gielow and Furlong (1988), published by Airflow Sciences Corporation. This reference was concerned with aerodynamic drag and train energy consumption. Other publications were primarily concerned with wind effects in subway tunnels, and therefore were not relevant to this present study.

However, one of the most useful and relevant documents was a comprehensive literature review undertaken by the Volpe Center in the spring of 1998, which is documented in a report titled *Assessment of Potential Aerodynamic Effects on Personnel and Equipment in Proximity to High-Speed Rail Operations* (DOT-VNTSC-FRA-98-3), written by Harvey S. Lee. Hereinafter referred to as Lee (1999), this report cites results from previous theoretical studies, full-scale tests, and other publications that focus on the aerodynamic effects of trains on other trains, persons, or objects, and/or the effects of various wind speeds or pressures. Some of the more pertinent findings from Lee (1999) and other documents are described in the section that follows.

2.2 Relevant Findings

2.2.1 Previous Theoretical Results and Measurements

As a train passes a station, airflow will be induced at three locations along the train's path of travel. One is at the front end of the train, in the form of a "bow wave", resulting from the forward motion of the train and the resultant displacement of the air ahead of it. The second is the "boundary layer" formed along the side of the moving train. The third is the "wake" at the rear of the train, which consists of a complex vortex field with turbulent flow. Therefore, people and objects close to a train passing at high speed could experience high wind forces. In addition, the wake can induce airflow velocities at the rear of the train that could stir up dust and debris around the track and propel it onto the station platform, and if high enough, can scatter luggage or other objects on the platform.

As noted by Gawthorpe (1972) and summarized in Lee (1999), "It is generally felt that the wake produces effects which are the most destabilizing to trackside objects." Further information from discussions with Gawthorpe (1998) indicate that exceptions to this may be from situations with older passenger trains pulled by blunt-end locomotives or freight trains consisting of a mixture of a different types of cars, e.g. boxcars, coal cars, container cars, etc. In these cases, the maximum airflow velocities may be from the boundary layer and not from the wake.

A summary of the theoretical results and measurements that are available in the literature regarding induced airflows alongside passing trains was compiled by Lee (1999) and is shown in Figure 2-1. This figure shows a plot of airflow speed non-dimensionalized to train speed (i.e., divided by train speed) versus lateral distance in meters from the side of the train. The figure contains theoretical results from Hammitt (1973), as well as several sets of measurements from Neppert and Sanderson (1977) and Gawthorpe (1972). While Figure 2-1 presents a convenient summary of what is readily available in the literature, there are some factors to consider in terms of its practical application:

- The theoretical results from Hammitt (1973) are based on simplifying assumptions that convert a complex 3-dimensional problem into a simplified model for which a purely mathematical solution could be derived. It assumes a 1/7 power law velocity distribution for flow within the boundary layer, and relates the boundary layer thickness to the drag coefficient through the momentum equation. This is limited because the 1/7 power law is usually associated with moderate Reynolds numbers on the order of 10^6 or 10^7. The Reynolds number is the dimensionless ratio of the momentum force to the viscous force. For the high speed train calculation, it is equal the speed of the train times the air density times the length of the trainset, divided by the viscosity of the air. The Reynolds number is an indicator of the different types of air flow and the degree of turbulence in the flow. In general, the higher the Reynolds number, the more turbulent the flow. The Reynolds number associated with the high-speed passage of trains is on the order of 10^9, and would thus require some modification to the 1/7 power law.

- The theoretical results are for the boundary layer, while the severest results may be from the wake.

- Most of the measurements are for a location at or near the end of the train, which would represent a boundary layer situation (Lee, 1998a). However, for the British Rail (BR) data, Gawthorpe (1998) has indicated that British Rail generally collected data focusing on the maximum velocity, without noting in particular whether it was from the wake or the boundary layer.

- In summary, Figure 2-1, while useful as a summary, contains a mixture of information and data for comparisons.

2.2.2 Air Velocity and Pressure Effects on People and Wayside Objects

A useful and widely accepted indicator of the effects of wind on people and objects is provided by the Beaufort scale. This scale was originated by Sir Francis Beaufort in the mid-1800s and was originally developed for nautical applications. A description of the Beaufort scale can be

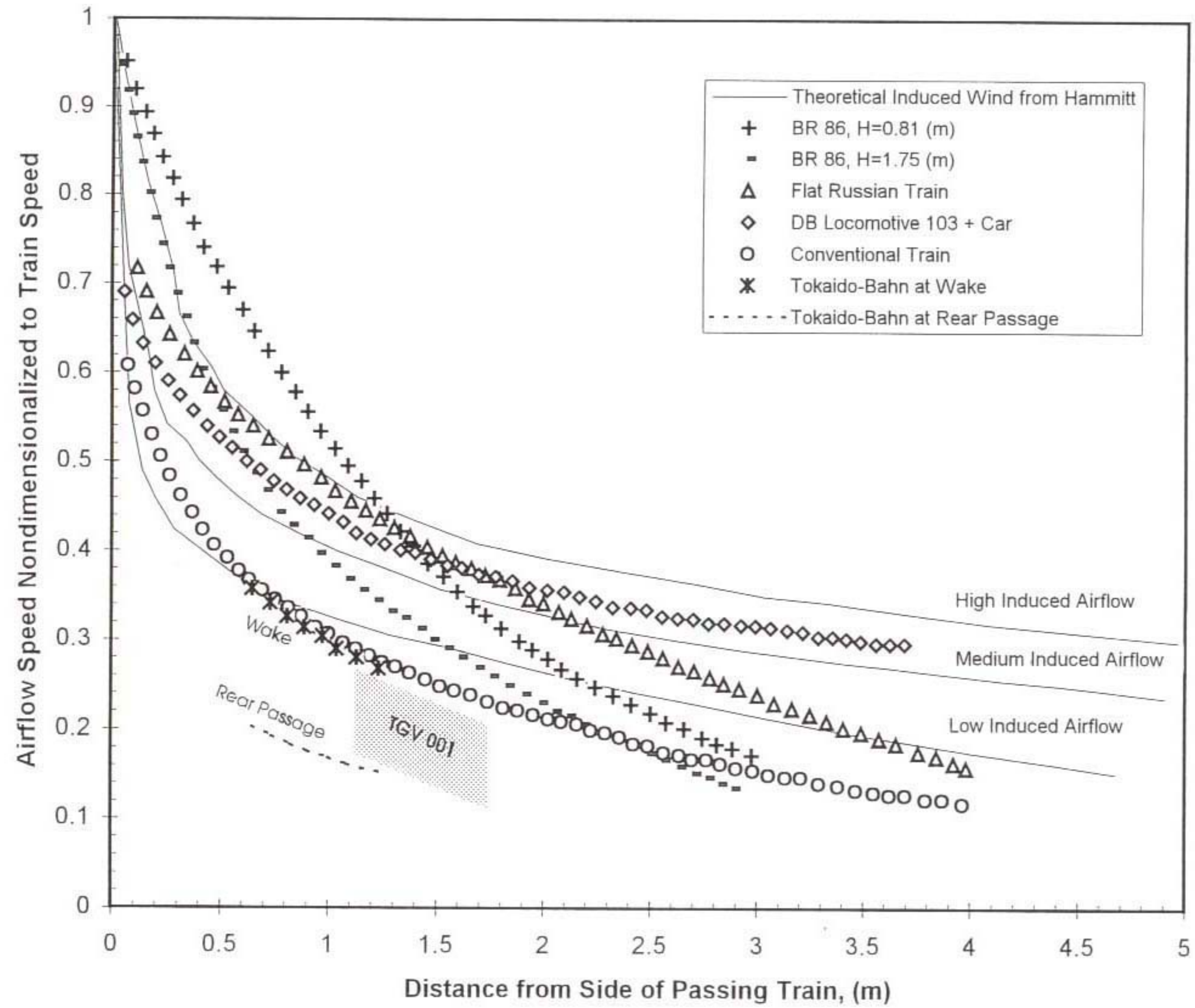

Figure 2-1. Theoretical and Experimental Induced Airflow Speed From a Passing Train, From Lee (1999)

found in the book *Piloting, Seamanship and Small Boat Handling*, written by C. F. Chapman (1970). Lee (1998) also provides a summary of the Beaufort Scale, Table 2-1, and it is also employed in the *Subway Environmental Design Handbook*, written by Associated Engineers (1976). It should be noted that there are minor inconsistencies among these and possibly other references, probably caused by the conversion and rounding of numbers for the Beaufort Scale data from knots to miles per hour, to feet per minute, and then to kilometers per hour.

Table 2-1. Beaufort Scale

Beaufort Number	Name	Wind Speed (Mph)	Description
0	Calm	Less than 1	Calm; smoke rises vertically.
1	Light Air	1-3	Direction of wind shown by smoke, but not by wind vanes.
2	Light Breeze	4-7	Wind felt on face; leaves rustle; ordinary vane moved by wind.
3	Gentle Breeze	8-12	Leaves and small twigs in constant motion; wind extends light flag.
4	Moderate Breeze	13-18	Raises dust and loose paper; small branches are moved.
5	Fresh Breeze	19-24	Small trees in leaf begin to sway; crested wavelets form on inland waters.
6	Strong Breeze	25-31	Large branches in motion; telegraph wires whistle; umbrellas used with difficulty.
7	Moderate Gale (or Near Gale)	32-38	Whole trees in motion; inconvenience in walking against wind.
8	Fresh Gale (or Gale)	39-46	Breaks twigs off trees; generally impedes progress.
9	Strong Gale	47-54	Slight structural damage occurs; chimney pots and slates removed.
10	Whole Gale (or Storm)	55-63	Trees uprooted; considerable structural damage occurs.
11	Storm (or Violent Storm)	64-72	Very rarely experienced; accompanied by widespread damage.
12	Hurricane	73-136	Devastation occurs.

(From Lee, 1999)

The direct effects on people are described in Chapman (1970) in terms of sustained wind speeds in miles per hour (mph). These effects may not be significant (<13 mph), be annoying or a nuisance (13 to 25 mph), cause inconvenience in walking (25 to 40 mph), or impede walking (>40 mph). The indirect effects on people include the movement of dust and debris. Air velocities greater than about 13 mph can move dust, leaves, and other loose objects.

While trains passing stations at high speed do not generate sustained winds, the transient induced airflows produced can reach significant velocities, with effects not unlike those described in the Beaufort Scale. Nevertheless, it is important to note that the transient induced airflows may not have as large an effect as a sustained wind of the same velocity.

Air velocities generate pressures, which if high enough, can move objects such as trash baskets and luggage, knock down signs, etc. For an outside air temperature of approximately zero degrees Fahrenheit, the dynamic pressure caused by the wind velocity is approximately $P = 0.00284 \times V^2$, where P is the pressure in pounds per square foot (psf) and V is the air velocity in mph. [Note: This formula is derived based on the equation for velocity pressure, i.e., $P = 0.5 \times (\text{density of air}) \times V^2$.] The pressures corresponding to various air velocities are provided in Table 2-2, below.

Table 2-2. Air Velocities and Approximate Dynamic Pressures

Air Velocity (mph)	Dynamic Pressure (psf)
13	0.48, or approximately ½
25	1.78, or approximately 2
40	4.55, or approximately 5
75	15.98, or approximately 16

Instantaneous pressure changes caused by passing high-speed trains can have physiologic impacts on a human body, including the ear, which can produce discomfort. According to Lee (1999), “An advisable limit that can be considered the instantaneous pressure change from a physiologic standpoint is 0.06 psi.”

For this report, the above finding from the Lee study was compared with the *Subway Environmental Design Handbook*, or SEDH, developed and written by the Associated Engineers for the Urban Mass Transit Administration (now the Federal Transit Administration) in 1976 (Associated Engineers, 1976). The area of concern was air pressure and its rate of change, causing ear discomfort, etc. The recommendation of the SEDH was selected because it has been satisfactorily used in the underground transportation and airline industries for the past 25 years. The recommendation is that for pressure changes greater than 14.4 psf (0.1 psi), the rate of pressure change should be less than 8.64 psf (0.06 psi)/second, to prevent hazards to people.

These velocity and pressure effects have the potential for adverse impacts upon more than the safety and comfort of people on station platforms. Indeed, British Rail (BR) has established safety parameters for the upper limit of induced air velocities to which patrons and employees are permitted to be exposed. For employees working along the tracks, BR suggests an exposure limit of 38 mph, corresponding to the upper end of the Beaufort Scale Number 7. For members of the public, the suggested limit is 25 mph, corresponding to the upper end of Beaufort Scale Number 5 (Lee, 1999).

Using the British Rail and other data, Lee (1999) was able to establish the level of aerodynamic forces and airflow that can be expected in proximity to a passing train:

- "For persons situated within 6.6 ft from the side of a train passing a station platform at a speed of 150 mph, the effects of pressure and induced airflow is high enough to be safety concern. The distance of 6.6 ft does not represent a safety limit, but it does indicate that when people are situated within that distance to a passing train, this can be a safety issue."

Another finding of the Lee (1999) study was:

- "When a train is passing a station platform at high speeds, the wake effect of the train with its turbulent fluctuations and buffeting in the air, along with any dust and debris that is blown or propelled, is a serious issue regarding the comfort and safety of people on the platform."

2.2.3 Effects of Streamlining on Rail Vehicle-Induced Air Pressures and Velocities

The documents reviewed clearly indicate the *potential* for adverse aerodynamic impacts from the wind velocities and pressures induced by passing high-speed trains. However, they also determined the potential for these impacts to be ameliorated by the design of the high-speed rail vehicles:

> "Train geometry, particularly the shape of the train nose, has a significant influence on the strength of the aerodynamic forces. There are sufficient variations in the strength of the aerodynamic forces to indicate that a train with a slender nose traveling at 150 mph creates aerodynamic forces that are no more severe than a train with a bluff nose traveling at a speed of 110 mph. If a train proposed for high-speed operation has a streamlined body design with a slender nose, it is possible that its favorable aerodynamic characteristics can offset the higher aerodynamic forces that would otherwise be generated by its increase in speed." (Lee, 1999.)

As a prelude to the results presented in Section 3 of this report, this observation documented by Lee (1999) is relevant in interpreting the results of the CFD analyses. In fact, the CFD analyses show that the more streamlined Acela trainset may mitigate some of the increase in air velocities in portions of the air velocity field of the trainset.

3. NUMERICAL MODELING OF AERODYNAMIC EFFECTS OF HIGH-SPEED TRAINS

3.1 General Methodology

Numerical analysis of the aerodynamic effects of the Acela trainset passing a passenger station platform was performed using a technique known as Computational Fluid Dynamics (CFD). The study considered the effects of Acela trainset passing the platform at 110 and 150 mph, and Amfleet equipment passing the platform at 125 mph.

In brief, CFD is the finite-volume modeling of fluid flow, and is analogous to the technique of finite element modeling for stress analysis. CFD is a powerful tool that has been used in the last two decades in many industries. It is used by federal agencies, national laboratories, the aircraft industry, and the automobile industry, for aerodynamic analysis, design, and the verification of experimental data. Specific users include the National Aeronautics and Space Agency (NASA), Boeing, McDonnell Douglas, Pratt and Whitney, Lockheed, Allied Signal, Ford Motor Company, General Motors, Chrysler, Mercedes Benz, and Bavarian Motor Works (BMW). Since the creation of supercomputers and powerful workstations, this tool has become even more attractive, working hand-in-hand with experimental investigations.

The methodology in CFD is based on the solution of conservation of mass and momentum equations. In addition, depending on the parameters involved, such as the flow regime (laminar or turbulent), other equations are utilized to solve the problem. The governing equations are discretized on a curvilinear grid to enable computations in complex/irregular geometries. The equations are solved by the Semi-Implicit Method for Pressure-Linked Equations (SIMPLE) algorithm, or by the Semi-Implicit Method for Pressure-Linked Equations Consistent (SIMPLEC) algorithm. Both algorithms use an iterative line-by-line matrix solver and multigrid acceleration. More details of the mathematical concepts of CFD are presented in Appendix A.

CFD software that was used in this study was the FLUENT program (Fluent, Inc., 1996). FLUENT is a general-purpose computer program for modeling fluid flow, heat transfer, and chemical reactions. FLUENT incorporates up-to-date modeling techniques and a wide range of physical models for simulating numerous types of fluid problems, and has been previously used by Parsons Brinckerhoff for numerous other applications.

The CFD technique was used for evaluating the aerodynamic effects of Amtrak's new Acela trainset assuming three train/station platform configurations, modeled as follows:

- Low-level platform with the Acela trainset.
- High-level platform with the Acela trainset on the track next to the platform.
- High-level platform with the Acela trainset on the second track away from the platform.

[It should be noted that the low-level platform condition is, for modeling purposes, the same as having a no platform condition. The low-level platform is for practical purposes the same as ground level, i.e., a condition where the platform can be modeled the same as the ground.]

For purposes of establishing a baseline for comparison with the Acela trainset results and the instrumentation field measurements, CFD analysis of the existing Amfleet cars was performed assuming a single train/platform configuration, as follows:

- Low-level platform with the Amfleet trainset.

In the low-platform simulations (for the Acela and the Amfleet trainsets), there was no height differentiation between the rails and the platform; both were modeled as being at ground level. Since there was no asymmetry presented by platform conditions, and the computational domain was wide enough, one model could be used to calculate both the effect of the passing train when it was either near the platform or one track away from it.

The physical characteristics of the Acela trainsets, as modeled by the train's manufacturer in scale-model tests, were obtained from Amtrak (Bombardier, 1998). Extensive data, including experimental analyses and measurement of the drag coefficient were available (Lanneville, 1998). The physical characteristics of the Amtrak Amfleet equipment (AEM 7-type locomotive and cars) and its theoretical drag force were also obtained from Amtrak. However, the information provided for the Amfleet did not include experimental data, or the same level of detail, and thus required additional assumptions and calculations in this study.

3.2 Details for Acela Trainset Model

The CFD computational domain for the Acela trainset was modeled as being 1,322 ft long, 40 ft high, and 67 ft wide. The trainset consisted of six coach cars located between two power cars. The domain must be large enough so that the effects of the train passage are negligible at the edges of the computational domain, i.e., to represent ambient air conditions without train passage effects. Thus the domain was sized to exceed the boundary layer thickness by at least an order of magnitude. As mentioned previously, three platform configurations were used to analyze this problem. The first case used a flat platform (low-level), as depicted in Figure 3-1. The second case, shown in Figure 3-2, used a platform 5 ft high with the train moving on the track next to the platform (high-level). The third case, shown in Figure 3-3, used the same platform configuration as the second case, but the train was traveling on the second track from the platform, with track centers 12 ft apart. The grid that was used was 157x31x41 cells in the three directions, respectively. This grid density was arrived at after confirming that the results of the simulation are grid-independent. This grid density is fine enough that numerical errors are avoided in the velocity results obtained. The corresponding grid spacing varied from as small as 0.06 ft at or near the wall of the train to a spacing of 2.0 ft at edge of the CFD model domain. Figure 3-4 shows the type of grid that was used around the cars.

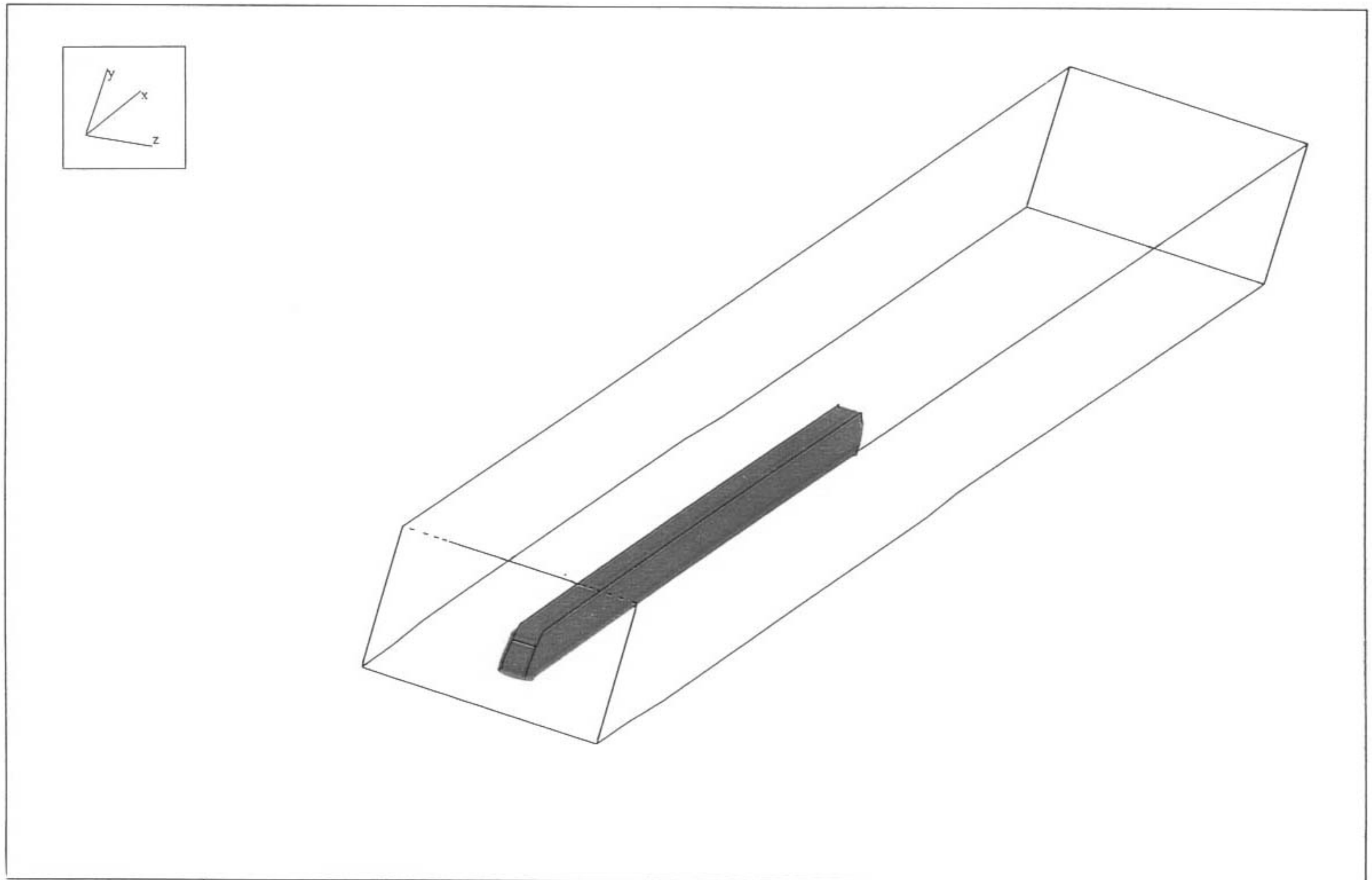

Figure 3-1. CFD Model – Isometric View – Acela Trainset with Low-Level Platform (at ground level) – Grid (157 x 131 x 41) – Dimension (1322 x 40 x 67) ft

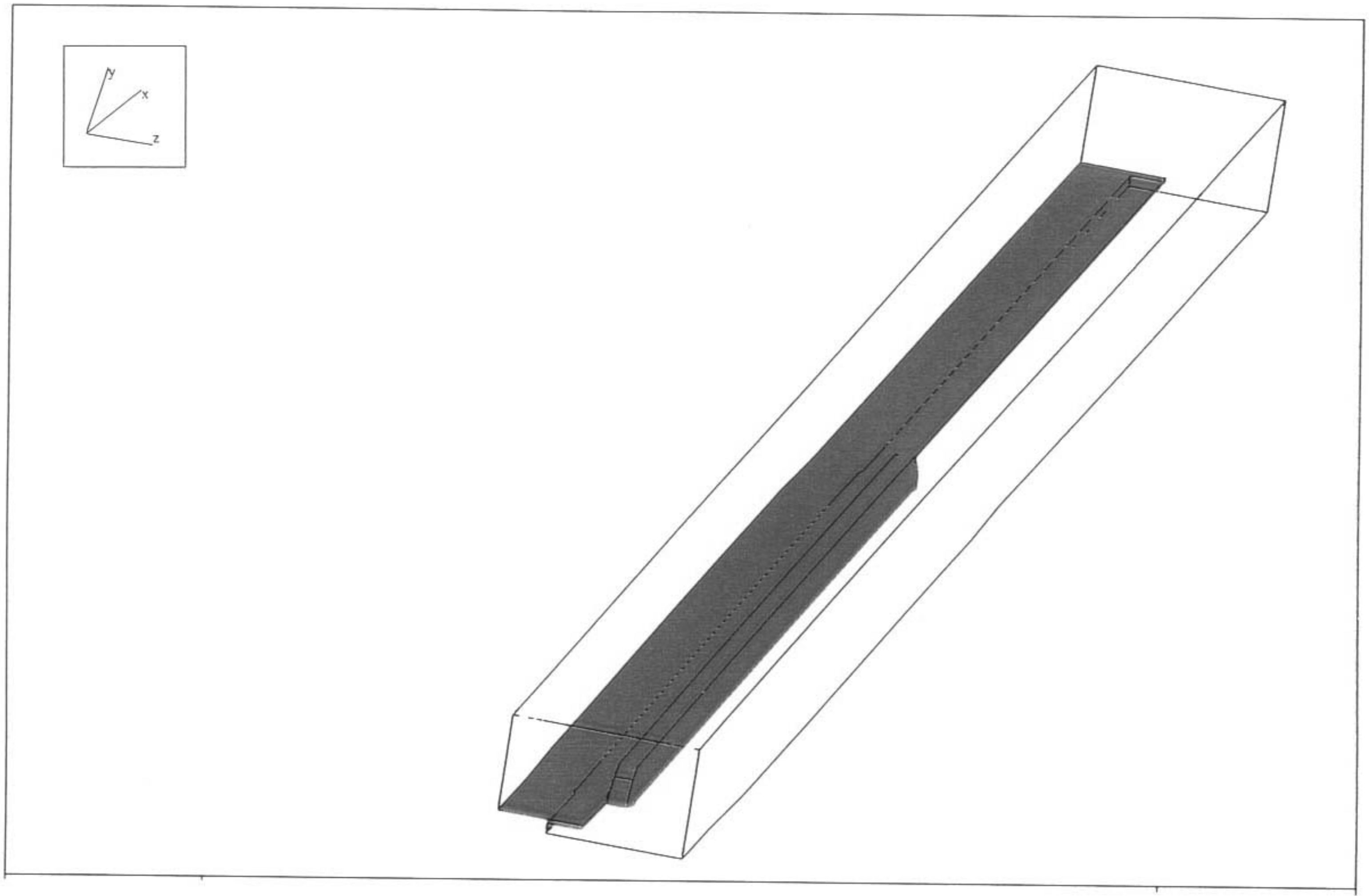

Figure 3-2. CFD Model – Isometric View – Acela Trainset Next to Platform – Grid (157 x 31 x 41) – Dimension (1322 x 40 x 67) ft

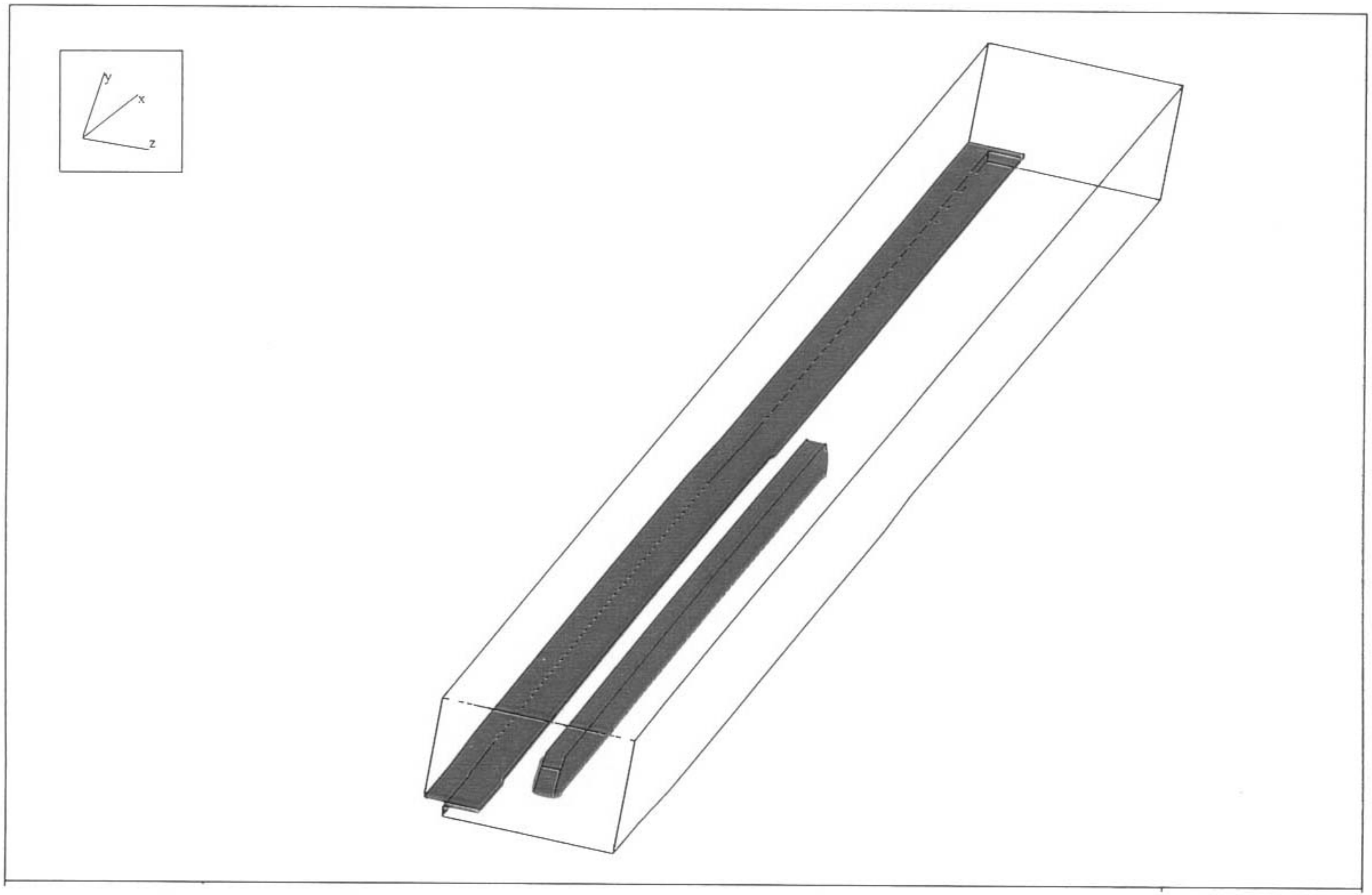

Figure 3-3. CFD Model – Isometric View – Acela Trainset Second Track From Platform – Grid (157 x 31 x 41) – Dimension (1322 x 40 x 67) ft

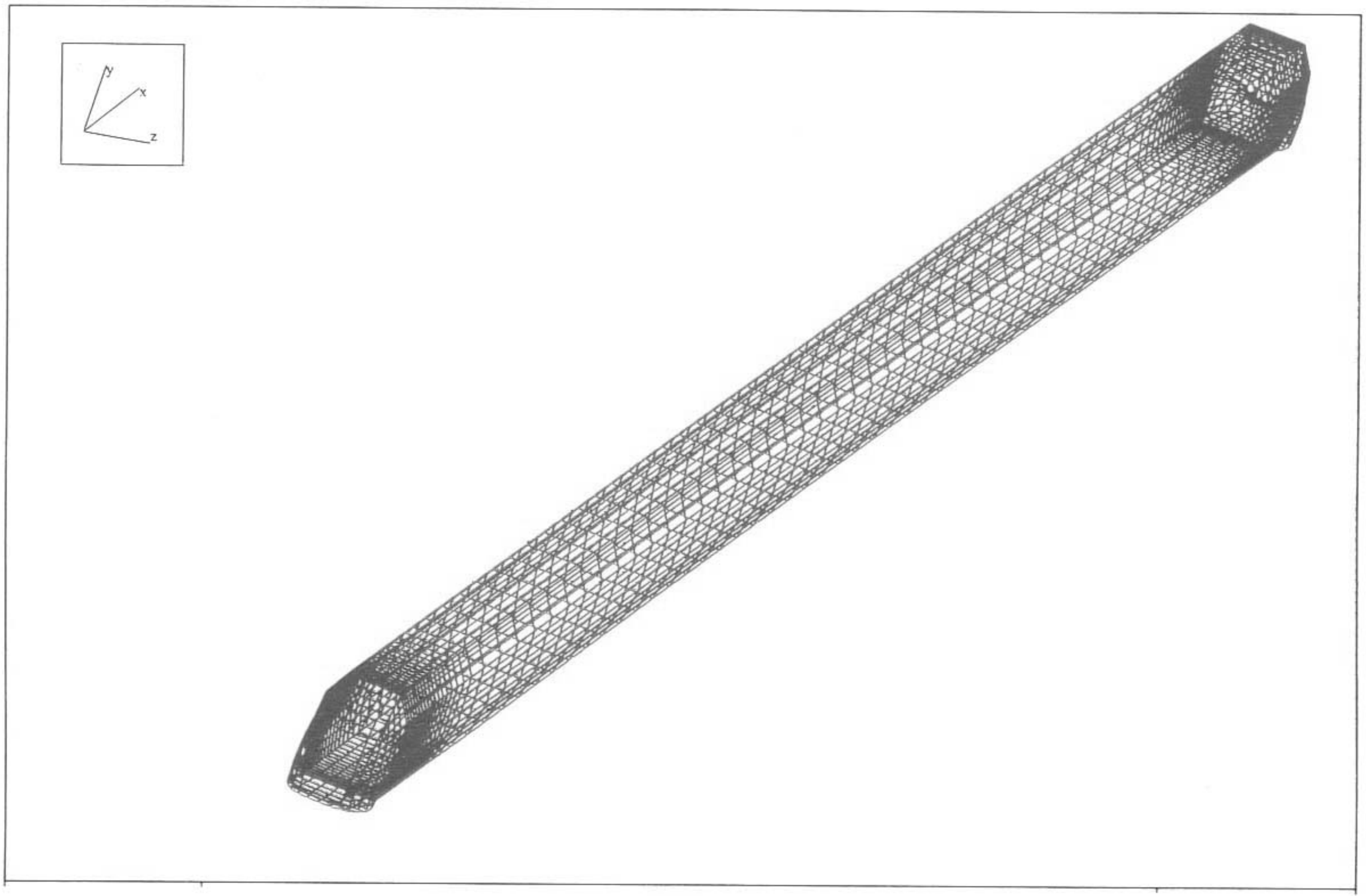

Figure 3-4. CFD Model – Acela Trainset Computational Grid – Grid (157 x 31 x 41)

Six simulations were done, with train speeds of 150 and 110 mph for each of the three configurations. The problem was analyzed isothermally, i.e., so that there are no temperature gradients within the model, an assumption that is required for the analysis, and that reasonably reflects actual conditions. The Renormalization Group (RNG) turbulence model (see Appendix A) was used to represent turbulence in the problem. For the simulation, the problem was solved in a coordinate system that was fixed relative to the train. In this system, the train was stopped while the air, the ground, and the observer were moved at the desired velocity in the direction opposite from what would be the train's normal motion.

There were six boundary conditions, corresponding to the six sides of the computational model, two in each of the x, y, and z directions, respectively. These directions are referred to as front and back (x), bottom and top (y), and left and right sides (z), respectively (see Figure 3-1). The inlet (front) velocity boundary condition was 80 ft in advance of the train. A moving ground was used for the bottom, and pressure boundaries were used on both sides, top and back of the computational domain. The coordinate system was fixed relative to the train, and the induced airflow velocities relative to the ground had to be calculated by subtracting out the speed of the train through post-processing algorithms for the data output. The back of the computational domain was put far enough from the tail of the train to provide a proper boundary condition. Different subroutines were written in conjunction with the main computer program, FLUENT (see Appendix A), to provide different output results pertinent to the problem.

3.3 Results of Acela Trainset Analyses

3.3.1 General Characteristics of Results

Per the previous discussion in Section 2.2.1, as a train passes a station, airflow will be induced at three locations along the train's path of travel that, relative to stationary objects, is felt as wind. One location is at the front end of the train, in the form of a "bow wave", resulting from the forward movement of the train and the resultant displacement of the air ahead of it. The second is the "boundary layer" formed along the side of the moving train, where the viscosity of air will cause a moving train to drag air with it, resulting in an induced airflow. The third is the "wake" at the rear of the train, which consists of a complex vortex field with turbulent flow. Therefore, people and objects close to a train passing at high speed could experience high wind forces. In addition, the wake can induce airflow velocities at the rear of the train that could stir up dust and debris around the track and propel it onto the station platform, and if high enough, can scatter luggage or other objects on the platform.

The CFD results depicting the *mean* air velocities in the direction of the train movement for train speeds of 110 mph and 150 mph and vehicles 10 ft wide are shown in Figures 3-5 through 3-16. Contour plots at 2.5 ft and 5 ft above the platform are plotted and shown in Figures 3-5, 3-7, 3-9, 3-11, 3-13 and 3-15. The results at 2.5 ft above the platform are relevant to potential effects that may be felt by small children or objects, such as luggage, at or near the platform level. Values of

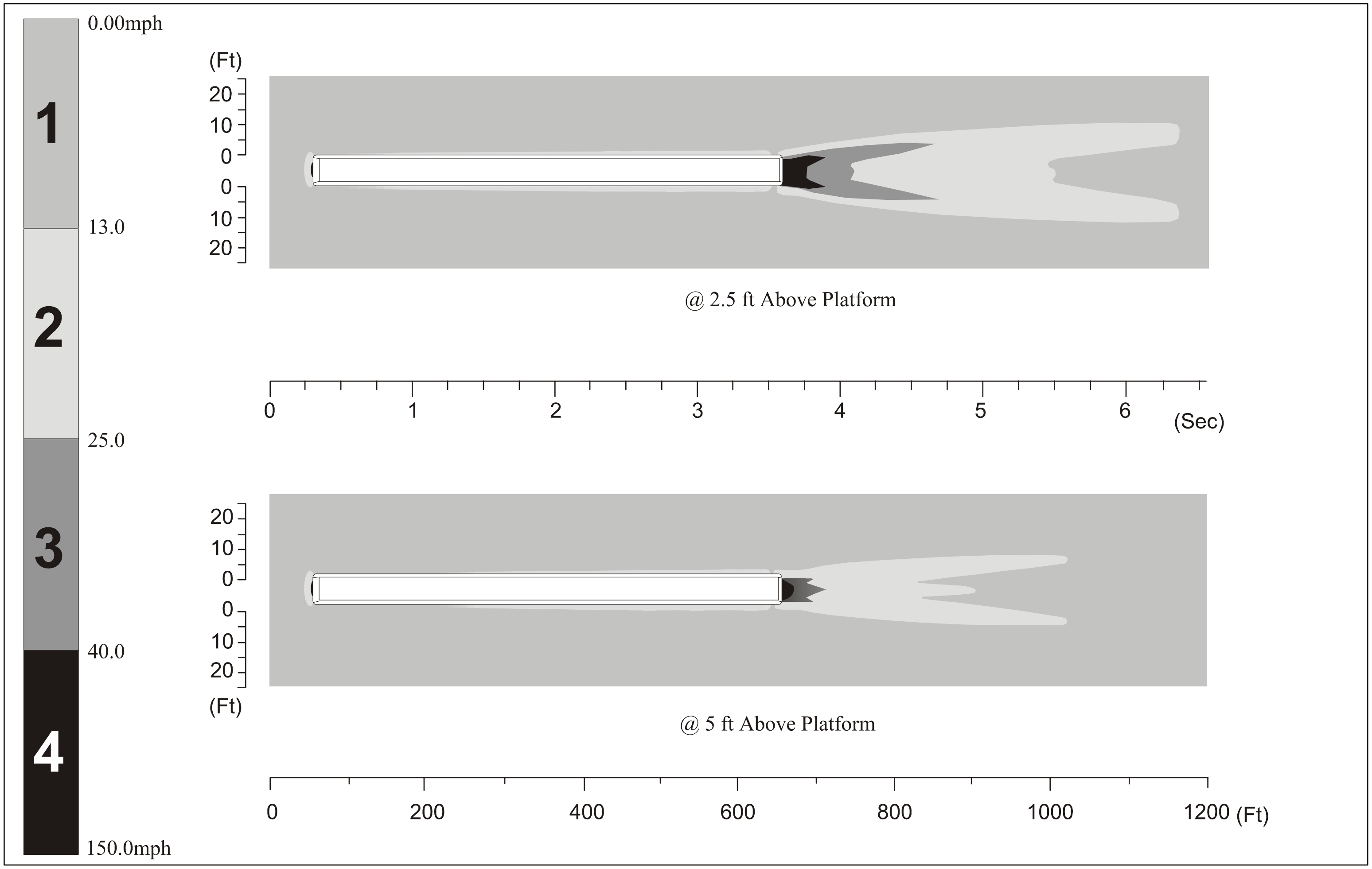

[Note: Axes coordinate orientation - x is the longitudinal direction ; y is the vertical direction; z is the transverse direction]

Figure 3-5. CFD Analysis Results – Low-Level Platform – Horizontal Mean Induced Airflow Velocity – Acela Trainset Speed = 150 mph

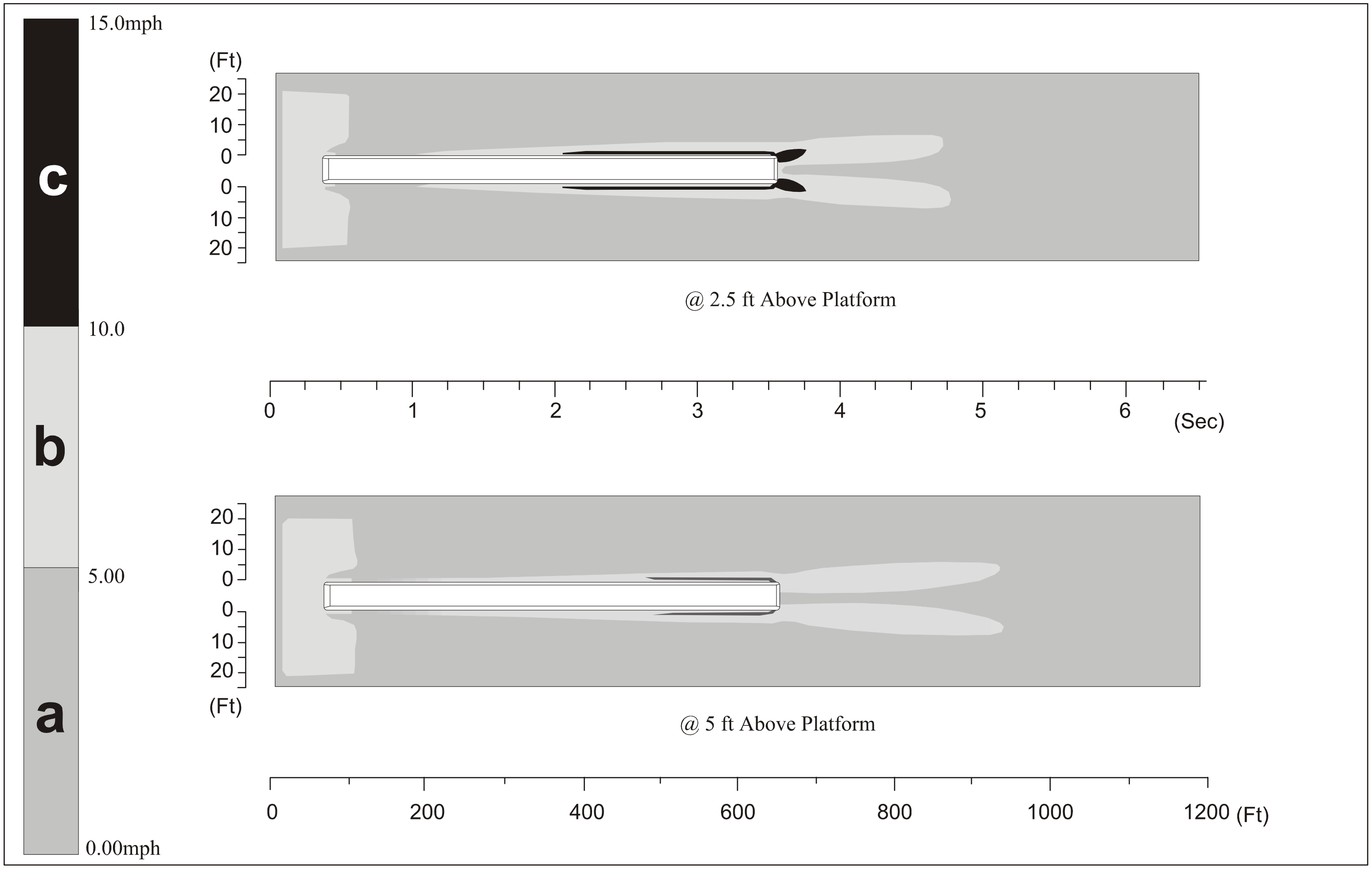

[Note: Axes coordinate orientation - x is the longitudinal direction ; y is the vertical direction; z is the transverse direction]

Figure 3-6. CFD Analysis Results – Low-Level Platform – Fluctuating Component of the Horizontal Velocity – Acela Trainset Speed = 150 mph

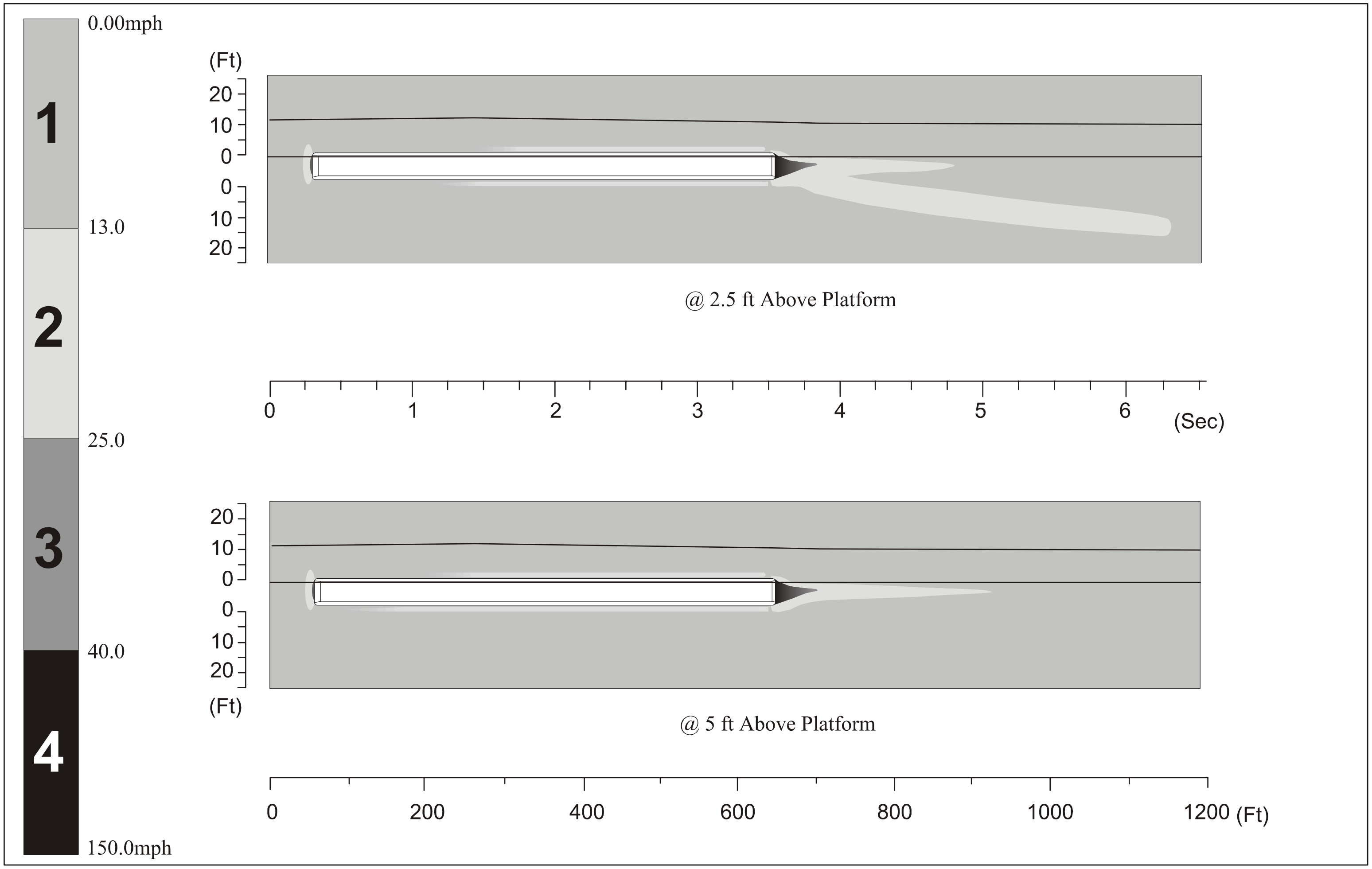

[Note: Axes coordinate orientation - x is the longitudinal direction ; y is the vertical direction; z is the transverse direction]

Figure 3-7. CFD Analysis Results – High-Level Platform – Horizontal Mean Induced Airflow Velocity – Acela Trainset Speed = 150 mph – Trainset Next to High-Level Platform

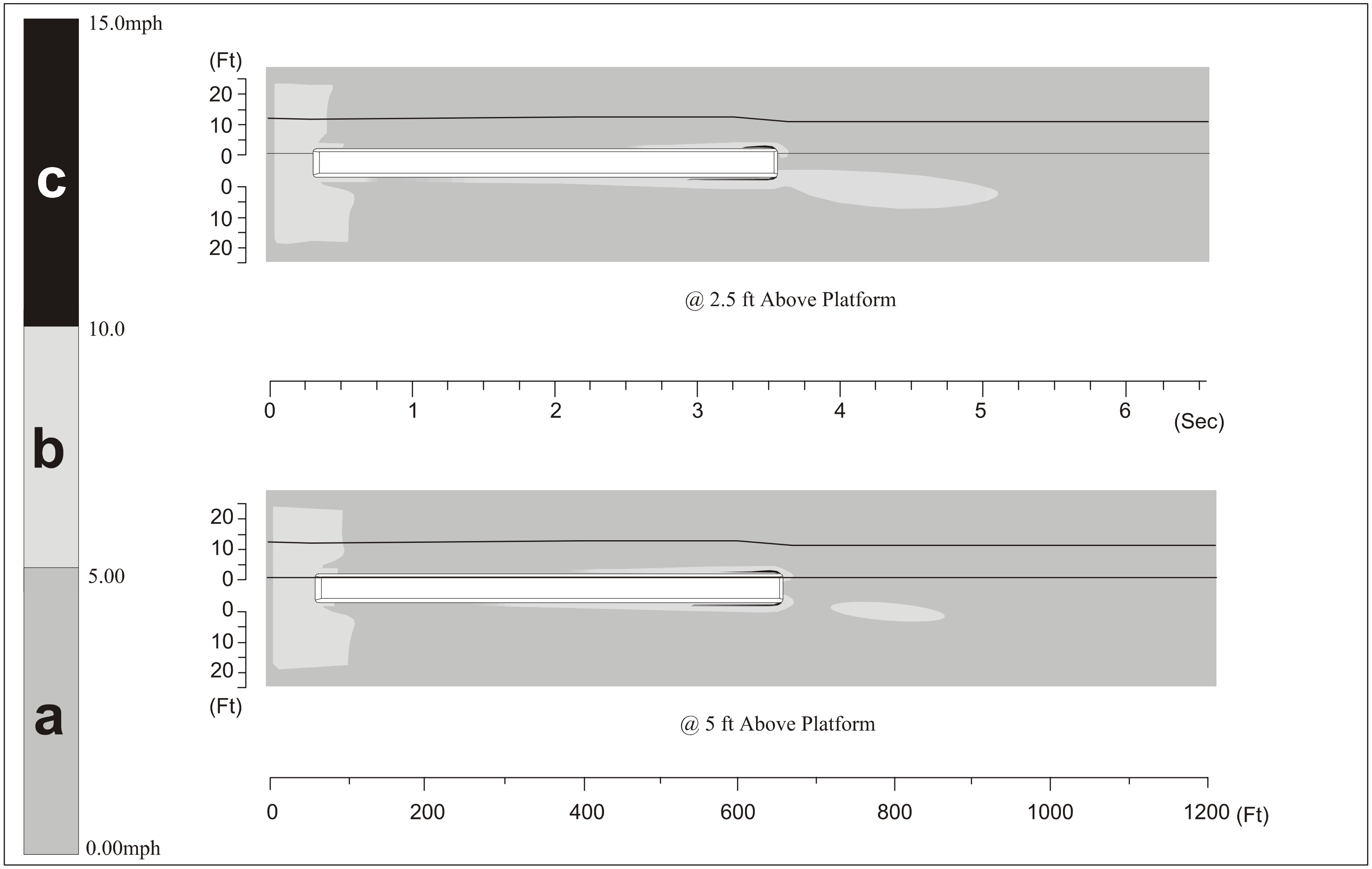

[Note: Axes coordinate orientation - x is the longitudinal direction ; y is the vertical direction; z is the transverse direction]

Figure 3-8. CFD Analysis Results – High-Level Platform – Fluctuating Component of the Horizontal Velocity – Acela Trainset Speed = 150 mph – Trainset Next to Platform

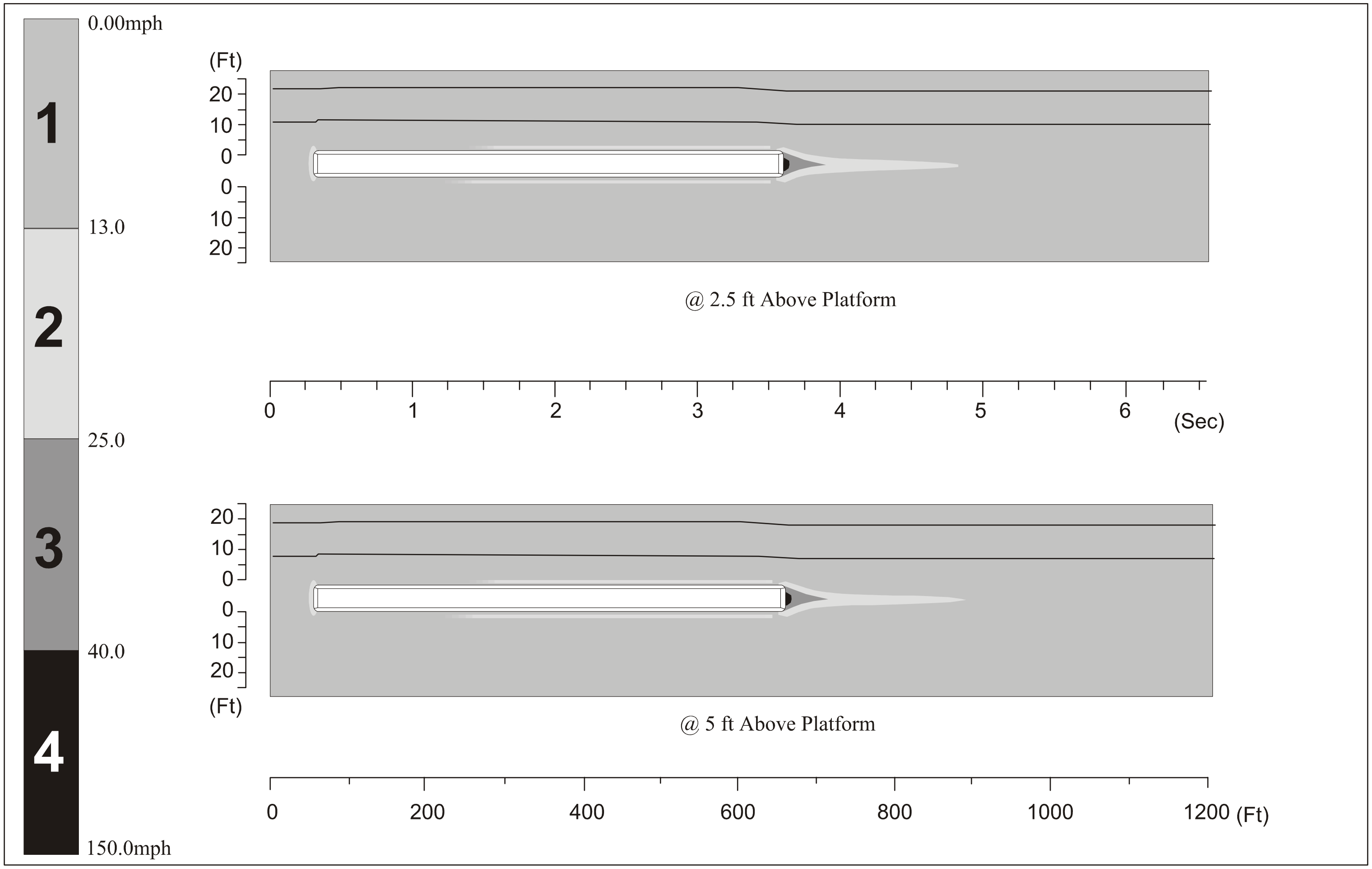

[Note: Axes coordinate orientation - x is the longitudinal direction ; y is the vertical direction; z is the transverse direction]

Figure 3-9. CFD Analysis Results – High-Level Platform – Mean Induced Airflow Velocity – Acela Trainset Speed = 150 mph – Trainset on Second Track from Platform

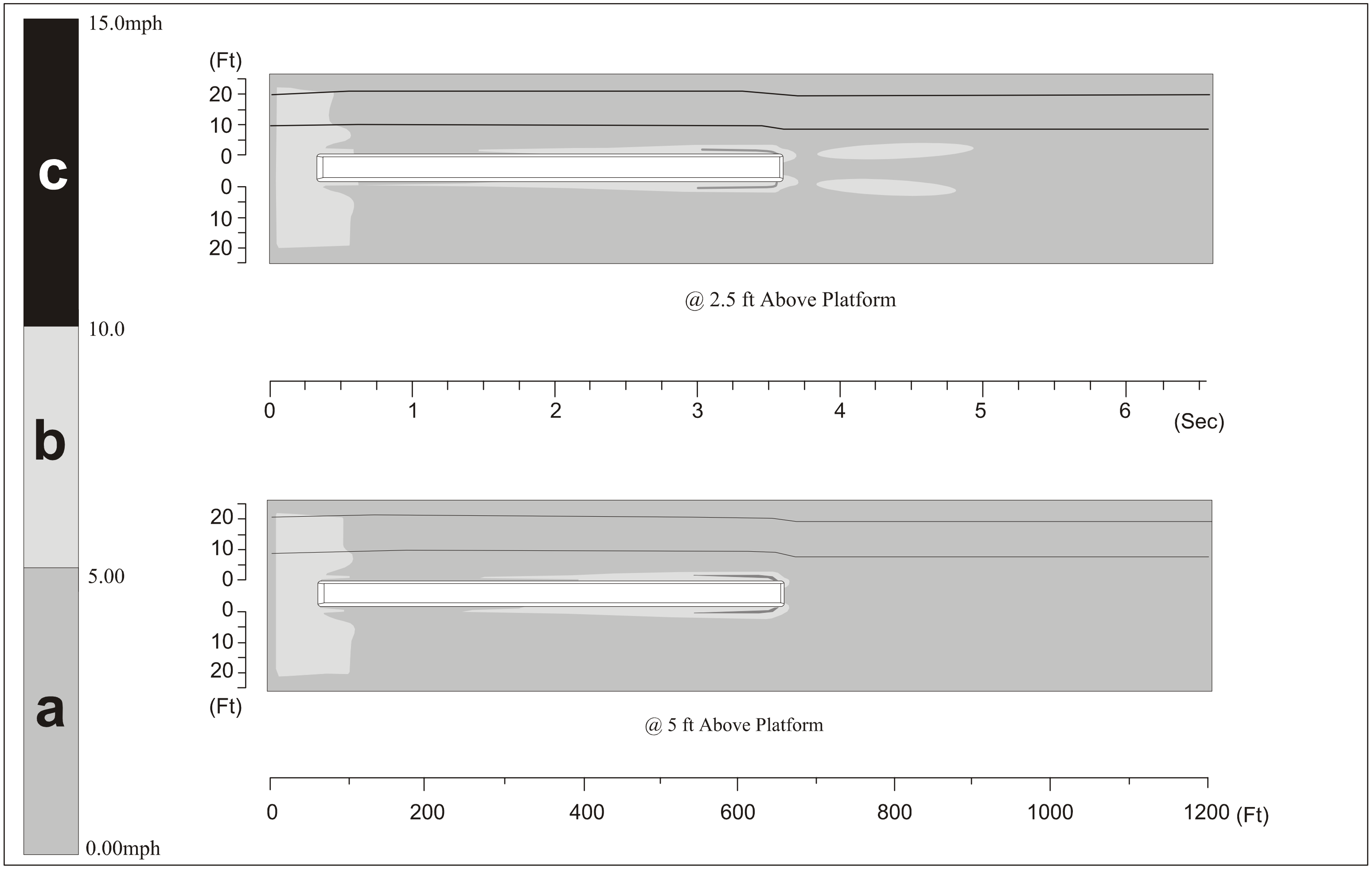

[Note: Axes coordinate orientation - x is the longitudinal direction ; y is the vertical direction; z is the transverse direction]

Figure 3-10. CFD Analysis Results – High-Level Platform – Fluctuating Component of the Horizontal Velocity – Acela Trainset Speed = 150 mph – Trainset on Second Track from Platform

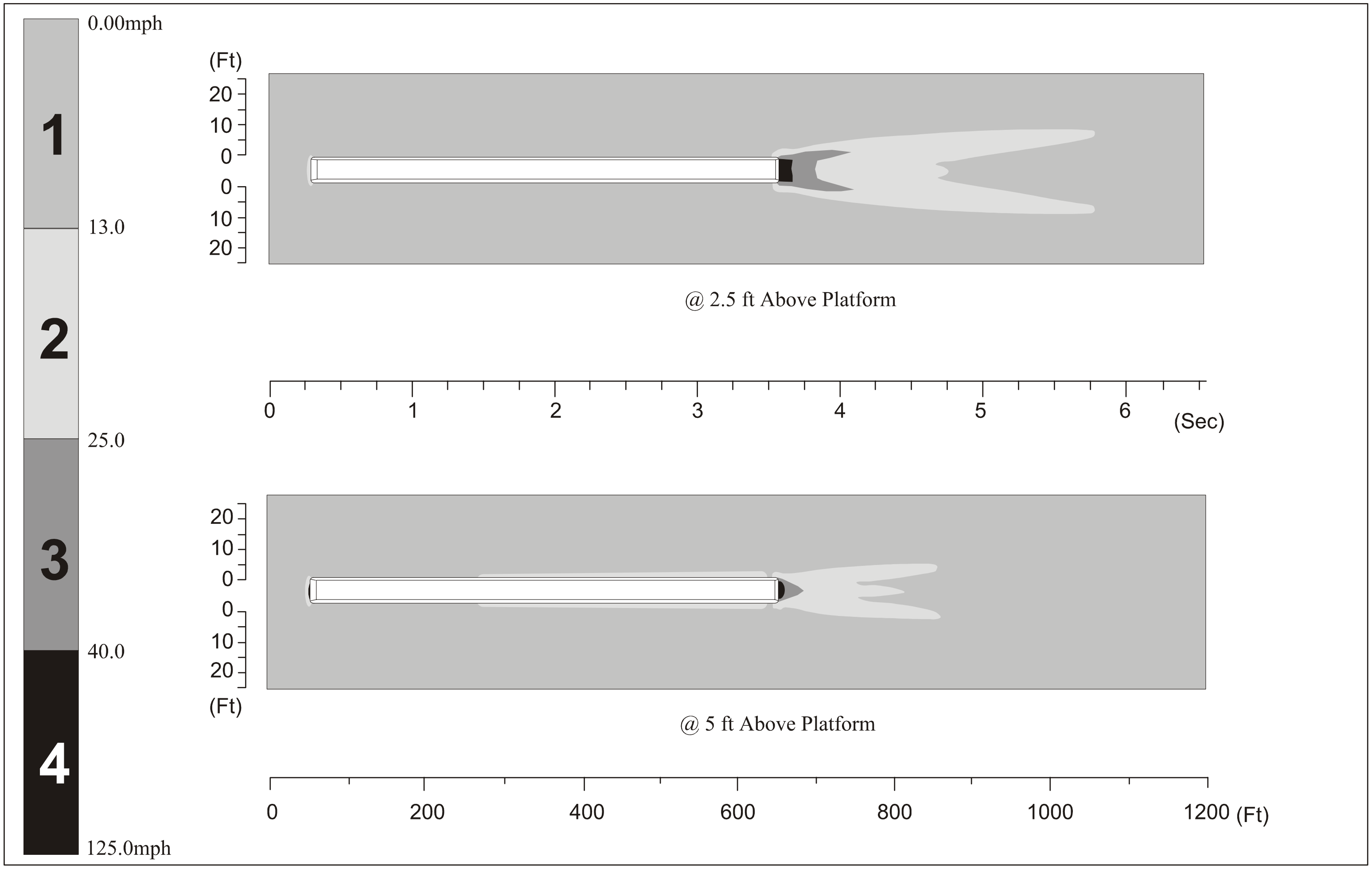

[Note: Axes coordinate orientation - x is the longitudinal direction ; y is the vertical direction; z is the transverse direction]

Figure 3-11. CFD Analysis Results – Low-Level Platform – Horizontal Mean Induced Airflow Velocity – Acela Trainset Speed = 110 mph

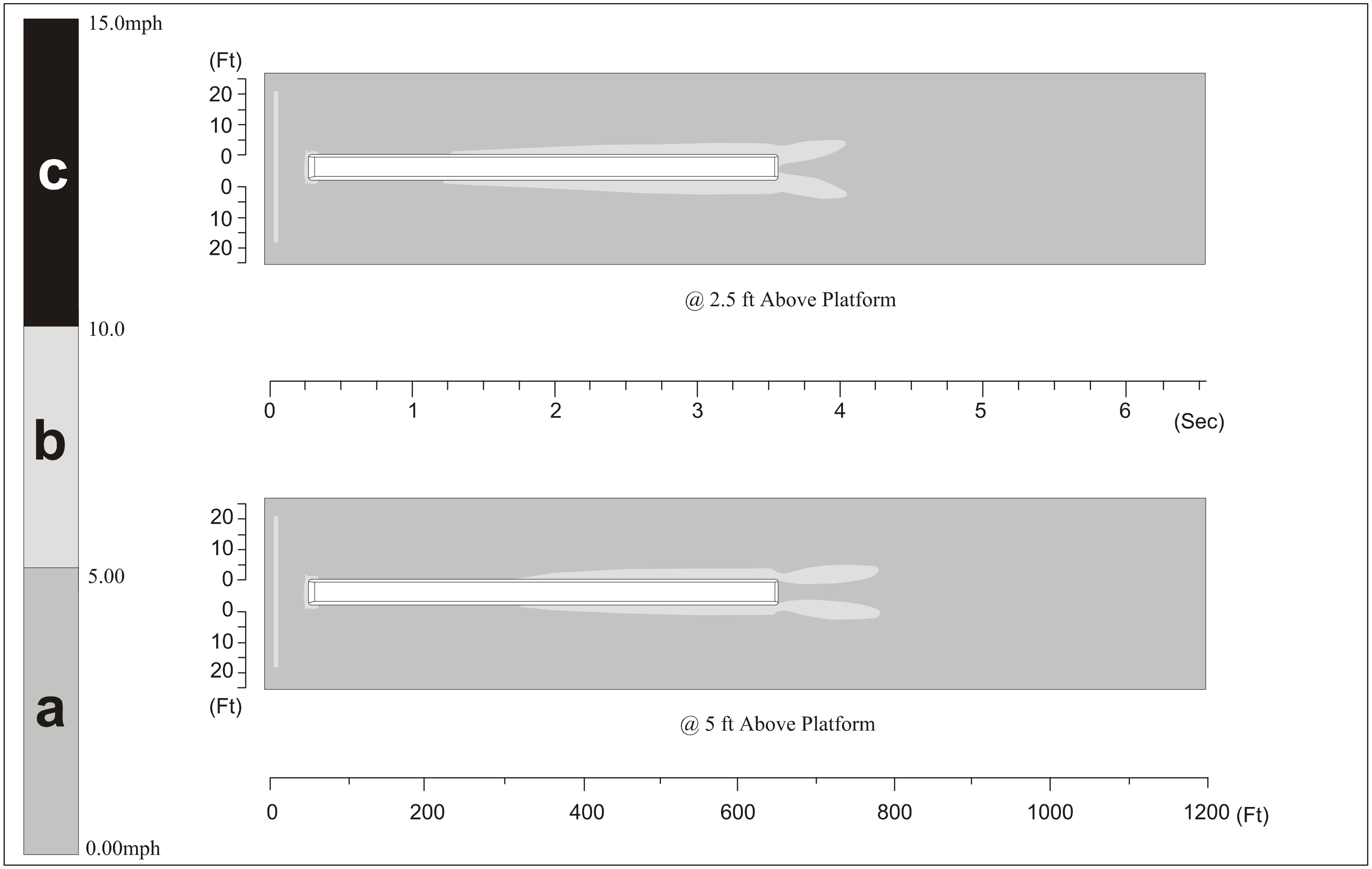

[Note: Axes coordinate orientation - x is the longitudinal direction ; y is the vertical direction; z is the transverse direction]

Figure 3-12. CFD Analysis Results – Low-Level Platform – Fluctuating Component of the Horizontal Velocity – Acela Trainset Speed = 110 mph

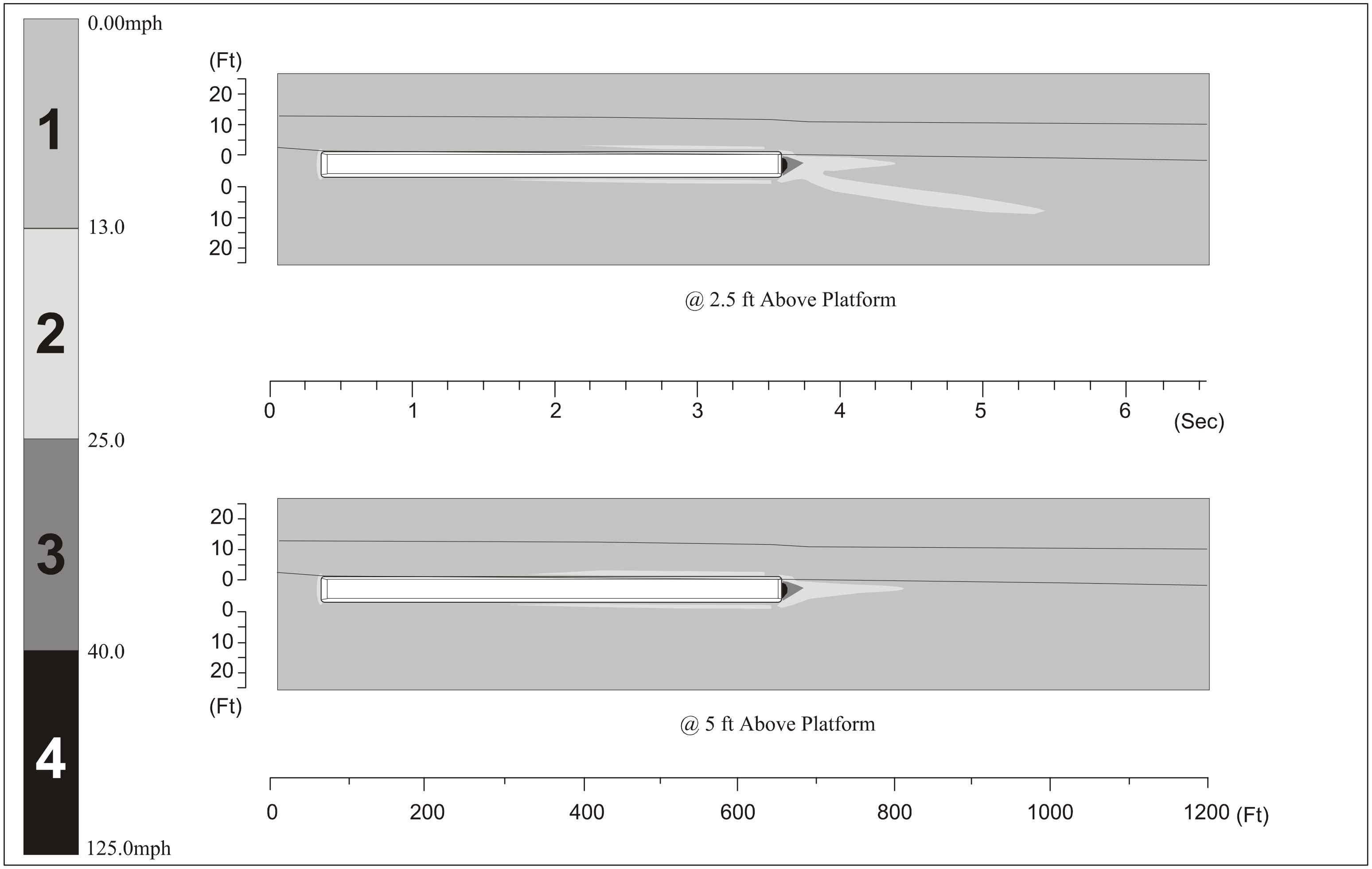

[Note: Axes coordinate orientation - x is the longitudinal direction ; y is the vertical direction; z is the transverse direction]

Figure 3-13. CFD Analysis Results – Low-Level Platform – Horizontal Mean Induced Airflow Velocity – Acela Trainset Speed = 110 mph – Trainset Next to Platform

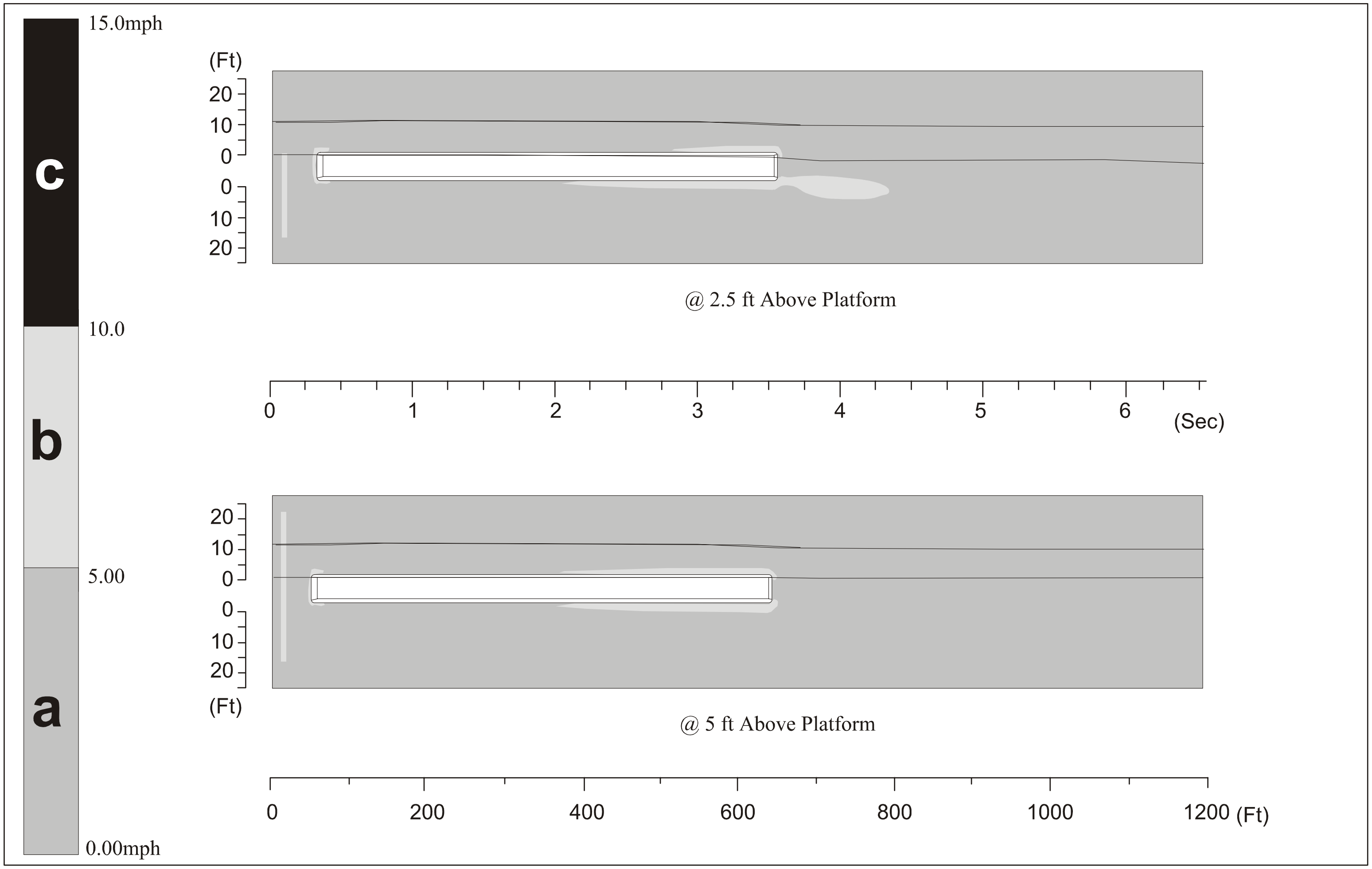

[Note: Axes coordinate orientation - x is the longitudinal direction ; y is the vertical direction; z is the transverse direction]

Figure 3-14. CFD Analysis Results – High-Level Platform – Fluctuating Component of the Horizontal Velocity – Acela Trainset Speed = 110 mph – Trainset Next to Platform

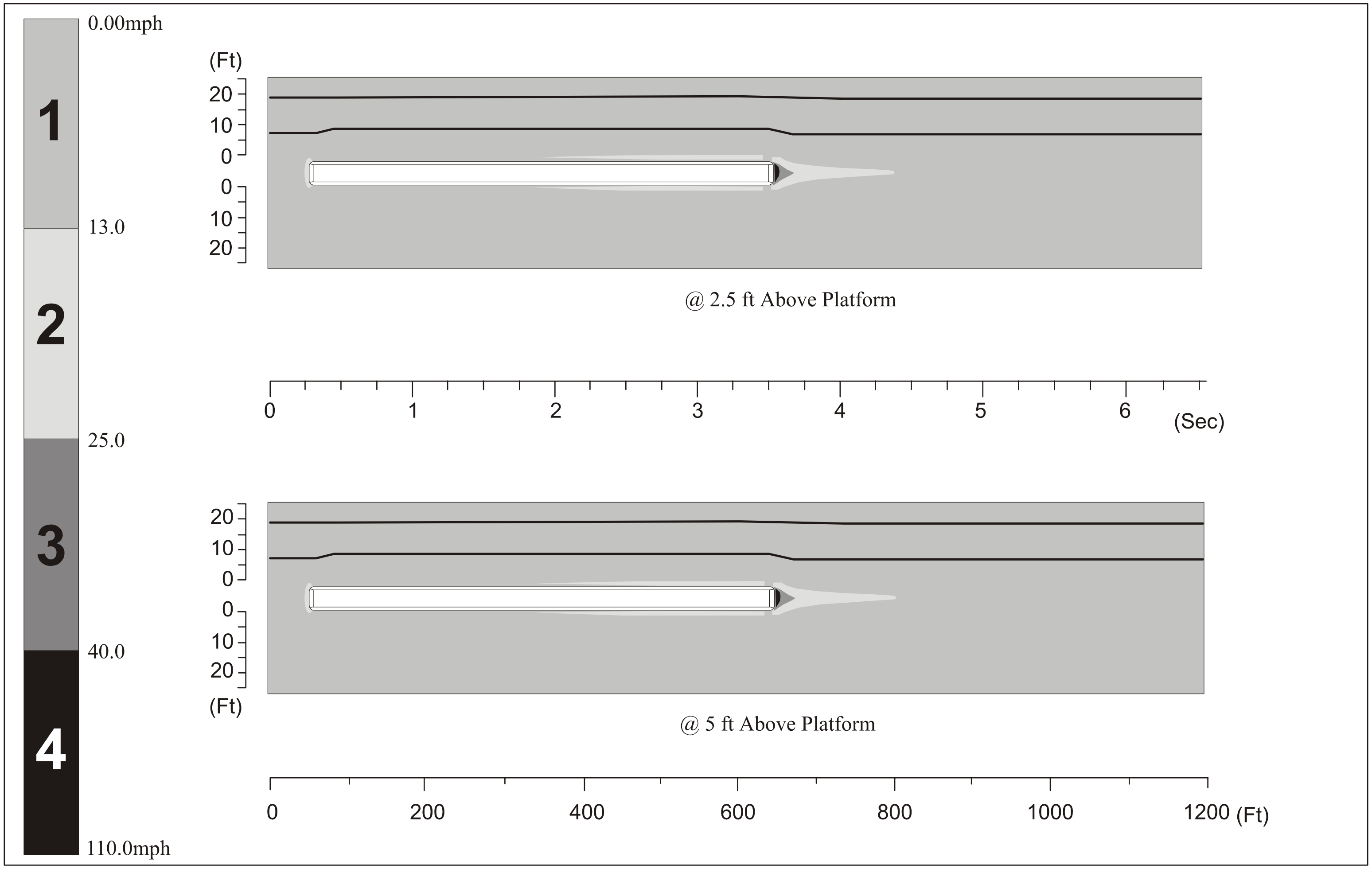

[Note: Axes coordinate orientation - x is the longitudinal direction ; y is the vertical direction; z is the transverse direction]

Figure 3-15. CFD Analysis Results – Low-Level Platform – Horizontal Mean Induced Airflow Velocity – Acela Trainset Speed = 110 mph – Second Track from Platform

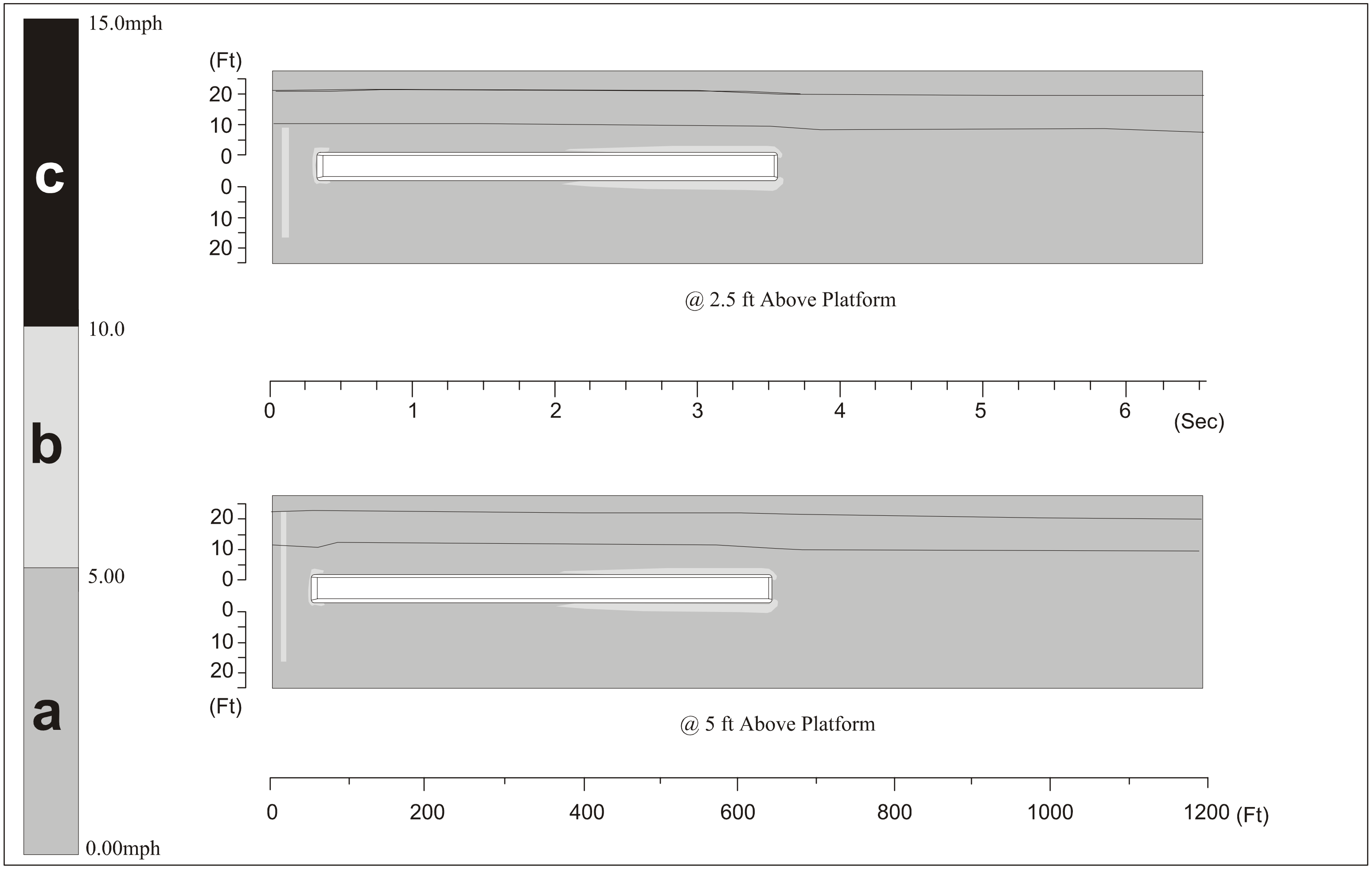

[Note: Axes coordinate orientation - x is the longitudinal direction ; y is the vertical direction; z is the transverse direction]

Figure 3-16. CFD Analysis Results – Low-Level Platform – Fluctuating Component of the Horizontal Velocity – Acela Trainset Speed = 110 mph – Trainset on Second Track from Platform the air velocity fluctuation contours due to turbulence are also plotted and shown in Figures 3-6, 3-8, 3-10, 3-12, 3-14 and 3-16 for 2.5 ft and 5 ft above the platform. The range of actual induced airflow velocity is obtained by adding or subtracting the fluctuating component of velocity to/from the mean air velocity, as explained in Appendix E.

Four ranges of mean air velocities were represented in the velocity contours, as based on the Beaufort scale (Chapman, 1970; Lee, 1999). The plots generated by the CFD computer program are color coded as follows to show these air velocity ranges:

- 0 to 13 mph – (1)- no nuisance
- 13 to 25 mph – (2) - nuisance
- 25 to 40 mph – (3) - difficulty in walking
- Above 40 mph – (4) - walking impeded or worse

Similarly, the fluctuation contours (used to describe the range of variation of the actual velocity from the mean velocity values, see Appendix E) were plotted using three ranges:

- 0 to 5 mph – (a)
- 5 to 10 mph – (b)
- 10 to 15 mph – (c)

The fluctuation component reflects the turbulent and somewhat random component of the airflows. To obtain the upper and lower ranges of induced airflow velocities, the random component should respectively be added or subtracted from the mean component.

All the figures are magnified four times in width to facilitate visualizing the flow behavior around the train. Note also that, along the longitudinal axis, there are length and time scales. Thus, from a bystander's frame of reference, the air velocity and fluctuation contours represent effects relative to the position of the train, or the effects at any time relative to the arrival and passage of the train. The horizontal velocities indicated on the figures reflect the velocities primarily in the longitudinal direction rather than in a direction transverse to the train.

3.3.2 Bow Wave and Boundary Layer Effects

These CFD results show that there are no hazards or nuisances resulting from the bow wave and the boundary layer along the train for both the 110 mph and 150 mph train speeds beyond a distance of 3 ft from the side of the train for the low-level platform, or 2 ft for the high-level platform. These observations were expected (see Hoerner, 1965) due to the high-flow Reynolds Numbers (the ratio of the momentum force to the viscous force) in all the cases studied. The Reynolds Numbers were 8.1×10^8 and 5.9×10^8 when the train traveled at 150 mph and 110 mph, respectively. The boundary layer thickness increases along the train, as can be seen in Figures 3-5, 3-7, 3-9, 3-11, 3-13, and 3-15, but not enough to create a nuisance or hazard to the patrons on the nearby platform, beyond the distances stated above.

3.3.3 Wake Effects

The effects of airflow in the wake regions are considered to have potentially the largest impacts along the platform where people are standing. The magnitude of the wake problem depends on the type of the platform configuration, low-level or high-level, the condition of the trackbed, e.g., whether loose sand and grit are present, and the presence or absence of walls or movable objects on the platform.

The wake does not apparently create a danger or a nuisance to people or property in the case of a high-speed train passing a high-level platform. The velocity of the air in the cases with high platforms is 13 mph or lower on the platform for train speeds of both 110 mph and 150 mph, as seen in Figures 3-7 and 3-13 for the train close to platform, and Figures 3-9 and 3-15 when the train is on the second track. Due to turbulence, these values can fluctuate by as much as ±5 mph, as shown in the Figures 3-8 and 3-14 for the train close to the platform, and Figures 3-10 and 3-16 when the train is on the second track.

The figures for the case of the low-level platform for both train speeds of 110 and 150 mph, as shown in velocity Figures 3-5 and 3-11 and fluctuation Figures 3-6 and 3-12, presented a different outcome. The wake boundaries with higher velocities extended to distances where people could be standing. The instantaneous velocity (i.e., the sum of the mean and fluctuating values) is shown in Figures 3-17 and 3-18. When the train is moving with a speed of 150 mph, Figure 3-17 shows that at a height of 2.5 ft above the low-level platform, a velocity field that could be as high as 25 mph is seen to reach people and objects that are 12 ft away from the side of the train. The exposure time is estimated to be 2 to 3 seconds. At the same height, a velocity as high as 40 mph can exist at a distance 3-6 ft away from the side of the train. The exposure time is estimated to be 1 second. At 5 ft above the platform, the velocity of the air can reach 25 mph at a distance of 8 ft away from the side of the train. The exposure time is calculated to be 2 seconds.

When the train is passing a low-level platform at a speed of 110 mph, the distances covered by relatively higher values of velocities are less far-reaching than at 150 mph. At 2.5 ft above the platform, for the instantaneous velocity value, Figure 3-18 shows a velocity of 25 mph at a distance 9 ft away from the side of the train. The exposure time is estimated to be 3 seconds. At the same height, a velocity of up to 40 mph can reach people that are 2 ft away from the side of the train. The exposure time is estimated to be 0.5 to 1.0 second. At 5 ft above the platform, a velocity of 25 mph reaches a distance of 4 ft away from the train's side, as can be seen in the same figure. The exposure time is calculated to be 2 seconds.

When the train is on the first track (i.e., closest to the platform), the high-level platform effect can be seen as shown in Figures 3-7, 3-8, 3-13, and 3-14. The mean velocity and fluctuations are damped on the side of the train next to the platform, due to the presence of the underpinning

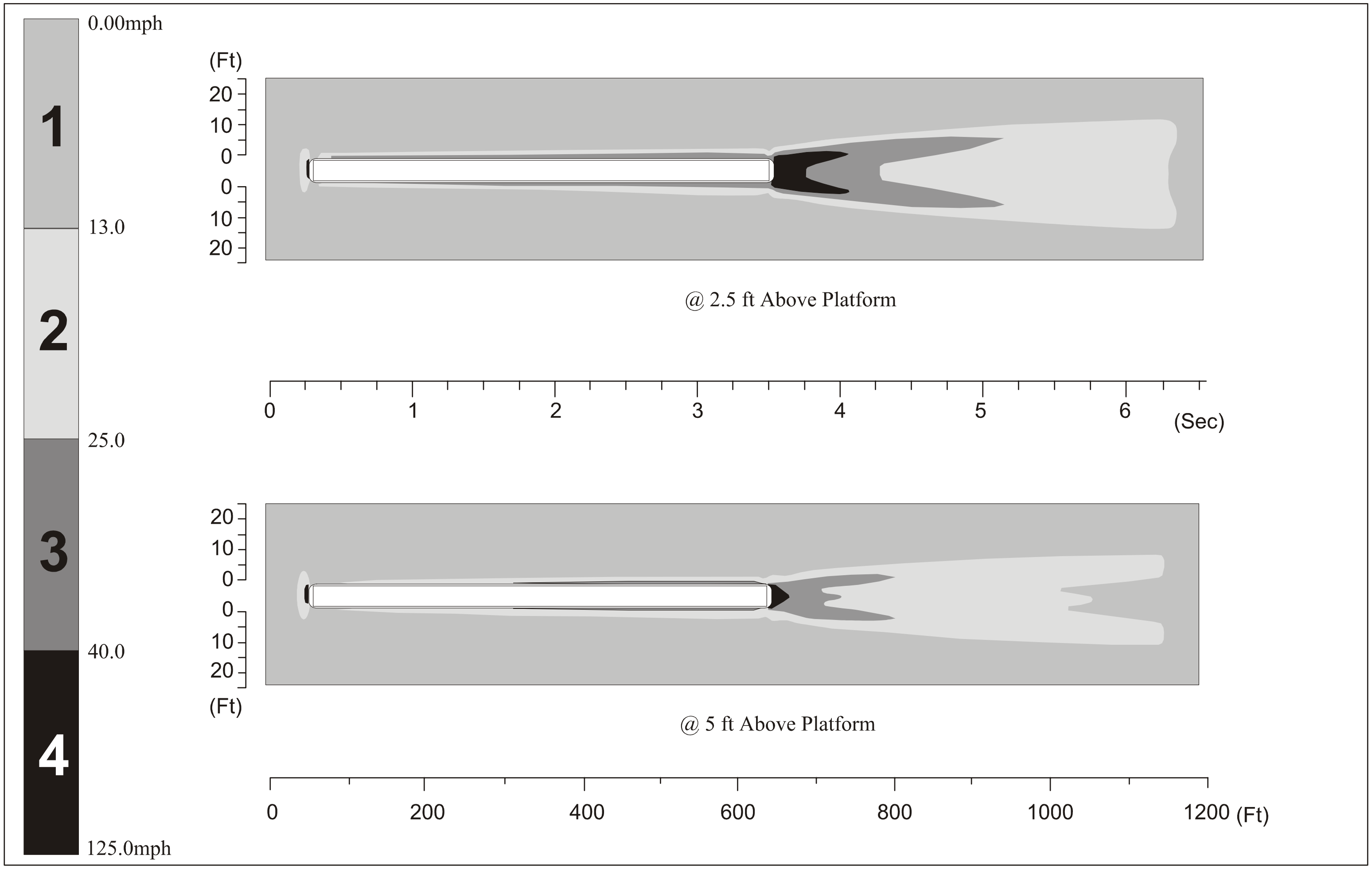

[Note: Axes coordinate orientation - x is the longitudinal direction ; y is the vertical direction; z is the transverse direction]

Figure 3-17. CFD Results – Low-Level Platform – Horizontal Induced Airflow Velocity – Mean Plus Fluctuating Component - Acela Trainset Speed = 150 mph

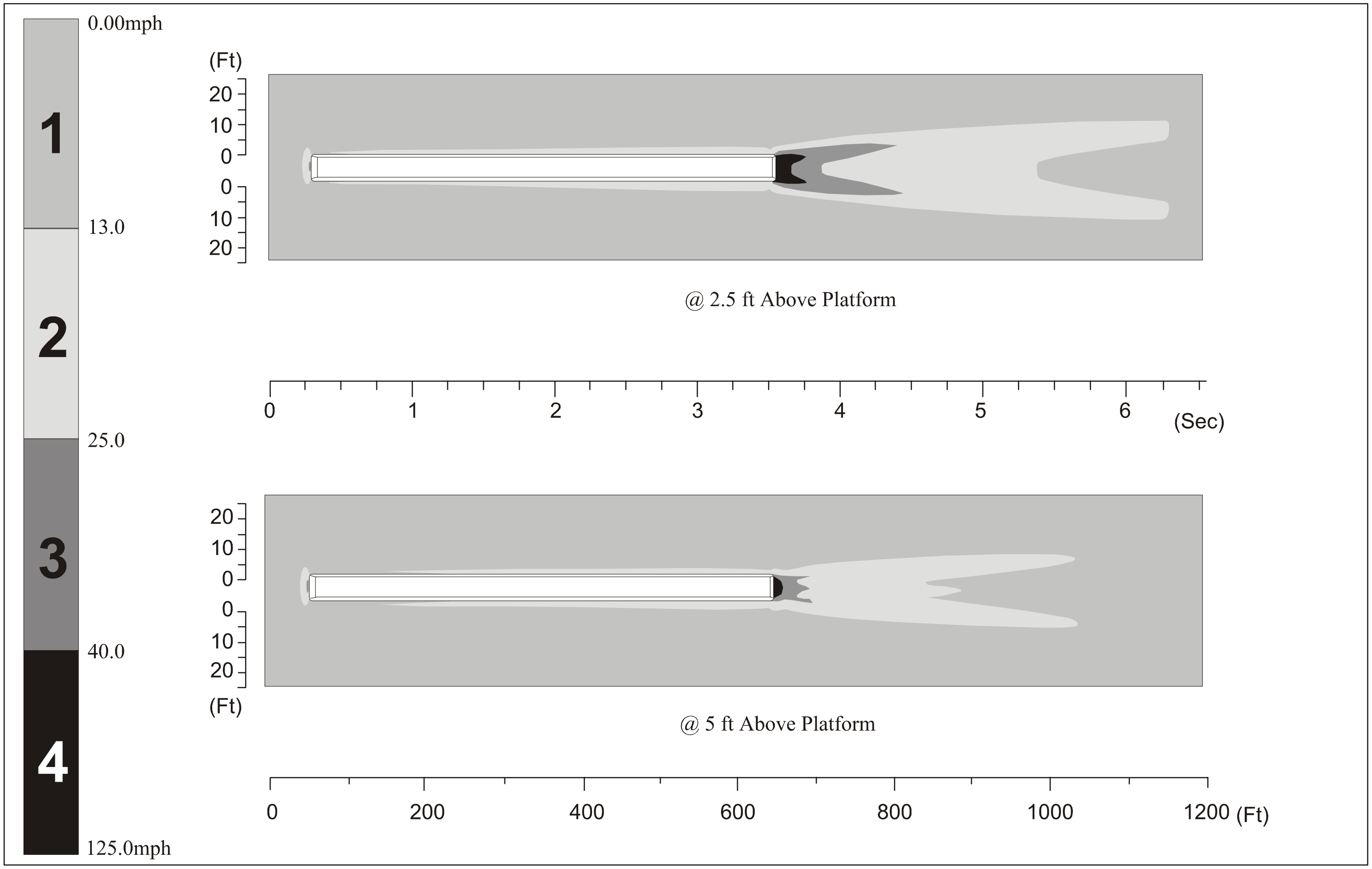

[Note: Axes coordinate orientation - x is the longitudinal direction ; y is the vertical direction; z is the transverse direction]

Figure 3-18. CFD Results – Low-Level Platform – Horizontal Induced Airflow Velocity – Fluctuating Component - Acela Trainset Speed = 110 mph support wall of the platform structure. However, the velocity contours behave roughly the same as the free-field condition on the side opposite the platform, forming a shape like a tail, as seen in Figures 3-7 and 3-13. [The lengths and the shapes of the wake contours should be compared to Figures 3-5 and 3-11 respectively, for conditions for the low-level platform.] The effect is less noticeable as the height above the platform increases, as can be seen in Figures 3-7 and 3-13 when comparing the contours at 2.5 ft and 5 ft above the platform. The mean velocity contours are not symmetrical with respect to the longitudinal axis along the train, as was observed in the mean velocity and fluctuation contours for the low-level platform case (see Figures 3-5, 3-6, 3-11, and 3-12). The effect of the high-level platform presence on the mean velocity and fluctuation contours is less pronounced and weaker when the train is in the second track from the platform, as seen in Figures 3-9, 3-10, 3-15, and 3-16.

Comparing the above CFD results with the British Rail exposure limits of 25 mph for the general public and 38 mph for employees along the track, it is clear that the CFD results (mean plus fluctuating component) for low-level platforms would exceed these exposure limits. The results are also consistent with the estimate by Lee (1999) that for a person standing less than 6.6 ft away from the side of the train, the effects would be high enough to be of concern. Mitigating these concerns, however, is that the air velocities have relatively short durations and are transient in nature. Related to this factor, these exposure limits are based to some extent on the Beaufort scale, which was originally developed for sustained wind rather than transient air velocity effects. Also, these air velocities are anticipated to be slightly to moderately greater than those currently experienced as the result of the currently operating Amfleet service and other express train services along the Northeast Corridor. Trains pulled by locomotives with a more blunt front end than an AEM-7, such as the F40PH Diesel or the E-60 electric, could have induced air velocities greater than the Acela trainsets.

3.4 Model Details for Amfleet Trainset Analyses

CFD analysis was performed on the Amfleet trainsets, for comparison with the Acela trainset analysis and with the actual field measurements described in Section 4.

The Amfleet cars consisted of an AEM-7 electric locomotive trailed by six coach cars, modeled as shown in Figures 3-19 and 3-20. The dimensions of the train were 563 ft in overall length, 10.25 ft wide, and 12.5 ft high. The computational domain was 1,200 ft long, 40 ft high, and 60 ft wide, as shown in Figure 3-19. As for the Acela trainset model described in Section 3.2, the computational domain must be large enough so that the effects of the train passage are negligible at the edges of the domain, i.e., to represent ambient air conditions without train passage effects. Similar to the model for the Acela trainset, the domain was sized to exceed the boundary layer thickness by at least an order of magnitude. The inlet free stream boundary started 70 ft ahead of the train's nose. The case that was analyzed assumed a train speed of 125 mph with a low-level platform. Recall also, that the low-level platform condition is, for modeling purposes, the same as having a no platform condition. The low-level platform is for practical purposes the same as ground level, i.e., a condition where the platform can be modeled the same as the ground.

Runs were performed to compare and adjust the coefficient of drag, which was the only data provided by Amtrak. The coefficient of drag is a dimensionless number obtained by taking the drag force and dividing it by the dynamic pressure force on the front of the train. Amtrak used the Davis Equation (see Baumeister et al, 1979) during design to compute train drag coefficient. Generally lower drag coefficients indicate more streamlined trains or objects. At 125 mph, the train's aerodynamic drag was calculated to be of 8,000 lbf. The drag force consists of two components: pressure drag and frictional drag. In the CFD model, the frictional force can be adjusted as explained in Appendix C. After three runs and adjustments, the value of the drag force obtained by the CFD model was 7,800 lbf. This value differs by only 2.5% from the value computed with the Davis Equation. However, as noted previously, the level of detail on information provided for the Amfleet trainset was less than that provided for the Acela, and required additional assumptions and calculations to enable the analysis. This resulted in somewhat less accurate results for the Amfleet runs compared with the Acela trainset runs.

The final coefficient of drag used for the Amfleet trainset was 1.61. For purposes of comparison, it should be noted that the coefficient of drag used for the Acela trainset was 1.32.

3.5 Results for Amfleet Trainset Analyses

Figure 3-21 depicts the component of the velocity along the body of the train, and Figure 3-22 shows the fluctuating component of the airflow. Two plan sections for the velocity contours are shown in these Figures, one at 2.5 ft and the other at 5 ft above the rails. The results at 2.5 ft above the platform are relevant to potential effects that may be felt by small children or objects, such as luggage, at or near the platform level. The phenomenon of excessive flow separation can be seen in Figure 3-21, at the corners at the head of the train. The contours are discontinuous, meaning that the flow lines at the head of the train separate from the train body, and then re-attach further back along the side of the train. This indicator of poor aerodynamic performance is essentially due to the shape of the nose. The profile shape of the vehicle leads to an increase in the pressure drag, which represents the major drag component on the train.

Figure 3-21 shows that the velocity of the air at 4 ft on the side near the head of the train can reach a value of 40 mph, or higher. At about 150 ft back from the head of the train, the velocity of the air can attain a value of 25 mph up to 6 ft away from the side of the train, which persists for almost 500 ft behind the train, which corresponds to a calculated 2 to 3 second duration of exposure for a person standing on the platform.

As with the Acela trainset results, a comparison with the British Rail exposure limits of 25 mph for the general public and 38 mph for employees along the track shows that the Amfleet results (mean plus fluctuating component) for low-level platforms also exceed these exposure limits.

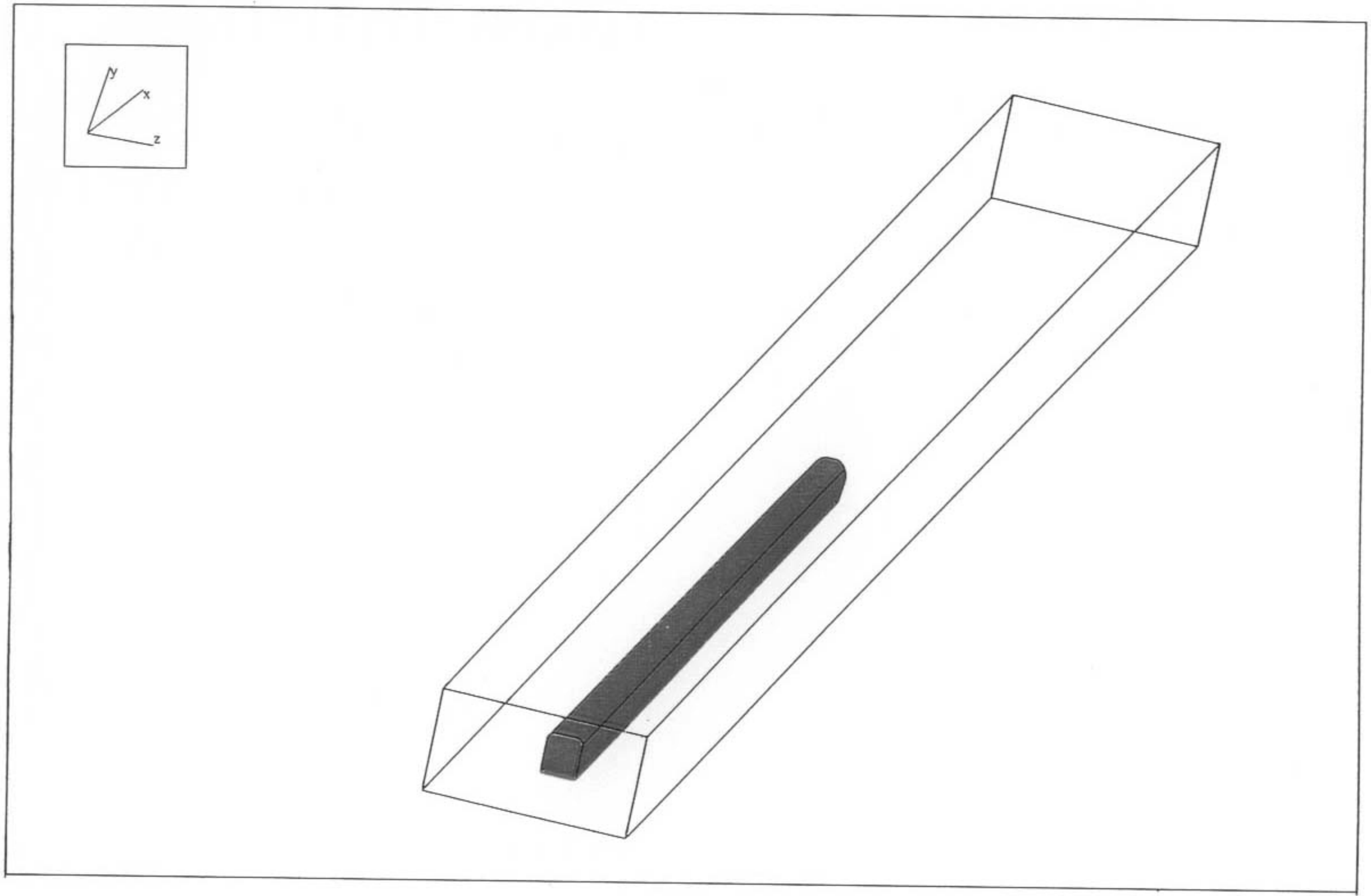

Figure 3-19. CFD Model Isometric View – Amfleet Trainset with Low-Level Platform – Grid (160 x 38 x 53) – Dimension (1200 x 40 x 60) ft

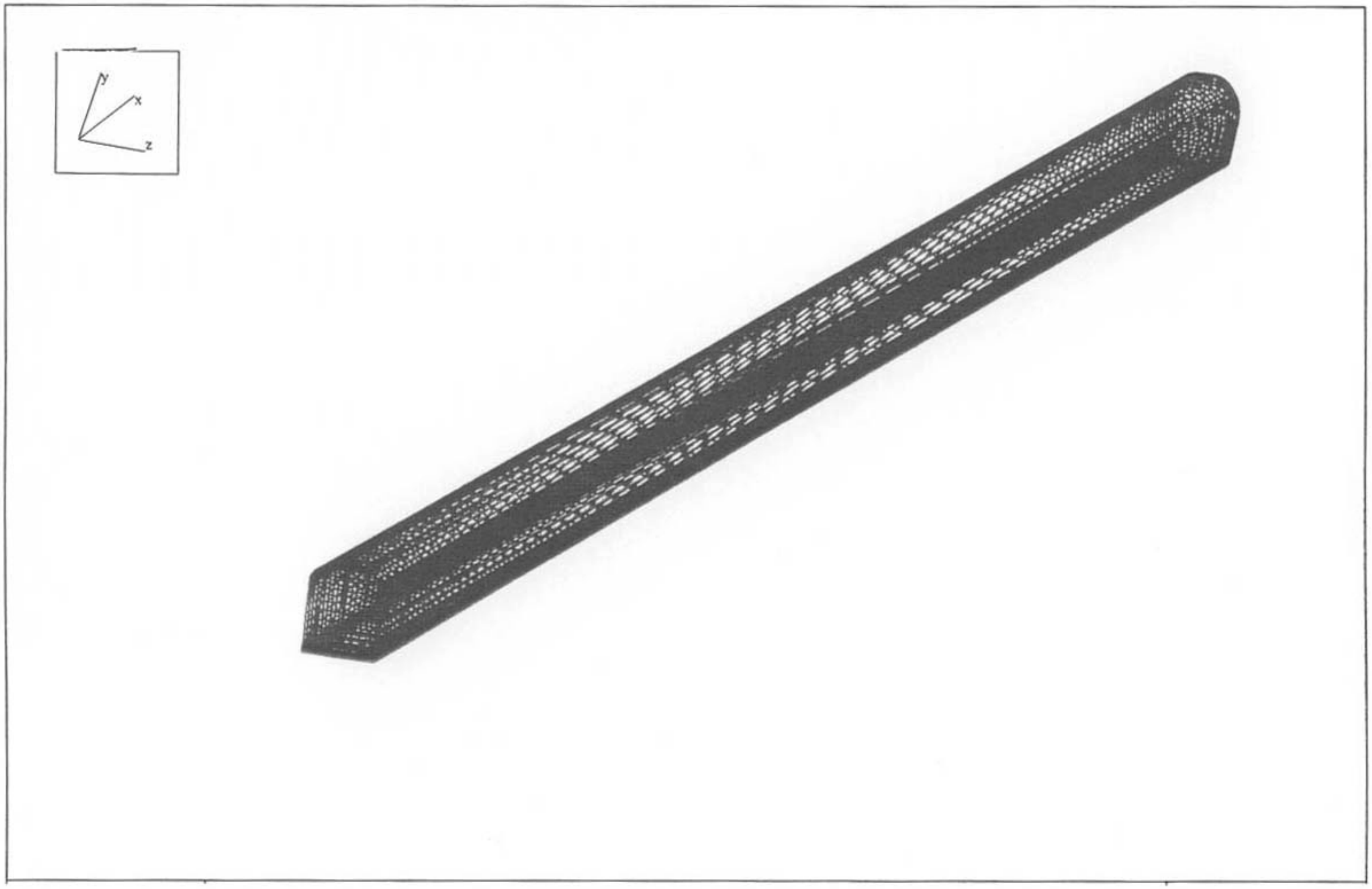

Figure 3-20. CFD Model – Amfleet Trainset Computational Grid - Grid (160 x 38 x 53)

3.6 Comparison of Acela Model with Amfleet Model Results

Comparison of Figures 3-21 for the Amfleet with equivalent Figure 3-5 for the Acela trainset for the low-level platform condition indicates the following observations regarding the CFD results:

- The bow wave for the Amfleet trainset is much more pronounced than the bow wave of the Acela trainset.

- The boundary layer effects for the Amfleet are much more severe, with the zone of velocities between 13 to 25 mph (nuisance/yellow zone) extending outward 7 ft to 9 ft from the side of the train, compared to the Acela, where the boundary layer effects only extend out to approximately 2 ft, at a height of 2.5 ft above the platform/rail. Similar conclusions can be arrived at when comparing conditions at a height of 5 ft.

- The wake effects of the Amfleet have higher intensity over a larger area directly behind the train. However, the wake effects behind the Acela trainset appear to offset the benefits of the Acela trainset streamlining, by spreading out the airflow effects into a fishtail pattern behind the cars. For a height above platform of 2.5 ft, the nuisance (yellow) zone thus extends outward from the side of the train for a width of 2 ft directly behind the Acela trainset to 10 ft at a distance of 500 ft behind the train. By comparison, the Amfleet results indicate a width of the nuisance zone that is more uniform and is about 5 to 6 feet.

Other conclusions from comparing the results of the Amfleet and the Acela can be seen in the fluctuating components, Figure 3-22 for the Amfleet trainset versus Figure 3-6 for the Acela trainset.

- The Amfleet results (Figure 3-22) show larger magnitudes over a significantly larger area around the train, indicating much more turbulence in the flow field for the Amfleet than for the Acela trainset (Figure 3-6).

- In the airflow field behind the trains, the zone of fluctuations between 5 mph and 10 mph extends out to a width of about 10 ft for both the Acela and the Amfleet trainsets.

In order to compare the total effects, the values of the mean components of the induced airflow were added to the turbulent fluctuations for the Amfleet trainset (results shown in Figure 3-23), and the Acela trainset (results shown in Figures 3-17 and 3-18). The results indicate that the Acela trainset traveling at 150 mph produces airflow effects and impacts that are less than or no worse than the Amfleet (at 125 mph), within most of the train time-distance domain. The only instances where the impacts of the Acela trainset are greater is for the wake, starting immediately after passage of the train to about 100 ft behind the train at a “difficulty in walking” (orange) level for less that 1.0 second; and then at about 300 ft behind the back of the train at a “nuisance” (yellow) level, lasting for no more than 1.5 seconds.

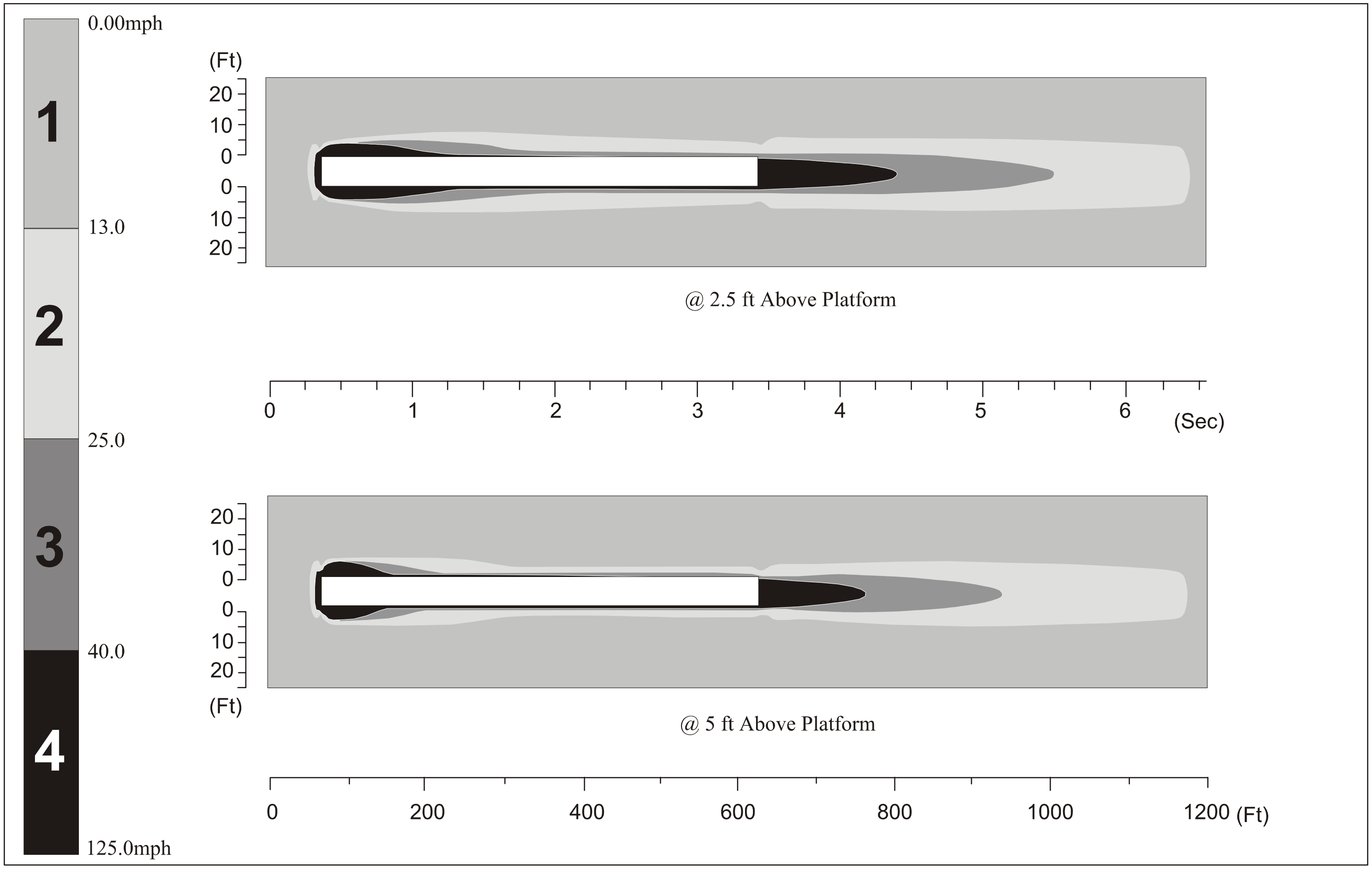

[Note: Axes coordinate orientation - x is the longitudinal direction ; y is the vertical direction; z is the transverse direction]

Figure 3-21. CFR Results – Low-Level Platform – Horizontal Mean Induced Airflow Velocity – Amfleet Trainset Speed = 125 mph

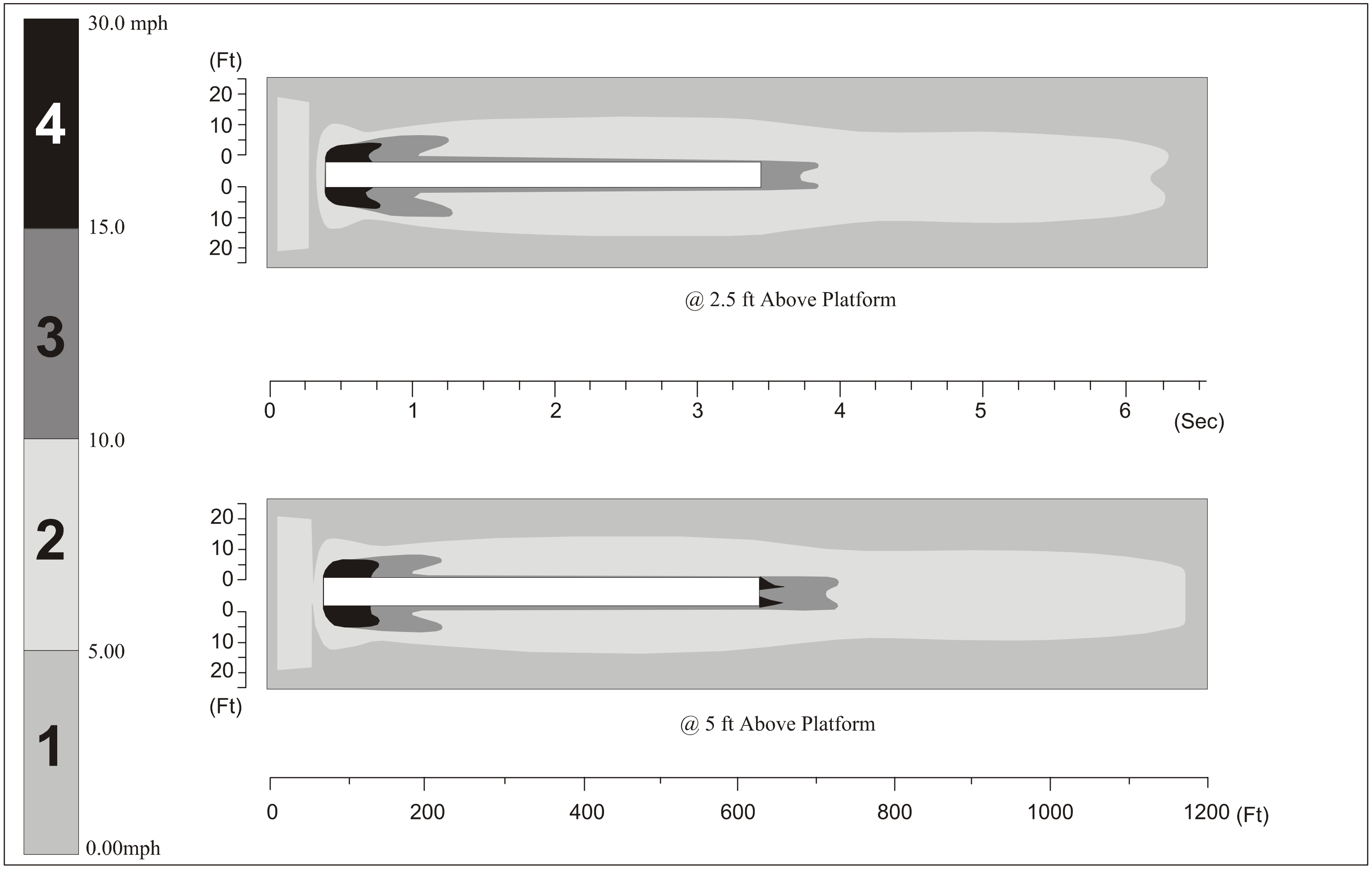

[Note: Axes coordinate orientation - x is the longitudinal direction ; y is the vertical direction; z is the transverse direction]

Figure 3-22. CFR Results – Low-Level Platform – Fluctuating Component of the Horizontal Velocity – Amfleet Trainset Speed = 125 mph

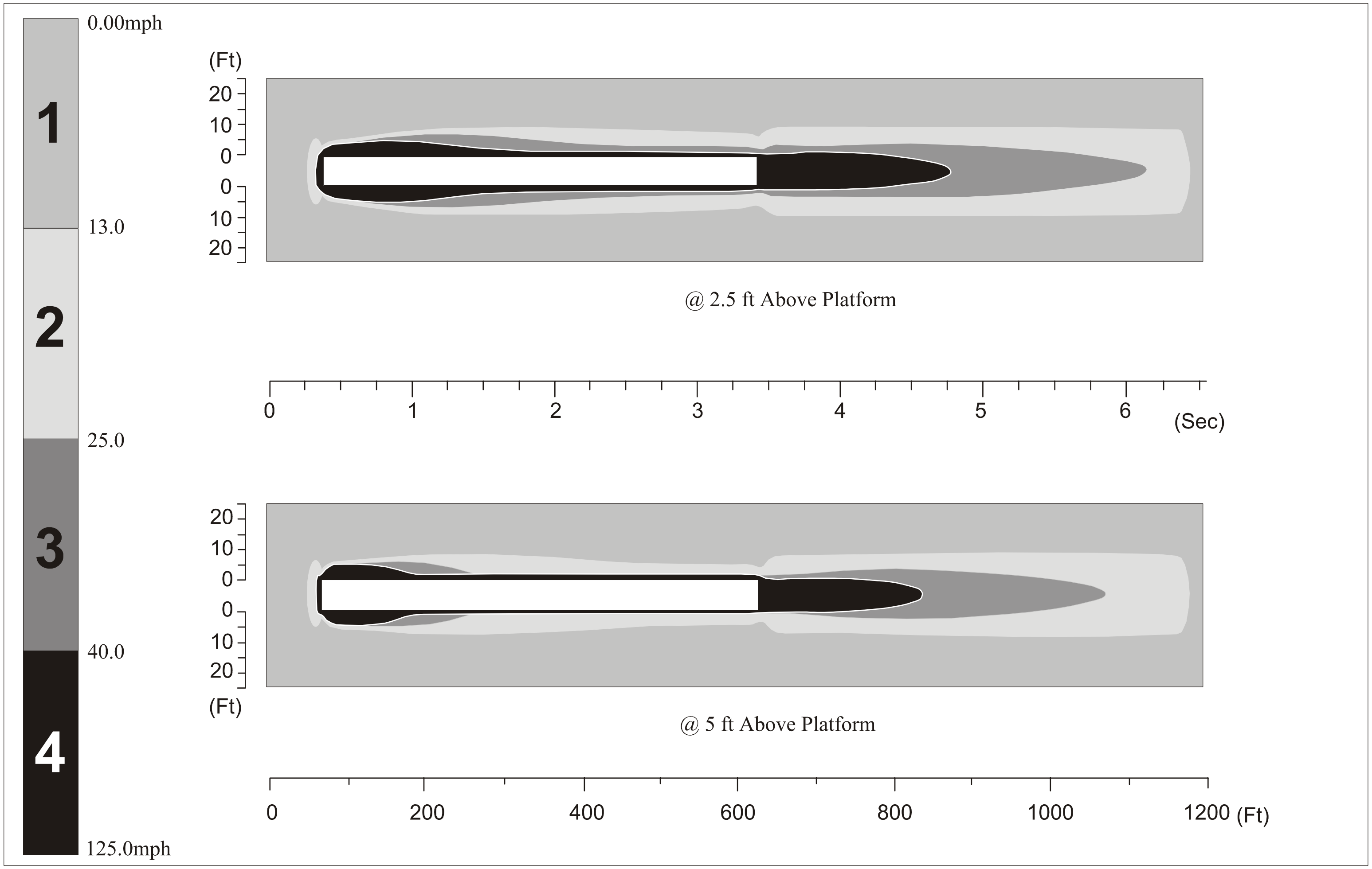

[Note: Axes coordinate orientation - x is the longitudinal direction ; y is the vertical direction; z is the transverse direction]

Figure 3-23. CFR Results – Low-Level Platform – Horizontal Induced Airflow Velocity – Mean Plus Fluctuating Component - Amfleet Trainset Speed = 125 mph

A tabular summary of the airflow effects, which represent the “worst-case” results of the preceding Acela and Amfleet CFD analyses, have been summarized in Tables 3-1 and 3-2 below. “Worst case” is defined as the maximum induced airflows (mean plus maximum fluctuating velocities) at 2.5 feet above a low-level platform, with the train on the track next to the platform passing at 150 mph (Acela) or 125 mph (Amfleet). As mentioned previously, the results at 2.5 ft above the platform are relevant to potential effects that may be felt by small children or objects at or near the platform level. The corresponding Beaufort Scale numbers are also included in the Tables. The data in the Tables should be compared with the British Rail safety parameter of 25 mph maximum induced air velocity exposure for members of the public. It should also be compared with Lee’s (1999) estimate of the distance of 6.6 feet from the side of a passing 150 mph train, where there may be a safety issue. As stated previously, the CFD results are consistent with Lee’s (1999) estimate and there are values for both the Acela trainsets and the Amfleet which exceed the British Rail exposure limit, especially at the closer distances from the side of the train. The values identified by asterisks in Table 3-1 indicate the conditions where the Acela trainset airflow velocities exceed the Amfleet trainset airflow velocities. Note that this occurs for only three of the tabulated values, i.e. in the wake at distances of 3 ft, 6 ft, and 12 ft from the side of the train. In all other instances, the “worst-case” Amfleet velocities are greater than or equal to the Acela results.

Table 3-1. Summary of Worst-Case Conditions at 2.5 Feet Above Platform, Acela Trainset Passing a Low-Level Platform on the Near Track at 150 mph

Induced Air Flow Element	Maximum Air Velocity (in mph) at the Distances Shown from the Side of the Train					Beaufort Scale Numbers for the Maximum Air Velocities at the Distances Shown From Side of Train			
	3 ft	6 ft	9 ft	12 ft		3 ft	6 ft	9 ft	12 ft
Bow Wave	13-25	<13	<13	<13		4-6	3	3	3
Boundary Layer	13-25	<13	<13	<13		4-6	3	3	3
Wake	>40*	25-40*	13-25	13-25*		>8*	6-8*	4-6	4-6*

* Note: Asterisk indicates the condition where the Acela trainset airflow velocities exceed the Amfleet airflow velocities.

Table 3-2. Summary of Worst-Case Conditions at 2.5 Feet Above Platform, Amfleet Trainset Passing a Low-Level Platform on the Near Track at 125 mph

Induced Air Flow Element	Maximum Air Velocity (in mph) at the Distances Shown from the Side of the Train					Beaufort Scale Numbers for the Maximum Air Velocities at the Distances Shown From Side of Train			
	3 ft	6 ft	9 ft	12 ft		3 ft	6 ft	9 ft	12 ft
Bow Wave	13-25	13-25	<13	<13		4-6	4-6	3	3
Boundary Layer	>40	25-40	13-25	<13		>8	6-8	4-6	3
Wake	25-40	13-25	13-25	<13		6-8	4-6	4-6	3

In summary, one of the most significant results of the CFD calculations is that the new high-speed Acela trainset, running at 150 mph past a station, is calculated to have generally less intense to somewhat more intense effects and impacts than an existing Amfleet trainset running past a station at 125 mph. This comparison is specifically of the computational fluid dynamics (CFD) results for trains passing a station with a low-level platform, which represents the most severe condition in terms of aerodynamic effects. The reason why the effects are not greater can be partially attributed to the fact that the Acela trainset is much better aerodynamically streamlined than the Amfleet trainset, and thus would mitigate the otherwise expected disruption and turbulence of the air surrounding the train as it passes.

3.7 Comparison with Previous Results and Accuracy of the CFD Analyses

Figure 3-24 presents a comparison of the CFD results with previous theoretical results by Hammitt (1973), as reported in Lee (1999). CFD results are shown for the Acela and Amfleet trainsets at or near the end of the cars at vertical distances above platform level of y = 2.5 ft and y = 5.0 ft. Both sets of CFD results are for the low-level platform condition. This figure indicates that the trends in the CFD results are in general agreement with previously derived theoretical trends reported by Hammitt (1973). The theoretical results from Hammitt (1973) are based on simplifying assumptions that convert a complex 3-dimensional problem into a simplified model for which a purely mathematical solution could be derived. Thus while the trends are comparable, it is not surprising that the numerical values do not compare as well. This figure also provides an additional comparison of the CFD results of the Acela and Amfleet analyses, graphically indicating a faster decay of airflow effects as a function of distance from the side of the passing train for the Acela trainset.

Figure 3-25 provides an additional comparison of the CFD results with experimental data from Neppert and Sanderson (1977), also as reported in Lee (1999). Figure 3-25 presents the theoretical results for Hammitt (1973) and only a selection of the previous experimental data to avoid the clutter of data in order to enhance the comparisons. The CFD results are clearly within the order of magnitude of previous measurements. Note that the Acela trainset results are consistent with (for the relevant distance from the side of the moving train), though somewhat lower than the gray band marked TGV 001, which represents measurement results from the French high-speed rail system.

The comparisons in Figures 3-24 and 3-25 provide a confirmation that the results of the CFD models are reasonable relative to results previously reported in the literature, and thus provide a degree of confidence regarding the accuracy of the CFD technique and models. Adding to the confidence in the results, it should be noted that there may be assumptions that limit the absolute predictive accuracy of the CFD models. However, the comparative accuracy of the CFD models has more validity than the absolute accuracy, e.g., comparison of the relative wind velocities due to different cars are more valid than absolute values of the calculated velocities themselves. Thus the models provide a relatively high level of confidence for comparing the Acela trainset impacts to the Amfleet trainset impacts.

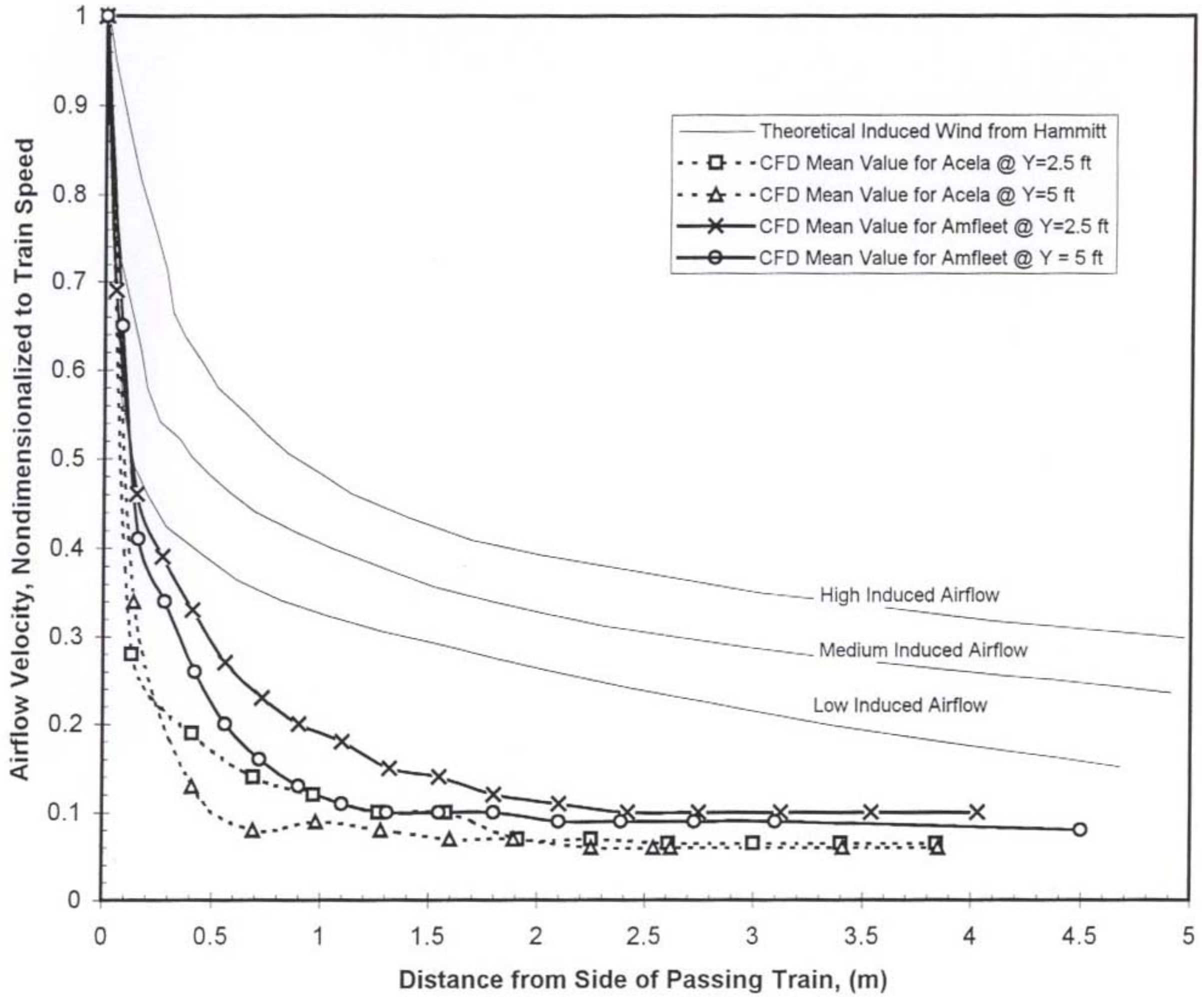

Figure 3-24. Results from CFD Model versus Theoretical Results from Hammitt (1973) for Induced Airflow Velocity from a Passing Train, Excerpted from Lee (1999)

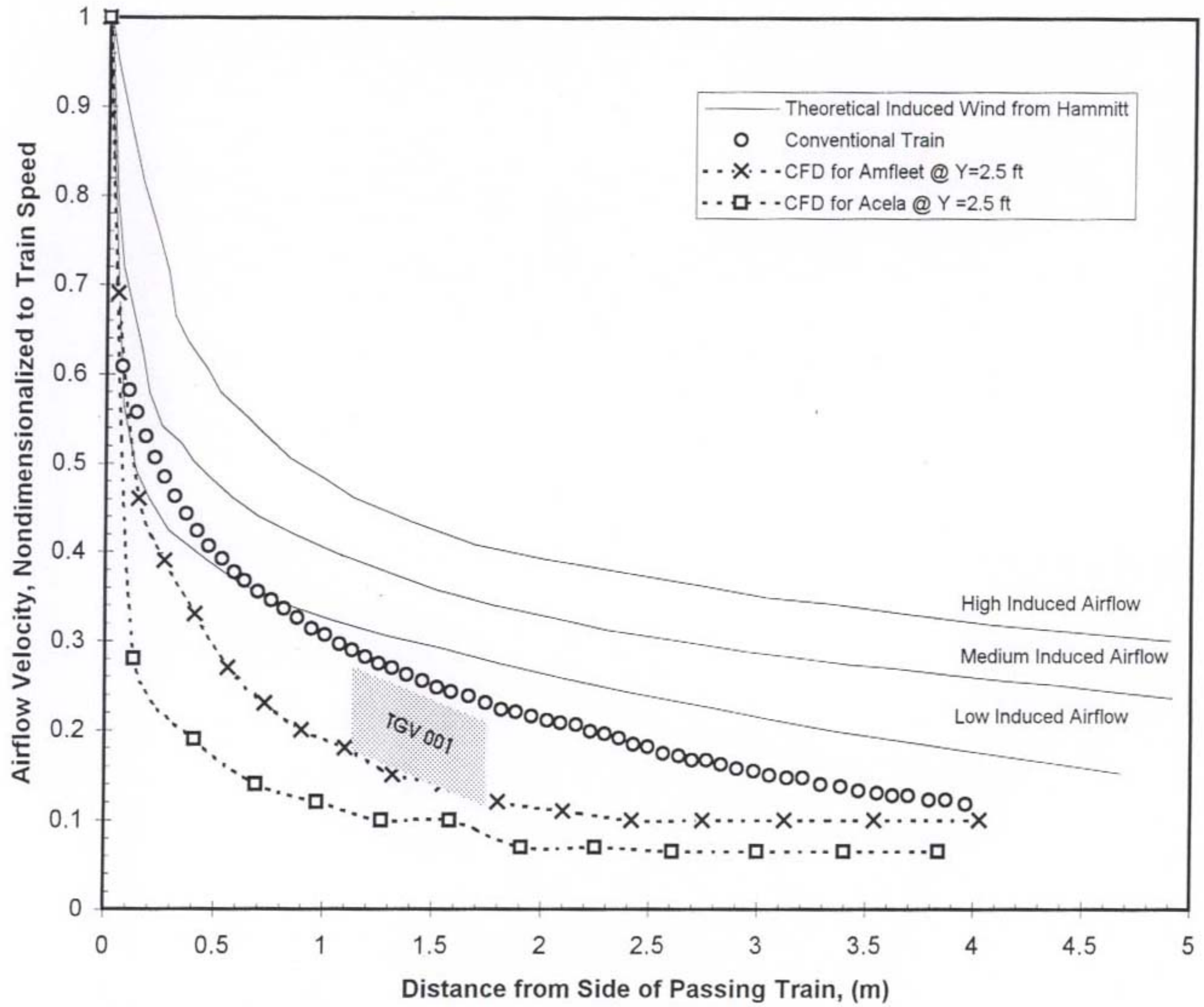

Figure 3-25. Comparison of Theoretical versus Previously Measured Results Reported by Neppert and Sanderson (1977), Excerpted From Lee (1999)

It should also be noted that the comparisons shown in Figures 3-24 and 3-25 do not reflect the most severe conditions and impacts of airflows induced by passing trains. This is because the results shown represent for a line of values along a transverse axis at or near the tail of the train. The maximum effects are expected to occur in the wake after the passage of the train, but analytical solutions needed for comparison at these locations have not been previously derived.

4. FIELD MEASUREMENTS

4.1. Description of Field Measurement Methodology

Airflow velocities induced by the passage of the existing Amfleet cars were measured at three sites at two stations on the Northeast Corridor. The purpose of obtaining these measurements was to provide a comparison with the air velocities predicted by the CFD computer program for Amfleet trains, and thus to provide additional verification that the model and its implementation were appropriate for the task at hand. Details of the measurements are presented in Appendix J.

All the measurements were done using an Alnor Velometer (Pitot tube device) having a maximum range of 2,500 feet per minute [~28 miles per hour (mph)] and a response time of about one second. The Alnor Velometer was mounted at an elevation of about 5.5 ft above platform level. In the case of a low-level platform, the platform level can be considered to be equivalent to the top of rail. The Velometer Pitot tube was positioned parallel to the track with its opening oriented to face the oncoming train. The Pitot tube was mounted to a test stand to avoid movement during train passage. Depending on the site, the Pitot tube opening was from about 5.5 ft to about 18 ft from the side of the train

4.2 Results of Measurements

The measurements were done at three sites on the NEC, as follows:

Site 1: **Princeton Junction, NJ**, measuring device straddling the west rail of Track 4 about 1000 ft north of the railroad station, on 1 September 1998. The purpose of measurements at this location was to obtain a reading for an equivalent low-level platform situation to compare to CFD results.

Site 2: **Princeton Junction, NJ**, Railroad Station northbound high-level platform, on 8 September 1998. The purpose of measurements at this location was to compare with the high-level platform CFD results.

Site 3: **Newark, DE,** Railroad Station southbound platform, on 17 September 1998. This station has a low-level platform. The purpose of measurements at this station was to obtain data for an unusual station geometry where a "back wall" was conjectured to influence the low-level platform air velocities. The "back wall" was about 5 ft high, about 77 ft long, and about 8.5 ft from the side of the train. The measuring device was positioned at the south, or exiting, end of the wall.

In all cases, the maximum measurement of air velocity occurred in the wake after the train had passed. Though there was a bow wave felt in some instances, velocities of this bow wave did not register on the Pitot tube instrument, possibly due to the very short duration of the bow wave or possibly the orientation of the Pitot tube relative to the direction of the bow wave air velocity or pressure. A summary of the results of the measurements at the three sites are presented in Table 4-1 below.

Table 4-1. Summary of Velocity Measurements

Site	High or Low-Level Platform	Approximate Distance From the Side of the Train (ft)	Train Speed (mph)	Maximum Air Velocity (mph)	Comments	Air Velocity Extrapolated to 125 mph (mph)	Air Velocity Extrapolated to 150 mph (mph)
1	Low	9.0	125	17		17	21
1	Low	4.5	125	~17	Observation only	~17	21
2	High	5.5	110	10		12	14
2	High	18.0	125	8		8	10
3	Low	5.5	~125	28	At south end of back wall 8.5 ft from train	28	34
3	Low	17.0	110	2		3	3

At Sites 1 and 2 (Princeton Junction, NJ), the speed of the train was obtained by contacting Amtrak Train Control and through communication with the drivers of the trains, who were notified prior to passage regarding the need and reasons for a speedometer reading. At Site 3 (Newark, DE), the measurements were obtained by Amtrak personnel using a radar speed gun.

Extrapolations of measurements to reflect higher train speeds were based on multiplying the measured airflow velocity times the ratio of the projected train speed to the actual train speed. For the extrapolation to 150 mph, this represents an estimate of the maximum velocity that might be caused by the Acela trainset. This is believed to be potentially an upper bound value, since the Amfleet is not as well streamlined as the Acela trainset.

Note that for Site 3, the test results showed that for a low-level platform with a back wall, the air velocities at 5.5 ft could cause inconvenience in walking. For a low-level platform without a back wall (Site 1), the train wake air velocities at a distance of 4.5 ft from the side of the train or greater could be annoying, but only a risk to safety if loose materials were stirred up by the passing train. Thus it is conjectured that the effect of a back wall close to a low-level platform could be important, and may also be important for high-level platforms as well. Additional field measurements and analyses would be required to confirm this.

4.3 Comparison of Measurements with Amfleet CFD Results

Figures 4-1 and 4-2 provide a comparison of the field measurements with the CFD results, plotting the airflow velocity versus distance behind the end of the train. (See Appendix J for details regarding the data.) Note that the distance scale on the horizontal axis can be translated to an equivalent time scale, and thus this plot is similar to a time history of air velocities at a stationary point. The display of these results reflects the fact that there were no significant readings measured by the Pitot tube instrument as the train approached and was immediately adjacent to the platform. Figure 4-1 shows the results of measurements at Site 1 (Princeton Junction, NJ – equivalent low-level platform condition) at a distance of 9 ft from the side of the train. Figure 4-2 shows the results of measurements at Site 3 (Newark, DE – low-level platform) at a distance of 5 ft from the side of the train. The CFD results, both from the same model shown in Figures 3-19 and 3-20, are also plotted. There are some minor inconsistencies among the models and the measurements that should be noted:

- The CFD model is for a theoretical train speed of 125 mph. The actual train speeds may differ somewhat from this theoretical velocity.

- The Newark, DE platform includes a back wall, which is not incorporated as part of the CFD models.

- The measurement instruments may have a response time that may not have fully captured all of the fluctuations of the induced airflow as calculated by the CFD models.

However, despite the minor inconsistencies above, the field data compare fairly well with the CFD results, and are either within the range of the mean velocity plus or minus the fluctuating components, or are slightly higher than the upper range.

Figure 4-3 presents a comparison between measurements at Site 2, representing a high-level platform, and Site 3, representing a low-level platform. Although there are also some minor inconsistencies between the measurements, the comparison clearly shows that the airflow velocities at a low-level platform are expected to be more severe. Although these measurements are for the Amfleet trainset passage, this confirms the CFD results for the Acela trainset that examined high-level versus low-level platform configurations.

It should be noted that there are error bars in Figures 4-1 through 4-3, which indicate the range of distances behind the train for the readings to be correlated with the CFD results and for other comparisons. For Figures 4-2 and 4-3, the range of distances was estimated based on the timing of the peak readings occurring about 2 seconds after passage of the end of the train (see Appendix J). It was estimated that the actual timing of the readings could have been between 1 to 2 seconds. These times were then multiplied with the corresponding train speed to estimate the distance range shown in the figures.

The fact that the maximum measurements were recorded for the wake effects reflect, to a large extent, the placement of the instruments relative to the side of the passing train, and also possibly

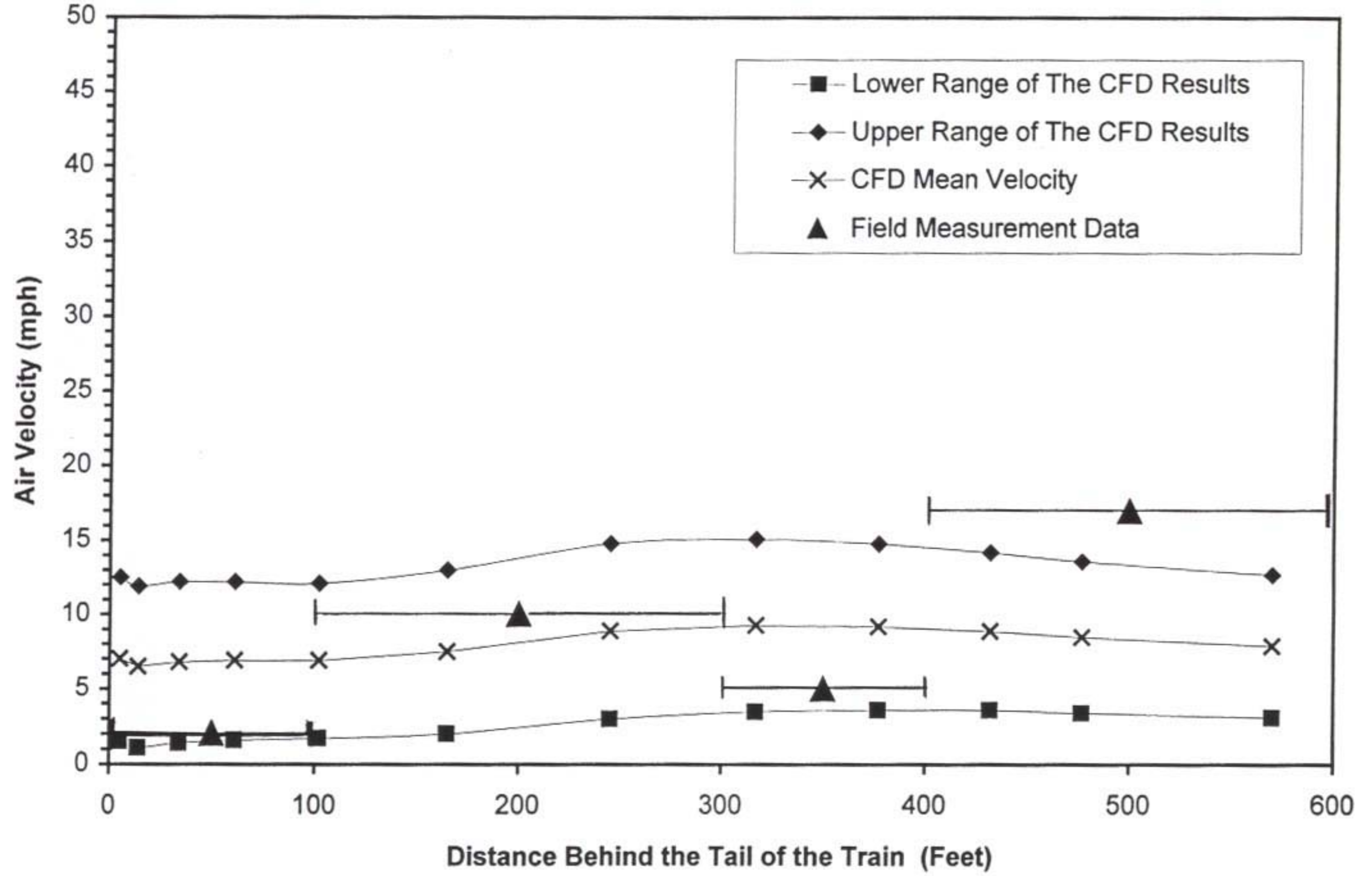

Figure 4-1. Comparison of CFD Analysis with Measured Airflow Velocities at Princeton Junction, NJ, at 9 ft from Side of Train – 5 ft Above Equivalent Low-Level Platform Condition (Rail/Ground) – CFD Train Speed = 125 mph, Field Train Speed = 125 +/- mph.

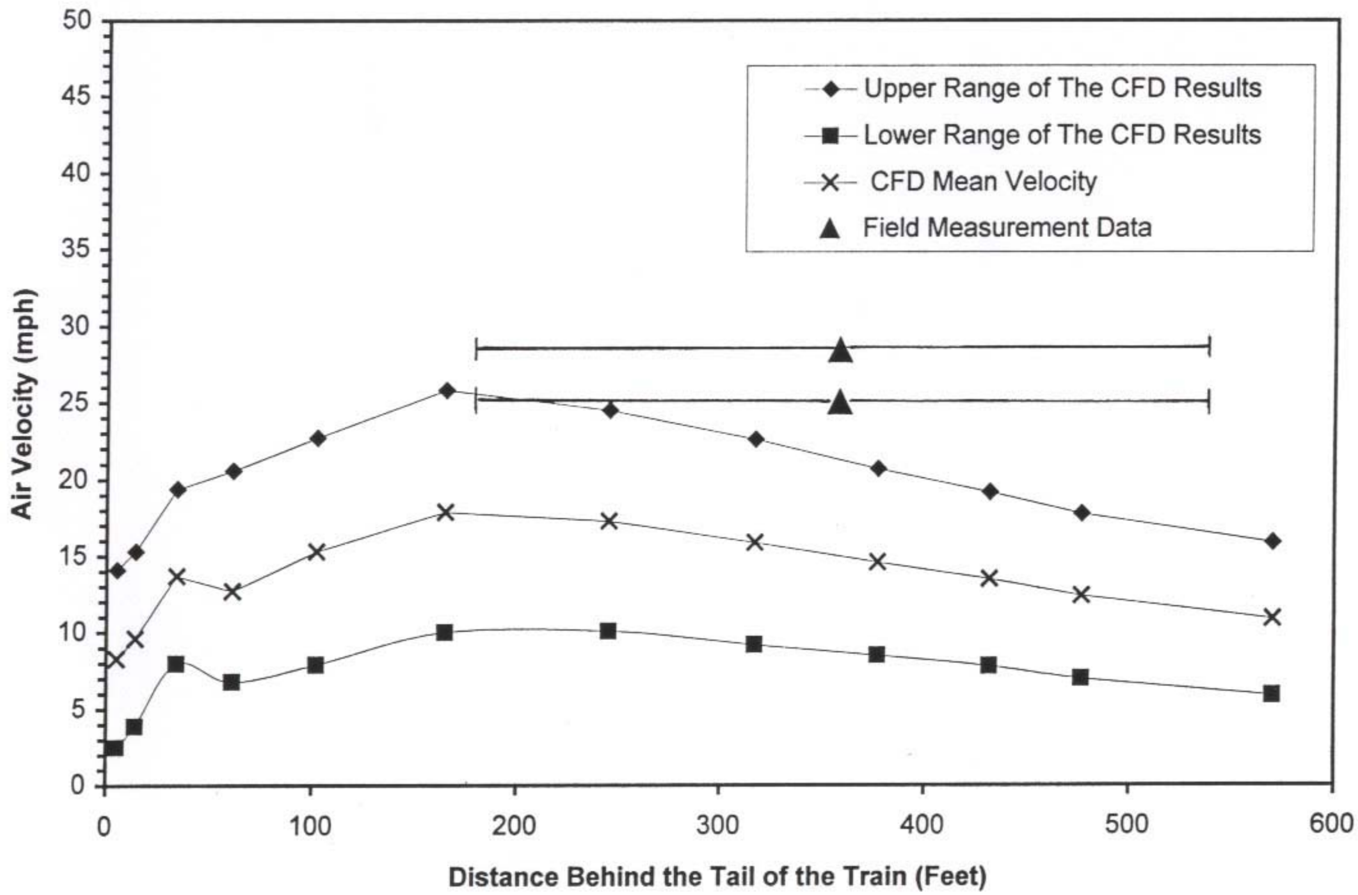

Figure 4-2. Comparison of CFD Analysis with Measured Airflow Velocities at Newark, DE – 5.5 ft from Side of Train – 5.5 ft Above Low-Level Platform – CFD Train Speed = 125 mph, Field Train Speed = 122 +/- mph

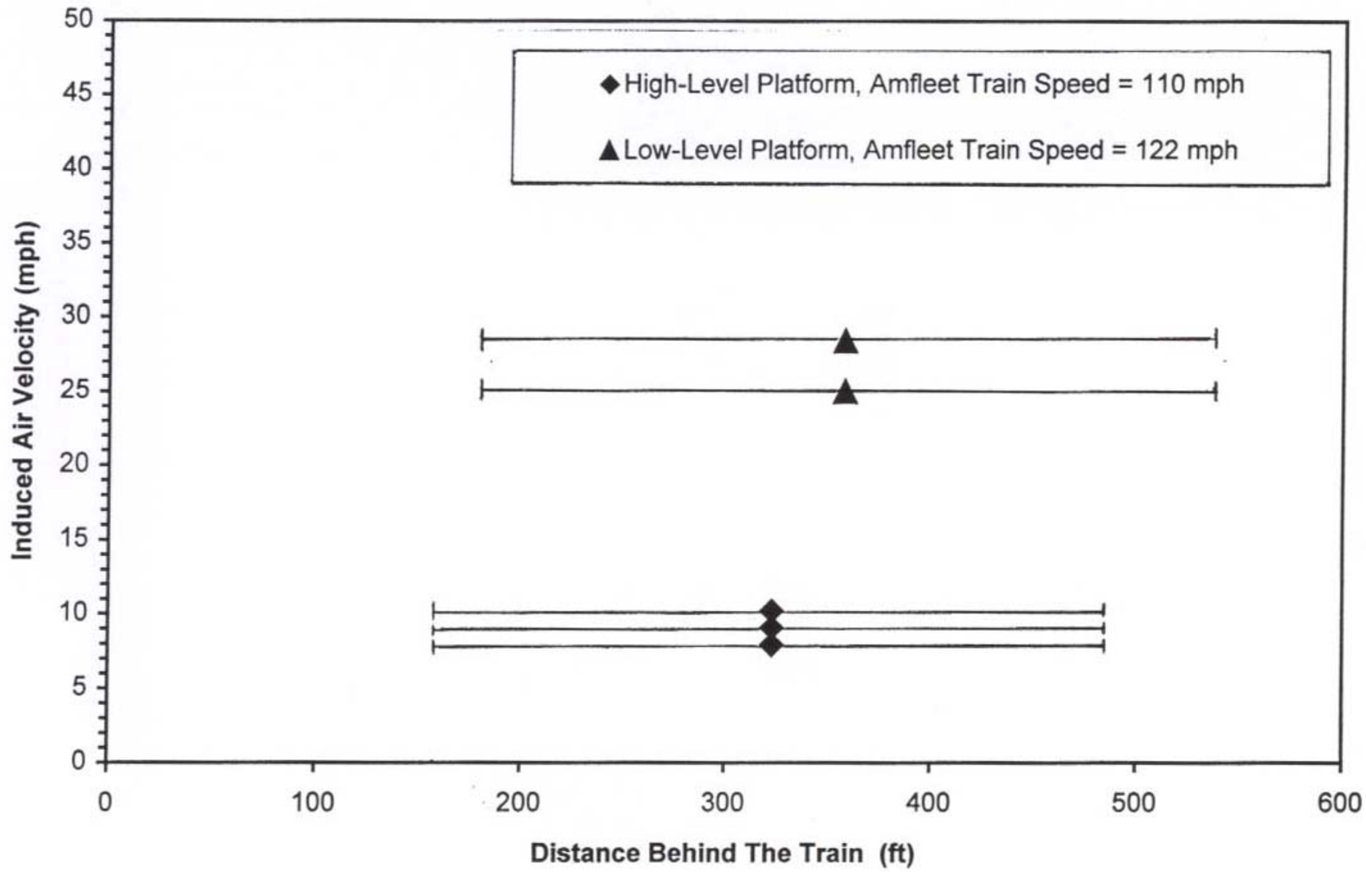

Figure 4-3. Comparison of Measured Air Velocities for Low versus High-Level Platform at 9 ft from Side of Train – 5.5 ft Above Platform Level – Low-Level Platform at Newark, DE and High-Level Platform at Princeton, Junction, NJ

the orientation of the Pitot tube opening. The absence of readings as the train approached and was immediately adjacent to the platform, however, tend to support the CFD results as follows:

- For the front of the train, the CFD results show a "bow wave" extending slightly less than 5 ft out from the side of the train. However, the change from a high air velocity to a low air velocity regime in the bow wave is predicted to occur over a very short distance (less than a foot). The field measurements support this, because if the bow wave were of a longer duration, this effect would have registered on the instrument.

- Along the train, the CFD results show a very thin boundary layer, which defines the region of high velocity flow immediately adjacent to the train. The change from a high velocity airflow (inside the boundary layer) to a low velocity airflow (outside the boundary layer) is predicted to occur over a very short distance (less than a foot). The field measurements support this, because there was no registration of significant velocities when the Pitot tube was positioned at 4 ft to 5 ft from the side of the train (outside the calculated limit of the boundary layer), and as the train was running along the platform.

An observation during the field measurements indicates that there might be an important discrepancy between the perceived air velocities and those predicted by the CFD model. There were no measurements, but felt-air velocities indicated that the lateral extent of the airflow effects seemed to be more widespread than is shown for the Amfleet CFD model in Figure 3-19. Correspondingly, based on engineering judgment, one would expect a greater fanning out of the wake behind the Amfleet trainset, similar to that which was calculated for the Acela trainset. This discrepancy might be attributed to the minimal data available to model the Amfleet trainset versus the much more detailed information available for the Acela trainset. Some improvement in the prediction of the wake velocities might have been obtained by more detailed modeling of the rear of the train. Additional information on aerodynamic drag characteristics in particular would have been desirable to provide more confidence and accuracy for the Amfleet model.

4.4 Conclusions from Field Measurement Results

In general, the field measurements supported the predictions of the CFD model for the Amfleet trainset and provided verification of the modeling technique. Considering the assumptions and level of information available for modeling, the results of the field measurements agreed fairly well. The data obtained also indicate that the current air velocities experienced on low-level platforms probably routinely exceed the British Rail threshold level of 25 mph for members of the public standing on platforms. Based on the measurements, it is also conjectured that the effect of back walls close to low-level platforms could be important, and may amplify train-induced air velocities. This effect may also be important for high-level platforms as well.

5. STATION SURVEYS

5.1 General Methodology

The initial approach to the visual field surveys of passenger stations (station surveys) was to determine their number and location. Public timetables were obtained for Amtrak and the commuter rail services in the Northeast Corridor, and track charts for Amtrak and Metro North Railroad (MNR) were consulted. A list of stations was compiled, and arranged in station order from Washington, DC, Union Station to South Station, Boston. The list was supplemented with stations that were under construction or planned, as information about them was obtained from a growing list of personal contacts at the various passenger rail operating and/or oversight agencies in the Corridor.

Amtrak and MNR provided current Employee Timetable and Special Instructions books. From these references, current maximum authorized speeds (MAS) past the stations in the Corridor were obtained. Amtrak provided the proposed MAS for its new Acela trainsets past each of the stations in the Corridor, and also identified the stations at which the Acela trainsets will stop. Additional information about the stations in the Corridor was obtained from the commuter rail operating agencies, and/or state departments of transportation charged with commuter rail oversight. State agencies responsible for cataloging and preserving historic sites provided information regarding the status of stations listed in the National Register of Historic Places.

A checklist for recording relevant information was prepared for use in the field inspections. As much information as possible was recorded in advance on the checklist for each station, from data or documents previously obtained. This was done in order to try and reduce the time that would actually have to be spent at each station. Two survey team members worked together in order to efficiently collect the multiplicity of data required. Even though the team members did not enter the track area, the presence of two persons helped to ensure safety while working on the station platforms.

Observations included the physical presence and condition of platforms, structures, and appurtenances. Measurements of platform length and width were taken, along with the length and width of any platform-edge safety zone. The immediate surroundings of the stations were noted. Also noted were the presence and condition of any safety-related signage or message boards, and whether a public address system was present and/or being used. Train movements were observed and experienced, from the aerodynamic perspective. The actions of passengers and others were observed as they boarded and alighted from trains, as trains approached and passed, and between trains. It should be noted that no two of the stations inspected were *exactly* alike. Indeed, it was rare when both platforms at a single station were found to be of identical dimensions and directly facing each other. Nearly every station inspected was asymmetrical and presented the equivalent of two different platform conditions per station.

A determination was made that the most cost-effective approach to the field surveys was to begin initially at Princeton Junction Station and work southward toward Philadelphia. After the surveys to the south of Princeton Junction, the team then began surveys to the north, from Jersey Avenue, in New Brunswick, NJ, to Linden, NJ. The team then progressed to Newark, DE, and worked northward to Glenolden, PA. The surveys in New England began in Boston, at the Ruggles Station. The team surveyed each of the stations in Massachusetts, Rhode Island, and Connecticut that will experience the highest speeds of passing Acela trainsets. None of the stations in Connecticut south of New Haven or in New York State, except New Rochelle, were surveyed. This was due to time constraints and consideration of the fact that these stations, for the most part, were going to experience very minimal, if any, increases in the speed of passing trains. These stations also had the lowest current MAS's in the Northeast Corridor. The last segment of the field surveys covered stations in Maryland, beginning at Seabrook and working northward to the Martin Airport (Middle River) Station. Though some of the stations inspected will experience little to no increase in the speed of passing non-express-stop trains, the current MAS's are some of the highest in the Corridor. Other stations in Maryland where Acela trainsets will stop, or where passing speeds will be low, were not surveyed.

In all, the visual field surveys were performed at 57 of the 101 existing stations between Washington, DC and Boston on various dates between July 7 and 31, 1998. Approximately 45 minutes to one hour were spent at each station, recording observations and conditions that have a bearing on the objectives of this study. The stations selected included all "non-express-stop" stations at which current MAS is greater than 100 mph, and that will see the greatest increase in the MAS upon the advent of Amtrak trainset service. None of the major stations at which all Acela trainsets trains will stop and through which they will move at slow speeds was inspected. From these inspections, relevant findings, examples of potential hazards, and inputs to recommendations were developed for this report.

5.2 Data Provided by Amtrak and Other Agencies

5.2.1 List of Stations on the Northeast Corridor and Other Information

Relevant information was obtained concerning the 101 passenger stations on the Northeast Corridor between Washington and Boston. Appendix F presents this data in tabular form. Such information as the passenger railroads providing service in the Corridor, the ownership of the right-of-way and responsibility for dispatching of trains, the specific stations by name and location, the highest maximum authorized speed past each station, and the types of passenger trains that stop at each station is presented.

5.2.2 Northeast Corridor Station Characteristics, by State

Additional information about the passenger stations on the Northeast Corridor is presented in Appendix G. Arranged by state, such information as the number of stations within each jurisdiction, who maintains them, whether they have safety systems installed and their accessibility to the disabled, their (National or State) Historical Landmark (Register of Historic Places) status, and other data are provided.

5.3 General Station Characteristics from Visual Field Surveys

For the sake of simplicity in this report, trains are considered to operate *northbound* toward Boston and *southbound* toward Washington, regardless of where they are on the Northeast Corridor. Also, main tracks are numbered from east to west. For example, Track No. 1 would be the easternmost and a northbound main track, and Track No. 4, the westernmost and a southbound. Where additional tracks are referred to, they are given the designation found in the Amtrak Employee Timetable and Special Instructions.

Summary data specific to each of the 57 stations subjected to field investigations are presented in Appendix H. These data include the number of tracks; the platform width; platform type, height, and extensions; whether there is a fence in the tracks separating the platforms (mid-track fence); and the present and planned speeds on the tracks closest to the platforms.

The physical conditions considered most germane to this study were platform type (side or island), platform height (high- or low-level), platform dimensions, the presence and dimensions of any platform-edge safety zones, the distance of the track used by non-express-stop trains from the platform, the presence and condition of platform passenger shelters, the presence and legibility of safety signs, the presence and type of any "safety systems", and the presence and type of any platform appurtenances (such as benches, trash receptacles, billboards, newspaper vending machines, etc.), or the existence of a back wall near the platform. These were considered germane because they are the elements that would be influenced by, and/or would create an influence upon, the aerodynamic effects of non-stop Acela trainsets. For example, the width of platforms and safety zones would determine the distance away from the side of passing trainsets that people could be standing and objects placed. Signage and warning systems likewise could help to determine how far away from a passing trainset people would stand.

Physical conditions varied widely between and among the stations that were visually surveyed (see Appendices H and I). The general findings were:

- The majority of stations had platforms on one or both sides of the tracks (side platforms). Where the platform was only on one side and there was more than one track, the platform had a limited-width ground level extension (frequently made of wood planking) that crossed the tracks to the other side or nestled between at least the first two tracks. These extensions cannot be considered true platforms, as they are not wide enough to permit persons safely to stand on them as trains pass. Even when there were platforms on both sides of the tracks and/or there were three or more tracks, platform extensions often exist and are used by passengers. See Figure 5-1 showing platform extensions at Bridesburg Station, Philadelphia, PA.

Figure 5-1. Photograph of Bridesburg Station, Philadelphia, PA, Showing Platform Extension Across Tracks; Also Showing Unsecured Wire Mesh Trash Basket

Figure 5-2. Photograph of New Brunswick Station, New Brunswick, NJ, Showing Crowded Northbound (High-Level) Platform at 8:10 AM, with People Standing in the Platform-edge Safety Zone.

- All station platforms visited in New Jersey and New York had high-level platforms. All station platforms visited in Delaware, Pennsylvania, Connecticut, and Rhode Island were low-level. Some of the platforms in Maryland and Massachusetts were high-level, and some low. In most cases where there were high-level platforms, short low-level platforms, sometimes with platform extensions, were provided off one or both ends of the high-level portions.

- Platforms ranged in width from less than 6 ft to 33 ft.

- Platform-edge safety zones ranged from none, to those denoted by a single yellow stripe, to those well marked and equipped with truncated-dome strips or tiles. In width measured from edge of the platform, the zones ranged from less than 2 ft to over 4 ft. Conditions of the markings ranged from very conspicuous to very inconspicuous, due to weathering.

- In four- or more-track territory from north of Wilmington, DE, through New Jersey, non-stop trains operate at the highest speeds only on tracks not immediately adjacent to station platforms. In three-main-track territory from south of Wilmington into Maryland, southbound non-stop trains operate at the highest speeds on a track next to the platform; northbound non-stop trains are one or more tracks removed from the platform.

- Passenger shelters vary from non-existent to full station buildings. In the latter case, the roof of the building is sometimes extended to provide cover over at least a portion of the platform. All shelter-types are at least partially open toward the tracks.

- Safety signs ranged from non-existent to very pertinent. The latter cautioned persons to stand back from the edge of the platform because of non-stop high-speed trains. Overall, most safety-related signage contained admonishments about not going onto the tracks or trespassing. Condition and placement of the signage ranged from very poor to good.

- Only two types of "safety systems" were observed. One, being developed by Amtrak, consisted of a LED message board and accompanying audio message. The message board was highly visible with bright red letters, and the audio portion was audible. It was observed at the Mystic Station, Connecticut. However, it was not in service for safety messages at the time of observation. The second type of safety system was found at several stations in Massachusetts, and has been developed by the Massachusetts Bay Transportation Authority (MBTA). It consisted of highly visible flashing amber lights accompanied by a loud bell. The MBTA devices are actuated when the approaching train is a considerable distance from the station platform. They continue to function as the train passes through the station (even during a stop), and cease only after the train is an equally considerable distance beyond the platform.

- Public address (PA) systems were observed at many station locations. But nowhere were they being used for safety purposes. A barely audible bell and barely visible message board were used in tandem at some stations in New Jersey to announce the approach of a train on the adjacent track. The usage was to alert patrons that their train was approaching, not to caution them to stand back from the platform edge.

- Almost all stations had appurtenances of one type or another on the platforms. The exception was the MARC stations in Maryland, which had appurtenance-free platforms.

5.4 Site Conditions Potentially Influencing/Influenced by Aerodynamic Effects of Passing Trains

The aerodynamic effects experienced or observed at the stations that were visually surveyed have been categorized in terms of their proximity effects, i.e., those effects related to the *distance* of people or objects from passing trains. The closer persons or objects are to passing trains, the higher the potential for greater aerodynamic effects from those trains.

Some examples of the aerodynamic effects of passing trains upon the field-survey team are presented below. These experiences, and the observation of conditions as they existed at the time of the inspections, have been used to provide input into the recommendations in Section 7.

- Platform type was a factor in the magnitude of the aerodynamic effects, i.e., they were greater for low-level than for high-level platforms. This may be because one is exposed to the full aerodynamic effects of the passing vehicle and its non-aerodynamic running gear at a low-level platform. At a high-level platform, part of the aerodynamic effects may be mitigated as the lower segment of the wind field passes under the platform, or blows against the support wall under the platform overhang.

- At many of the stations inspected, a platform-edge safety zone of 24 to 30 inches in width “separates” people from passing trains. Allowing for a four- to six-inch gap between the edge of the platform and the side of a train, people standing at the inner edge of the safety zone are 28 to 36 inches from a passing train.

- The safety zone varies from a single yellow stripe running all or part of the length of a platform, to yellow tactile tile plus a yellow line, to an area painted solid yellow, to nothing at all. Often, a stenciled admonition is located in or just before the edge of the safety zone. However, especially at busy stations where the platform is fairly narrow in overall width, people are often forced to stand within the safety zone, as at New Brunswick, New Jersey (see Figure 5-2). At this station, the overall width of the pictured northbound platform is 9 feet 5 inches, and the width of the safety zone is 35 inches, from inner edge of the stripe to outer edge of the wooden bump rail. People also often stand within the safety zone at stations to peer up and down the tracks.

- A number of the stations inspected had platforms or sections of platforms that were very narrow in overall width. The entire southbound platform at the Halethorpe, Maryland, Station is only 6 ft wide (see Figure 5-3).

Figure 5-3. Photograph of Halethorpe Station, Halethorpe, MD, Showing Narrow (6 feet wide) Southbound Platform Adjacent to High-Speed Track No. 3

Figure 5-4. Photograph of Odenton Station, Odenton, MD, Showing Appurtenances Installed Well Back from Station Platform

- A number of other stations had platforms or parts of platforms that were between 6 and 7 ft in total available width. At Sharon Station in Massachusetts, a member of the survey team sat on the only bench on the southbound platform as a two-unit (F40PHs) Amtrak passenger train passed. The maximum authorized speed (MAS) here is 100 mph. The bench was 6 feet 6 inches back from the edge of the platform. The blast of air (bow wave), as the locomotives passed, was experienced to physically push the observer, who weighs approximately 165 pounds. Severe air turbulence on the platform was experienced in the train's wake. Similar experiences occurred at other stations where the available platform width was similarly small. These observations are consistent with the CFD results, which indicate a significant bow wave associated with Amfleet passage. (See Table 3-2.)

- In general, neither any significant leading-end "bow wave" nor severe wake turbulence was experienced when trains passed a platform at high speed on the second track outboard from a platform's edge. This is consistent with the Amfleet CFD results, which show that induced airflow from a Amfleet is diminished severely beyond 12 ft from the side of the train.

- Two stations that were inspected would seem to have the potential for being affected by trains passing at high speed on a second track outboard from their platforms' edge. At Ruggles Station, in Boston, the platform is in a deep cut with a structure built over part of it creating a semi-tunnel effect. The retaining wall on the east side of the cut is separated from the platform by two tracks. The northbound high-speed track is alongside of the retaining wall. Trains are currently authorized to operate at 100 mph on this track; Acela trainsets will be authorized to operate at 120 mph. The other station is Forest Hills, also in Boston. The station's platform is, in essence, in a tunnel (a deep cut with a structure built over much of it). There are three tracks between the east side of the platform and the east-side retaining wall. The two easternmost tracks will be used by the Acela trainsets. They will be authorized to operate at 125 mph, 25 mph faster than the present MAS. Trains were observed passing on these tracks with very little wake effect felt on the platform. However, it may be advisable to study the aerodynamic effects at these two stations in more detail because of their unique physical characteristics. It should be noted that the CFD models used in this study dealt only with above-ground stations.

- Another type of aerodynamic proximity effect that is also a discomfort to persons is flying objects created by the air turbulence from passing trains. This was experienced during station inspections primarily when high-speed trains passed on the track closest to the platform. The survey team members tended to close their eyes as the train passed, and so avoided anything but some easily removed dust particles, generated by the wake well behind the train. This could be a problem, however, under some circumstances. If the track had recently been disturbed, large dust clouds would be generated. At Attleboro Station in Massachusetts, grading for a new track and catenary-pole installation were in progress south of the platforms. A passing high-speed train stirred-up large dust clouds that enveloped employees in the track area. The same thing could happen to persons waiting on platforms. These observations are consistent with the CFD analysis for low-level platforms, which indicate that the Amfleet can generate velocities in the wake upwards of 40 mph. During heavy rain or snowstorms, a train passing at high speed can cause swirls of water or snow on the platform. Especially with snow, persons on the platform could be temporarily blinded. Swirling dust and snow would probably cause problems on a platform even if a train was passing on a track not right next to it. Even though, as noted above, turbulence is greatly reduced when trains pass on the second track outboard from a platform, very fine and light particles could still have an effect on persons on the platform. The potential for this type of adverse aerodynamic effect may be increased with the Acela trainset, where the wake has been calculated by the CFD model to have a larger lateral zone of influence than the Amfleet. (See Tables 3-1 and 3-2.)

- It was found during the field inspections that in almost all cases the appurtenances provided are fixed objects, or are secured to the platform's columns, railings, etc. At Torresdale Station, in Philadelphia, the panels in the windscreen in front of the northbound platform shelter rattled in their frames as a northbound Amtrak train passed on the near track at high speed. At a few other locations a similar phenomenon was noted. Where the windscreen has been properly maintained, no rattling but some flexing was noted. Buffeting from passing trains may increase the frequency of maintenance needed to keep the panels tight in their frames, and mounting bolts secure in the platform. Experience elsewhere has shown that such buffeting, even at speeds as low as 20 to 40 mph, can cause fatigue of the fastening system for wayside signs to the point at which the signs fall to the ground. Some examples of damage to signs on mid-track fences that could have been caused by the constant buffeting from passing trains were observed during the field surveys. At a number of station platforms, a wire mesh basket with a plastic liner was used for trash. In most cases, the basket was found to be chained and locked to a secure element on the platform. One case where it was not was at the Bridesburg Station in Philadelphia (see Figure 5-3). The highest-speed tracks at Bridesburg are two tracks removed from the basket, but the photograph illustrates the potential problem. Experience with this type of receptacle indicates that the plastic liner can easily be blown inside-out by high wind, with its contents scattered. A passing high-speed train presumably could cause the same reaction.

- The potential for damage to or injury from unsecured platform appurtenances does exist, especially as the speed of passing trains increases. Perhaps because of this, MARC has taken a very practical approach to platform appurtenances at its commuter rail stations in Maryland: there are none. All newspaper vending machines, telephones, trash receptacles, bicycle racks, etc., are located on the approaches to the platforms, and not on the platforms themselves (see Figure 5-4). This also provides more standing room for people well away from the platform edge.

6. SUMMARY AND CONCLUSIONS

The most significant result of this study is that a new high-speed Acela trainset running at 150 mph past a passenger station is calculated to have overall aerodynamic effects and impacts ranging from less intense to somewhat more intense than an existing Amfleet trainset at 125 mph. It is likely that the percentage increase of the air velocities will be significantly less than the percentage increase in maximum train speed from 125 mph to 150 mph. This conclusion is largely attributed to the fact that the Acela trainset is much better aerodynamically streamlined than the Amfleet trainset, and thus would mitigate the otherwise expected disruption and turbulence of the air surrounding the train as it passes. However, the spatial and temporal distribution of the effects would differ for the Acela and the Amfleet trainsets, as noted previously in this report. Selected highlights of the computational fluid dynamics CFD results are as follows:

- For the Acela trainset passing at 150 mph, at a height of 2.5 ft above the low-level platform, air velocities could be as high as 25 mph, and can reach people and objects that are 12 ft away from the side of the train. The exposure time is estimated to be 3 seconds.

- For the Acela trainset passing at 150 mph, at a height of 2.5 ft above the low-level platform, air velocities as high as 40 mph can exist at a distance 3 ft to 6 ft away from the side of the train. The exposure time is estimated to be one second.

- For the Acela trainset passing at 150 mph, at 5 ft above the low-level platform, the velocity of the air can reach 25 mph at a distance of 8 ft away from the side of the train. The exposure time is calculated to be 2 seconds.

- The maximum airflow velocities induced by the Acela trainset service at low-level platforms is estimated to exceed the threshold values of 25 mph currently used by British Rail. However, based on the field measurements, this threshold is probably currently being exceeded routinely in the Northeast Corridor by the passage of Amfleet trainsets.

- Compared to the existing Amfleet trainset, the Acela trainset would induce less airflow at the head of the train as it approaches a station (bow wave), and along the sides while it is running adjacent to a station platform (boundary layer effects). But the wake effects after the train has passed would extend further laterally on the platform, though the effects would be of a shorter duration than the wake effects of the Amfleet. (See Figures 3-21 and 3-22; and Tables 3-1 and 3-2.)

- Induced airflow effects from a passing Acela trainset are calculated to be less severe at a high-level station platform than at a low-level platform.

- Induced airflow effects from a passing Acela trainset will be greater at 2.5 ft above a platform than at 5.0 ft above a platform, whether the platform is high-level or low-level.

Note that the above statements regarding results at a height of 2.5 ft above the platform are relevant to potential effects that may be felt by small children or unsecured objects, such as luggage, at or near the platform level. There are assumptions that limit the absolute predictive accuracy of the CFD models. However, the comparative accuracy of the CFD models has more validity than the absolute accuracy, e.g., comparison of the ratio of wind velocities due to different trainsets is more valid than the absolute values of the calculated velocities themselves. Thus, the models provide a relatively high level of confidence for comparing the Acela to the Amfleet results.

The field measurements for the Amfleet trainset compared well with the Amfleet CFD results, and thus provided a verification of the CFD analyses, and a confirmation of the calculated relative impacts of the new Acela trainset versus the Amfleet trainset. The maximum induced airspeeds measured at the stations were found to correlate well with the ranges of the mean airspeed combined with the fluctuating component from the CFD analyses.

Information on the stations in the Northeast Corridor was gathered from various agencies in the political jurisdictions in which the Acela trainsets will operate. The visual field surveys of the selected stations provided an inventory of conditions to confirm or identify station and platform characteristics that were either the same or different from the assumptions used in the CFD analyses, and the conditions at the location of the field velocity measurements. The data collected are provided as Appendices to the report, and can be useful to identify the relative potential aerodynamic impacts of the new high-speed Acela service at specific stations. Some general observations regarding stations and features are summarized below:

- Platform widths vary widely among stations along the Northeast Corridor.

- Safety signage advising people to stand back from the edge of the platform varies widely among stations. In many cases, the only signage that exists is that warning people not to enter upon the tracks.

- The type, dimensions, and quality of platform-edge safety zones vary widely among stations along the Northeast Corridor.

- Two types of safety systems, designed to provide an automatic warning to persons of an approaching high-speed train and cautioning them to stand back from the platform edge, are being developed or are in use. One of these, being developed by Amtrak, was observed in operation at Mystic Station, Connecticut, but not in the safety-system mode. The other was developed by the Massachusetts Bay Transportation Authority, and was observed in use at several of its commuter rail stations.

- Station platform or right-of-way signs and other appurtenances could be damaged or affected by the constant buffeting of winds induced by passing trains. It should be noted that the induced winds are repetitive in nature, and can induce failure from metal fatigue. For example, a sign designed for a 75 mph wind might fail from metal fatigue after the passage of many trains generating an air velocity of only 40 mph. This has certainly been an issue for signs, doors and other attached objects in subway tunnels, and may be an issue that should be considered in the design and securing of wayside objects along railroad lines.

7. RECOMMENDATIONS

The CFD modeling results and instrumentation field measurements are encouraging in terms of indicating that the overall increase of the aerodynamic effects will range from slight to moderate for the operation of Acela trainset service compared to the existing Amfleet trainset. Given that the aerodynamic effects of operating the Amfleet trainsets at the current speeds are acceptable, the Acela trainset should not pose any significant new impacts.

However, it is not certain that all the potential variables affecting the Acela trainset impacts at any given particular station have been accounted for. It may also be desired to mitigate existing impacts by instituting improvements to operations or facilities in the longer term. Thus, a prudent approach would be to develop a strategy now, which would be responsive to the possibility of unanticipated adverse impacts becoming noticeable only after the start of the high-speed service. This strategy would include two major components:

- **Observations or field measurements of the Acela trainset effects** - An observational approach should further confirm that the aerodynamic impacts of the Acela trainset are less than that of the existing Amfleet trainset, but could also offer advance warnings of unforeseen adverse aerodynamic impacts.

- **An action plan for possible mitigation –** In the event that there are unforeseen potentially adverse aerodynamic effects of the Acela trainsets, as identified by the observational component of the strategy, Amtrak or the FRA would be prepared to respond to these circumstances in a timely and effective manner. This action plan could also be part of or contain a long-term strategy for facility enhancements.

In terms of a long-term mitigation plan for aerodynamic impacts, there is evidence that wind speeds greater than about 13 mph can be annoying to people, and move dust, leaves, and other loose objects (Chapman, 1970). The existing Amfleet trainsets passing stations at a maximum of 125 mph currently induce wind speeds that exceed this value, and its effects were observed as part of the visual field surveys. The Acela trainset passing at 150 mph is calculated to have potentially a slightly to moderately greater impact than the Amfleet. It can induce wind velocities that could potentially cause a similar level of discomfort to persons on non-express-stop station platforms to various degrees, depending on the person's height above the platform and the distance he or she stands away from the side of the train. The height of the platform, whether high-level or low-level, is also a contributing factor to the degree of impact felt. Also of possible importance is the existence of a back wall that may influence the aerodynamic effects. Thus, consideration may be given to a long-term plan for enhancements to the comfort of people standing on platforms of the non-express-stop stations.

Possible considerations for the **observational component** of the strategy include:

- Observations and measurements of induced airflows could be incorporated as part of planned testing of the Acela trainset at the FRA's Transportation Technology Center (TTC) in Pueblo, CO.

- Observations and measurements of induced airflows could be planned during the Acela trainset field trials in the Northeast Corridor.

- Additional observations and measurements of induced airflows associated with the passage of the existing Amfleet trainsets may also be considered.

- The Northeast Corridor stations selected for proposed observations and measurements during Acela field trials and the existing Amfleet runs should be those that would be subjected to the largest increase in the speeds of passing trains upon the initiation of the high-speed Acela service, and those with unusual station and platform configurations.

- The measurements should be designed to verify the differences in the induced airflows between the Acela and Amfleet trainset passage, and between high-level and low-level platforms.

Possible considerations for the **action plan component** of the strategy include:

- A plan that could either be designed to meet the needs of each specific station that could be affected, or that could be generic, or a combination of both. Site-specific plans may be necessary, because of the wide variation between and among stations and their environments along the Northeast Corridor.

- As in the selection of stations for the observational component of the overall strategy, an action plan priority and focus should be those stations that will likely experience the greatest increase in the speeds of passing trains upon the initiation of high-speed Acela service, those with unusual station and platform configurations, and those where the field measurements indicate the highest potential for aerodynamically-induced effects and impacts. Based on the CFD results and field measurements and surveys that have been performed for this study, one particular focus should be those stations with low-level platforms.

- Definition of triggers or decision points that would cause a sequence of actions to be implemented.

- Consideration of warning and safety systems that can be implemented quickly and expediently on a temporary basis. These would primarily be measures to caution persons on station platforms to keep themselves and their luggage well back from the platform edge upon the approach of a non-stop train.

- Consideration of time of day and day of week of the high-speed Acela service for triggering actions. For example, the trigger for an action plan for the Acela trainset passing a station in the middle of the day should be considered differently than at a time in the morning during peak commuting hours, when the density of waiting commuters provides less overall room to step back. On the other hand, waiting commuters could be generally more familiar with safety procedures than infrequent users of commuter rail systems that would be present during the non-peak hours.

- The action plan should provide attention to the placement and securing of signs and appurtenances in the track area and on platforms. These are generally relatively low cost measures that can be implemented rapidly, but some measures could also be part of the long-term enhancements.

- Station environmental conditions, such as the proximity of residential housing, should be taken into account in the design of the safety systems, e.g., the acoustic impacts of the audible portions of temporary warning systems.

- Public awareness and education programs could be developed and implemented. The programs could emphasize, in a positive way, the increases in speed and frequency of trains. The programs should be tailored to local needs and conditions. The areas of greatest potential impact, such as between New Haven, Connecticut, and Boston, should be targeted for initial implementation of the programs.

- During periods of heavy snow, or after the trackbed has been disturbed during maintenance, consideration should be given to requiring a reduction in the speed of non-stop trains passing stations. This would mitigate the stirring up of particulate matter that could possibly impact persons on the platform. This reduction in speed could be accomplished through the use of the Amtrak Temporary Speed Restriction Bulletin (TSRB), issued beginning at 5:00 AM daily to train and engine crews. The determination of when these restrictions may be needed could be based on observations and reports of such conditions from the operating (train) crews, operations supervisors, or maintenance supervisors.

- As part of a long-term strategy for station enhancements, provide consideration of permanent warning signs and safety systems (visual and auditory) that can be implemented. The safety systems currently being developed by Amtrak or in use by the MBTA are examples of promising systems for consideration. Enhancement of platform-edge safety zones should be considered in conjunction with the warning signs and as part of the long-term strategy for safety systems.

- Many of the above action items cannot be implemented without consideration of other issues or requirements (e.g., ADA, FTA, NFPA and other standards or Environmental Impact Statement) or operational constraints imposed by Amtrak or the FRA.

The study recommendations are not prescriptive in nature, but rather suggest further steps that could be taken to minimize or mitigate potential effects of high-speed trains operating in the Northeast Corridor.

APPENDIX A

Description of Computational Fluid Dynamics Model Used in the Study

Computational Fluid Dynamics (CFD) is a powerful tool that has been used in the last two decades in many industries. It is used, by federal agencies, national laboratories, the aircraft industry, and the automobile industry, for aerodynamic analysis, design and, the verification of experimental data. Specific users include the National Aeronautics and Space Agency (NASA), Boeing, McDonnell Douglas, Pratt and Whitney, Lockheed, Allied Signal, Ford Motor Company, General Motors, Chrysler, Mercedes Benz, and Bavarian Motor Works (BMW). Since the creation of supercomputers and powerful workstations, this tool has become even more attractive, working hand-in-hand with experimental investigations. The methodology in CFD is based on the solution of conservation of mass and momentum equations. In addition, depending on the parameters involved, such as the flow regime (laminar or turbulent), other equations are utilized to solve the problem.

The CFD software that was used in this study was the FLUENT program (Fluent, Inc., 1996). FLUENT is a general-purpose computer program for modeling fluid flow, heat transfer, and chemical reactions. FLUENT incorporates up-to-date modeling techniques and a wide range of physical models for simulating numerous types of fluid problems, and has been previously used by Parsons Brinckerhoff for numerous other applications. When required, FLUENT can also be customized to specific modeling needs.

FLUENT can be used in a wide range of applications, such as:

- chemical and process engineering component design;
- combustion design and engineering, including gaseous combustion, liquid fuel combustion, and coal combustion;
- aerodynamic design;
- electronic cooling manufacture and design;
- power generation;
- heat transfer operations;
- material processing;
- chemical vapor deposition (CVD);
- spray drying or cooling;
- gas cleaning or particle classification;
- architectural design (internal and external air flow);
- fire research (open fires, fires in buildings);
- particle deposition or fouling;
- pollution control; and
- turbo-machinery component design.

FLUENT models a wide range of phenomena by solving the conservation equations for mass, momentum, energy, and chemical species using a control volume-based, finite-difference method. The governing equations are discretized on a curvilinear grid to enable computations in complex/irregular geometries. A non-staggered system is used for storage of discrete velocities and pressures. Interpolation is accomplished via higher order upwind schemes. The equations are solved by the Semi-Implicit Method for Pressure-Linked Equations (SIMPLE) algorithm, or by the Semi-Implicit Method for Pressure-Linked Equations Consistent SIMPLEC) algorithm. Both algorithms use an iterative line-by-line matrix solver and multigrid acceleration.

BASIC CONSERVATION EQUATIONS

The equations representing the conservation of mass, momentum, energy and species can be written as follows in Cartesian tensor notation:

Mass Conservation

$$\frac{\partial \rho}{\partial t} + \frac{\partial}{\partial x_i}(\rho u_i) = 0$$

Where: t is the time and x_i are the coordinates axis in the ith direction. ρ and u are the density and the velocity respectively of the fluid

Momentum Conservation

$$\frac{\partial}{\partial t}(\rho u_i) + \frac{\partial}{\partial x_j}(\rho u_i u_j) = \frac{\partial}{\partial x_j}(\tau_{ij}) - \frac{\partial P}{\partial x_i} + \rho g_i + F_i$$

The terms on the left side are the unsteady and convection terms of the momentum in the ith direction. P is the static pressure, τ_{ij} is the stress tensor acting on the ith face in the jth direction, g_i and F_i are the gravitational acceleration and external body forces in the i direction, respectively. The viscous stress tensor τ_{ij} is given by:

$$\tau_{ij} = \left[\mu \left(\frac{\partial u_i}{\partial x_j} + \frac{\partial u_j}{\partial x_i} \right) \right] - \frac{2}{3} \mu \frac{\partial u_l}{\partial x_l} \delta_{ij}$$

where μ is the molecular viscosity and the second term on the right hand side is the effect of volume dilatation. δ_{ij} is the Kronecker delta which is an isotropic tensor of rank 2 and has the following property: $\delta_{ij} = 0$ when $i \neq j$, and $\delta_{ij} = 1$ when i=j.

Species Mass Conservation Equation

The conservation of species I' is described by the following equation:

$$\frac{\partial}{\partial t}(\rho m_{i'}) + \frac{\partial}{\partial x_i}(\rho u_i m_{i'}) = \frac{\partial}{\partial x_i}(J_{i',i}) + S_{i'}$$

where $m_{i'}$ is the mass fraction of the species i′, $J_{i',i}$ is the diffusive mass flux of species i′ in the ith direction and $S_{i'}$ is the net rate of production of species i′ per unit volume due to chemical reaction or contribution from any other phenomena.
In general, the diffusive mass flux

$$J_{i',i} = -\rho D_{i',m} \frac{\partial m_{i'}}{\partial x_i} - \left(\frac{D_{i'}^T}{T}\right) \frac{\partial T}{\partial x_i}$$

where $D_{i',m}$ is the diffusion coefficient for species i′ in the mixture and $D_{i'}^T$ is the thermal diffusion coefficient. The first term is the contribution of concentration gradients to the diffusional mass flux vector and the second term represents the Soret effect, that is mass transfer due to temperature gradients.

Energy Equation

FLUENT solves the energy equation in terms of conservation of the static enthalpy, h, defined as:

$$h = \sum_{i'} m_{i'} h_{i'}$$

where

$$h_{i'} = \int_{T_{ref}}^{T} c_{p,i'} dT$$

where T_{ref} is a reference temperature and $c_{p,i'}$ is the specific heat at constant pressure of species i′ As in the species transport equations, the energy equation solved by FLUENT assumes that species diffusion due to pressure and external forces is negligible. Under this assumption, the energy equation cast in terms of h can be written:

$$\frac{\partial}{\partial t}(\rho h) + \frac{\partial}{\partial x_i}(\rho u_i h) = \frac{\partial}{\partial x_i}\left(k \frac{\partial T}{\partial x_i}\right) - \frac{\partial}{\partial x_i} \sum_{j'} h_{j'} J_{j'} + \frac{\partial P}{\partial t} + u_i \frac{\partial P}{\partial x_i} + \tau_{ij} \frac{\partial u_i}{\partial x_j} + S_h$$

where T is the temperature, τ_{ij} is the viscous stress tensor, $J_{j'}$ is the flux of species j', and k is the mixture thermal conductivity. S_h is a source term that includes sources of enthalpy due to chemical reaction, radiation and exchange of heat with the dispersed second phase.

Note the viscous heating term, $\tau_{ij} \frac{\partial u_i}{\partial x_j}$, can be activated as a modeling option when the viscous stresses are large and/or in compressible flows.

In solid regions, FLUENT solves a simple conduction equation that includes the heat flux due to conduction and volumetric heat sources within the solid:

$$\frac{\partial}{\partial t}\rho_w h_w = \frac{\partial}{\partial x_i} k_w \frac{\partial T}{\partial x_i} + \dot{q}'''$$

where ρ_w : wall density
h_w : wall enthalpy
k_w : wall conductivity
q''' : volumetric heat source.

TURBULENCE MODELING

In turbulent flows, the velocity at a point is considered as a sum of the mean (time averaged) and fluctuating components:

$$u_i = \overline{u}_i + u_i'$$

Substitution of expressions of this form into the Mass and Momentum conservation equations yields the ensemble-averaged momentum equations, applied by FLUENT for prediction of turbulent flows:

$$\frac{\partial}{\partial t}(\rho u_i) + \frac{\partial}{\partial x_j}(\rho u_i u_j) = \frac{\partial}{\partial x_j}\left(\mu\left(\frac{\partial u_i}{\partial x_j} + \frac{\partial u_j}{\partial x_i}\right)\right) - \frac{\partial p}{\partial x_i} + \rho g_i + F_i + \frac{\partial}{\partial x_j}\left(\rho \overline{u_i' u_j'}\right)$$

This equation has the same form as the fundamental momentum balance for laminar case with velocities now representing time-averaged (or mean flow) values and the effect of turbulence incorporated through the Reynolds stresses represented by $\rho \overline{u_i' u_j'}$.

FLUENT relates the Reynolds stresses to mean flow quantities via one of the three turbulence models.

- the standard k-ε model
- the RNG standard k-ε model
- the Reynolds Stress Model (RSM)

The Reynolds Stress Model involves a seven-equation (in 3D) model of turbulence. This can be compared to the two-equation model framework utilized in the k-ε and RNG models.

$$\rho u_i' u_j' = \rho\left(\frac{2}{3}\right) k \delta_{ij} - \mu_t \left(\frac{\partial u_i}{\partial x_j} + \frac{\partial u_j}{\partial x_i}\right) + \frac{2}{3}\mu_t \frac{\partial u_l}{\partial x_l}\delta_{ij}$$

The Reynolds stresses equation is analogous to that describing the shear stresses that arise in laminar flow with the turbulent viscosity μ_t playing the same role as the molecular viscosity μ.

Therefore the form of the Reynolds averaged momentum equations remain identical to the form of the laminar momentum equations except that μ is replaced by an effective viscosity, μ_{eff}:

$$\mu_{eff} = \mu + \mu_t$$

Using the Reynolds analogy between momentum, heat and mass transfer similar approach is used for the energy and species conservation equation. The conductivity in the energy equation and the diffusion coefficient in the species equation consists of the laminar and the turbulent terms.

$$k_{eff} = k + k_t$$

and

$$D_{i',m_{eff}} = D_{i',m} + D_{i'.mt}$$

Standard k-ε Model

In the k-ε model, Reynolds stresses are related to the mean flow via the Boussinesq hypothesis.

The turbulent viscosity, μ_t, is computed from a velocity scale ($k^{½}$) and a length scale ($k^{3/2}/\varepsilon$) which are predicted at each point in the flow via solution of transport equations for k and ε:

$$\frac{\partial}{\partial t}(\rho k) + \frac{\partial}{\partial x_i}(\rho u_i k) = \frac{\partial}{\partial x_i}\left(\frac{\mu}{\sigma_k}\right)\frac{\partial k}{\partial x_i} + G_k + G_b - \rho\varepsilon$$

and

$$\frac{\partial}{\partial t}(\rho\varepsilon) + \frac{\partial}{\partial t}(\rho u_i \varepsilon) = \frac{\partial}{\partial x_i}\left(\frac{\mu}{\sigma_\varepsilon}\right)\frac{\partial \varepsilon}{\partial x_i} + C_1\left(\frac{\varepsilon}{k}\right)\left(G_k + [1 - C_3]G_b\right) - C_2\rho\left(\frac{\varepsilon^2}{k}\right)$$

where G_k is the generation of k and is given by:

$$G_k = \mu_t\left(\frac{\partial u_j}{\partial x_i} + \frac{\partial u_i}{\partial x_j}\right)\frac{\partial u_i}{\partial x_i}$$

and G_b is generation of turbulence due to buoyancy:

$$G_b = -g_i \frac{\mu_t}{\rho\sigma_h}\frac{\partial u_i}{\partial x_i}$$

where σ_h is the turbulent Prandtl number, $\frac{\mu_t c_p}{k_t}$.

The turbulent viscosity is then related to k and ε by the expression:

$$\mu_t = \rho C_\mu \frac{k^2}{\varepsilon}$$

The coefficients C_1 ,C_2, C_μ, σ_k and σ_ε are empirical constants having the following values:

$C_1 = 1.44$, $C_2 = 1.92$, $C_\mu = 0.09$, $\sigma_k = 1.0$, $\sigma_\varepsilon = 1.3$

The Renormalization Group (RNG) Model

The RNG-based k-ε turbulence model follows the two-equation turbulence modeling framework and has been derived from the original equations for fluid flow using mathematical technique called Renormalization Group (RNG) methods. The RNG model provides a more general and fundamental model and yields improved predictions of near-wall flows (including flow separation), flows with high streamline curvature and high strain rate, low-Reynolds-number and transitional flow, wall heat/mass transfer, and detailed wake flow and vortex shedding behavior.

The RNG k-ε model differs from the standard k-ε in several important ways:

- Constants and functions in the RNG model are evaluated by the theory and not by empiricism. The model is therefore applicable without modification.
- Low Reynolds-number effects are included in the RNG theory, permitting laminar-like behavior to be predicted.
- New term appear in the dissipation rate equation, including a rate-of-strain term, which is important for treatment of non-equilibrium effects and flows in the rapid distortion limit like separated flows and stagnation flows.
-

The transport equations for k and ε in the RNG model

$$\frac{\partial k}{\partial t} + u_i \frac{\partial k}{\partial x_i} = \nu_t S^2 - \varepsilon + \frac{\partial}{\partial x_i} \alpha \nu_t \frac{\partial k}{\partial x_i}$$

and

$$\frac{\partial \varepsilon}{\partial t} + u_i \frac{\partial \varepsilon}{\partial x_i} = C_1 \frac{\varepsilon}{k} \nu_t S^2 - C_2 \frac{\varepsilon^2}{k} - R + \frac{\partial}{\partial x_i} \alpha \nu_t \frac{\partial \varepsilon}{\partial x_i}$$

where $\eta = \frac{Sk}{\varepsilon}$, $\eta_0 \approx 4.38$, $S^2 = 2 S_{ij} S_{ij}$ is the modulus of the rate of strain tensor, and

$$\nu_t = C_\mu \frac{k^2}{\varepsilon}.$$

The rate of strain term R is expressed as the following:

$$R = \frac{C_\mu \eta^3 \left(1 - \frac{\eta}{\eta_0}\right)}{1 + \beta\eta^3} \frac{\varepsilon^2}{k}$$

The values of the constants are as follows: C1=1.42 , C2=1.68, α= 1.39 , β= 0.012 and Cμ=0.085.

Reynolds Stress Model (RSM)

The RSM involves solving the transport equations for the individual stresses $\overline{u_i' u_j'}$. These equations can be derived from the momentum equations and contain triple order velocity correlations and pressure velocity correlations that must be modeled to obtain closure.

$$\frac{\partial \overline{u_i' u_j'}}{\partial t} + u_k \frac{\partial \overline{u_i' u_j'}}{\partial x_k} = \frac{\partial}{\partial x_k}\left(\frac{\nu_t}{\sigma_k} \frac{\partial \overline{u_i' u_j'}}{\partial x_k}\right) + P_{ij} + \Phi_{ij} - \varepsilon_{ij} + R_{ij} + S_{ij} + D_{ij}$$

where P_{ij} is the stress production rate, Φ_{ij} is a source/sink due to the pressure strain/strain correlation, ε_{ij} is the viscous dissipation, R_{ij} is the rotational term, and S_{ij} and D_{ij} are curvature related terms that arise when the equations are written in cylindrical coordinates.
The pressure/strain terms is modeled as

$$P_{ij} = -(\overline{u_i' u_j'} \frac{\partial u_j}{\partial x_k} + \overline{u_i' u_j'} \frac{\partial u_i}{\partial x_k})$$

$$\Phi_{ij} = -C_3 \frac{\varepsilon}{k}\left(\overline{u_i' u_j'} - \frac{2}{3}\delta_{ij} k\right) - C_4\left(P_{ij} - \frac{2}{3}\delta_{ij} P\right)$$

where P=1/2 P_{ii}, C3 and C4 are empirical constants whose values are 1.8 and 0.6, respectively.

The dissipation term is approximated by the isotropic dissipation rate ε:

$$\varepsilon_{ij} = \frac{2}{3}\delta_{ij}\varepsilon$$

As can be seen from these equations, the dissipation equation is solved for in the addition to the six equations of the Reynolds stresses in the RSM model.

CALCULATION OF FLUID PROPERTIES

FLUENT allows fluid properties to be defined by the user as constant or as temperature and/or composition dependent. In this section the equations employed by FLUENT for calculation of temperature and/or species dependent fluid properties are outlined.

Density

The density is computed based on the ideal gas law as:

$$\rho = \frac{P}{RT\sum_{i'} \frac{m_{i'}}{M_{i'}}}$$

where R is universal gas constant, $\Sigma m_{i'}/M_{i'}$ provides the molecular weight of the local mixture, $M_{i'}$ is the molecular weight of species i' and P is the pressure.
If the fluid is not an ideal gas, the density can be specified using functional relationships relating the density to the temperature $\rho = \rho(T)$. These functions can be polynomials or step varying.

Viscosity

In dilute mixtures or in pure-component flows, the fluid viscosity may be defined as $\mu=\mu(T)$ via input of a polynomial or a piecewise linear variation with temperature. Composition dependent viscosity may be of importance in non-dilute mixtures in laminar flow. When the viscosity is to be computed as a function of composition, the viscosity of each component (μ_i) must be defined. The individual pure-species viscosity's may be defined via polynomial or piecewise variation with temperature. The mixture viscosity will be computed based on a mass fraction average of the pure species viscosities:

$$\mu = \sum_{i} m_{i'} \mu_{i'}$$

For ideal gases the molecular viscosity for each component can be calculated using kinetic theory as:

$$\mu = 2.67 \times 10^{-6} \frac{\sqrt{MT}}{\sigma^2 \Omega_\mu}$$

$\Omega\mu$ is a reduced collision integral which function of T* ,where $T^* = \frac{T}{\varepsilon/k}$.

The Leonard-Jones parameters, σ and ε/k are user inputs to the kinetic theory calculation.

Thermal Conductivity

Thermal conductivities may be defined and computed in a manner very similar to that used for calculation of the fluid viscosity. The mixture conductivity may be input by the user as k = k(T) or it may be computed from pure species conductivities $k_i \cdot A$ mass fraction weighted average is used:

$$k = \sum_i m_{i'} k_{i'}$$

where $k_i = k_i$ (T) can be provided by the user via polynomial or piecewise linear input.

Also kinetic theory can be used, when ideal gas is present via the following:

$$k = \frac{15}{4} \frac{R}{M} \mu \left(\frac{4}{15} \frac{C_p M}{R} + \frac{1}{3} \right)$$

Mass Diffusion Coefficient

FLUENT allows the mass diffusion coefficient to be defined as function of temperature and/or composition:

$$D_{i',m} = D_{i',m}(T)$$

Kinetic theory can be used , where the diffusion coefficient is represented by:

$$D_{i'j'} = 0.0188 \frac{\left[T^3 \left(\frac{1}{M_{i'}} + \frac{1}{M_{j'}} \right) \right]^{1/2}}{p \sigma_{i'j'}^2 \Omega_D}$$

Likewise Soret diffusion coefficient is calculated through kinetic theory.

Specific Heat of Capacity

The mixture specific heat capacity, c_p, may be defined by the user as c_p, c_p(T), or it may be computed based on individual pure component heat capacities, $c_{p,i}$.

$$C_p = \sum_{i'} m_{i'} C_{p,i'}$$

Kinetic theory can be used for the ideal gas to define the specific heat as:

$$C_{p,i'} = \frac{1}{2} \frac{R}{M_{i'}} \left(f_{i'} + 2 \right)$$

where $f_{i'}$ is the degree of freedom for species i'.

SOLUTION PROCEDURE

FLUENT uses a control volume based technique to solve the conservation equations for mass, momentum, energy, species, and turbulence quantities described earlier. This control volume based technique consists of:

- Division of the domain into discrete control volumes using a general curvilinear grid.
- Integration of the governing equations on the individual control volumes to construct the algebraic equations for discrete unknowns (velocities, pressure, scalars).
- Solution of the discretized equations.

The governing partial differential equations for the conversion of mass, momentum, energy, and chemical species for the gaseous phase are rearranged into a general form which can be written as:

$$\frac{\partial}{\partial t}(\rho\Phi) + \frac{\partial}{\partial x_i}(\rho u_i \Phi) = \frac{\partial}{\partial x_i}\left(\frac{\Gamma_\Phi \partial\Phi}{\partial x_i}\right) + S_\Phi$$

where the terms are the temporal and the convection terms on (LHS), diffusion, and source terms on the other side. The equations are reduced to their finite-difference analogues by integration over the volume of the computational cells into which the domain is divided. Integration in time is fully implicit. FLUENT define the discrete control volumes using a non-staggered grid storage scheme. In this scheme, the same control volume is employed for integration of all the conservation equations and all variables are stored at the control volume cell center.

All the dependent variables, with the exception of velocity components, are calculated and stored at the nodal points which these cells encompass. The velocity components lie on the cell boundaries by means of a “staggered” grid. The interpolation to determine face values of the unknowns is accomplished via either the power law, blended second order upwind/central difference, or QUICK interpolation schemes.

The resulting algebraic equations can be written in the following common form:

$$\phi_p \sum_i \left(A_i - S_p\right) = \sum_i \left(A_i \phi_i\right) + S_c$$

Where the summation is over the neighboring finite difference cells i= N, S, E, W, F, B. The A’s are coefficients which contain contributions from the convective and diffusive fluxes and S_c and S_p are the components of the linearized source term, $S_F = S_c + S_p\,\Phi_p$. Power-law differencing scheme (or the optional Second Order Upwind or Quadratic Upwind Scheme) is used for interpolation between grid points and to calculate the derivatives of the flow variables. The set of simultaneous algebraic equations is solved by a semi-implicit iterative scheme which starts from arbitrary initial conditions (except at the boundaries) and converges to the correct solution (i.e., that which satisfies the governing equations) after performing a number of iterations.

Each iteration consists of the following steps:

1. The u, v, and w momentum equations are each solved in turn using current values for pressure, in order to update the velocity field.
2. Since the velocities obtained may not satisfy the mass continuity equation locally, a "Poisson-type" equation is derived from the continuity equation and the linearized momentum equations. This pressure correction equation is then solved to obtain the necessary corrections to the pressure field and the velocity components.
3. The turbulent kinetic energy and its dissipation equations are solved using the updated velocity field.
4. Any auxiliary equations (e.g. enthalpy, species, conservation, radiation, or turbulence quantities) are solved using the previously updated values of the other variables.
5. A check for convergence of the equations involved is made.

These steps can be continued until the error (residuals) has decreased to a required value.

BOUNDARY CONDITIONS

Because of the elliptic nature of the conservation equation, boundary conditions must be specified at all boundaries of the domain being considered.

FLUENT provides a wide variety of boundary condition options, including:

- Flow Inlets and Exits;
- Wall boundaries;
- Symmetry Boundaries;
- Periodic Boundaries; and
- Cyclic Boundaries.

Flow inlets and exits can be defined via pressure and/or velocity specification. Flow exits can alternately be defined in terms of zero normal gradient (or extrapolation) conditions. Wall boundaries can be stationary or moving, slip or non-slip, smooth or rough. Walls may be treated via a variety of thermal boundary conditions (fixed temperature, fixed heat flux, or fixed external heat transfer conditions). Symmetry, periodic and cyclic boundaries provide a means by which the scope of the computational model can be reduced by exploiting the repeating nature of the geometry and flow pattern.

For turbulent flows, wall functions, empirical in nature, are used at the near wall grid point to estimate the effect of the wall on the flow. These functions are used instead of resolving the entire turbulent boundary layer. This will eliminate the need to resolve finely the region near the wall. The wall function thus provides a great savings in the computer effort required for turbulent flows.

FLUENT provides two wall function options:

- the standard (equilibrium) wall function
- the non-equilibrium wall function

FLUENT OUTPUT

The final step of the computational fluid dynamics is to check the results, then generate graphical output of the data that are beneficial to the designer to judge the adequacy of the proposed analysis. The adequacy of the results is judged often using codes that dictate tenability limits set by different national associations. So as a first step, the final result are checked after the last iteration using the residuals that are provided at each iteration for each variable that is solved for. The residuals can be either supplied in a normalized form, or non-normalized if the absolute error is sought from iteration to the other. This test should not be the only deciding factor to judge convergence. The next step is to check the overall mass and heat balance using the total zone integration that is available in the alpha numerical menu. If a second specie is part of the problem set up, like smoke, overall mass balance of the specie should be checked using integration across different planes representing inlets and exits to and from the computational domain. These integrations are available in the alpha numerical menu.

For results presentation and check up at every point in the domain modeled, two methods are available. One is through alpha numerical menu that can tabulate all the variable of interest at every cell of the domain in a matrix form. The variable to be tabulated is selected from the select variable menu and the format of the matrix for the display is chosen by the user. The variables that are available from the select variable menu can be one of the variables that are solved for through the conservation equation as velocities, temperature, species, turbulent kinetic energy, dissipation, pressure or any other variable that can be derived from these primary variables and the geometry of the problems like shear stress, heat flux, or any of the physical properties.

In addition to the tables, graphical output is available. Contour as well as vector and profile forms are available to plot all sorts of variables that can be chosen from variable selection in the graphics menu.

APPENDIX B

HIGH-SPEED TRAINSET INPUT DATA

1. List of Drawings

Figures 3-1 through 3-4 show the three computational domains used for the three configurations used to analyze this problem, as well as the type of grid around the train.

Among the drawings that were used to create the geometry and the grid around the trainset are the following from the "Drawings for the Power Car and Coach Car," Bombardier, Inc., 1998 (Reference 7):

Drawing No.	Date	Title
HS-399-0011-2	24 December 1997	COACH SHELL ASSEMBLY
HS-936-0028-12	19 May 1998	INTERIOR DIAGRAM POWER CAR
HS-936-0050-4	10 November 1997	COACH CAR STRUTURAL DIAGRAM
HS-999-0066-2		HIGH SPEED TRAINSET CONSIST
HS-936-0028-1	19 May 1998	INTERIOR DIAGRAM POWER CAR
HS-936-0028-2	19 May 1998	INTERIOR DIAGRAM POWER CAR
HS-936-0028-6	19 May 1998	INTERIOR DIAGRAM POWER CAR
HS-936-0028-11	19 May 1998	INTERIOR DIAGRAM POWER CAR

2. Platform Measurement:

The following data were implemented in the model. These data were collected at Princeton Junction Station.

- Platform width = 11 feet.
- Platform thickness = 8 inches.
- Height from top of ballast to platform = 5 feet.
- Distance between edge of high level platform and centerline of closest track = 5 feet 7 inches.
- Distance between the two centerline tracks = 12 feet.

3. High-Speed Acela Trainset Dimensions:

	Length (ft)	Maximum Width (ft)	Height (rail to roof) (ft)
Power Car	69.61	10.42	14.17
Passenger car	87.42	10.38	13.89

4. Amfleet Trainset Dimensions:

	Length (ft)	Maximum Width (ft)	Height (rail to roof) (ft)
Power Car	51.48	10.0	12.47
Passenger Car	85.33	10.5	12.67

APPENDIX C

Adjustments of the Coefficient of Friction in the Computational Model

At the start of the runs, train walls were considered smooth. After convergence, result of the coefficient of friction for the train based on the frontal area was compared to the drag data supplied by the analysis performed by Sherbrooke University (Laneville, 1998). They obtained a friction coefficient of 0.46 when a train was travelling at 150 mph. Initially, when smooth walls were used a friction coefficient of 0.28 was obtained. To increase this coefficient, the walls roughness parameter was changed. After four trials a coefficient of friction of 0.48 was obtained.

In turbulent flows, large gradients are encountered in the vicinity of walls. In addition, the flow conditions in these regions are dominated by the molecular diffusion. Accurate representation of the wall boundary layers would require a very large number of grid points near the walls and the resulting computational effort will be excessive. In engineering models, such a detailed calculation is avoided by assuming a Couette flow approximation close to the wall. In this approach, the first grid point next to the wall is placed in the fully turbulent region, and wall functions, based on the universal logarithmic laws of wall, are used to represent the momentum fluxes between the near-wall grid point and the wall surface. The below algebraic terminology is defined in Appendix A.

For the momentum equations, the wall shear stress is given by :

$$\tau_w = \frac{\mu u\, y^+}{u^+\, y}$$

where μ is the dynamic viscosity of the air, u the velocity component parallel to the wall at near-wall grid point, located at a distance y from the wall. u^+ and y^+ are the dimensionless velocity and distance and are defined as:

$$u^+ = \frac{1}{\kappa} \ln\left(E\, y^+\right)$$

$$y^+ = \frac{\rho k^{1/2} c_\mu^{1/4}\, y}{\mu}$$

where ρ is the density of the air, κ = 0.41 is von Karman constant, C_μ= 0.085 and the constant E accounts for the effects of the laminar sub-layer. Its value depends on the wall roughness and is obtained as follows:

$E = 9$ for smooth walls $k^+ < 9.4$

$$E = \frac{210}{\left(k^+\right)^{1.409}}$$ for intermediate rough walls $9.4 < k^+ < 134$

$$E = \frac{28.5}{k^+}$$ for very rough walls $k^+ > 134$

In the above equations, K^+ is the nondimensional surface roughness height and is defined as:

$$k^+ = \frac{\rho e \sqrt{\tau_w / \rho}}{\mu}$$

where e is the roughness height.

For our analysis the values of E were altered in the four cases to match the shear stress (coefficient of friction) of the model to the measurement reported in Lanneville (1998). As can be seen from the equation shown, the coefficient of friction or the wall shear stress increase by decreasing the values of E. Values for E of 9, 1, 0.1 and 0.5 were used in order to match the coefficient of friction of the model to the supplied value in Lanneville (1998). The coefficient of friction corresponding to the E values of 9 and 1 were 0.28 and 0.35 while a value of 0.6 and 0.48 were the results for the values of 0.1 and 0.5, respectively. These results are summarized in the following table:

E	Coefficient of Friction
9	0.28
1	0.35
0.5	0.48
0.1	0.6

APPENDIX D

LINEAR INTERPOLATION FOR TRAIN VELOCITIES
Between 110 and 150 Miles Per Hour

The Reynolds number for the cases analyzed are 8.1×10^8 and 5.9×10^8 based on the length of the train and speeds of 150 and 110 mph respectively. The velocity difference between the two cases is about 25 percent. There is no critical point between these two Reynolds numbers where flow properties are anticipated to change drastically. Therefore, any data of interest for train velocities between the 110 mph and 150 mph should be found by linear interpolation without compromising the legitimacy of the obtained results. The flow patterns for the 110 mph and 150 mph cases showed a consistent behavior.

Two locations were chosen to confirm this approach. One location was in the boundary layer region on the side of the train, and the other was in the wake region of the train. The first location corresponds to the nodes I=100, J=8 and K=18, while the second point corresponds to I= 120, J=112 and K=25. The value of the horizontal velocity in the direction of train motion was chosen. Values of 112 ft/sec and 155 ft/sec were obtained from the simulation of 110 mph and 150 mph respectively for the first location. For the second chosen point, values of 115 ft/sec and 155 ft/sec were obtained from the 110 mph and 150 mph simulations, respectively.

As one can see, the value of the lower speed train can be predicted with a minimum of error by multiplying the high speed train value by 110/150 ratio. Therefore, the data for train speed between 110 mph and 150 mph can be obtained by a linear interpolation, using a linear relationship between 0 velocity and 150 mph to derive the data.

However, our concern is the air flow velocities at different locations for the train's speed between 110 and 150 mph. In this case, a linear interpolation between the 110 mph case and 150 mph will lead to better-predicted velocity values than using a linear interpolation between 0 and 150 mph. The improvement is due to the small range in which the interpolation will be performed. The smaller the interval in which the interpolation is made, the more accurate the prediction will be.

APPENDIX E

EXPLANATION OF TURBULENCE FLUCTUATIONS

Most fluid flows of scientific and technical interest are turbulent. Characteristics of turbulent flow are complex time-varying fields, random fluctuations in the flow variables, and rapid separation of neighboring fluid elements. Turbulence is one of the outstanding problems of classical physics, and there is no complete theory of turbulence derived from basic principles. If one subscribes to the view, as we will, that the Navier-Stokes equations form the correct basis for turbulence theory, then one might hope that numerical methods could be used directly to calculate turbulent flow. But as explained and proven in many papers, this is impractical for high Reynolds numbers. In the absence of general theories to calculate turbulence, there is a large body of literature devoted to phenomenological models of turbulence which enable turbulence to be accounted for in a large class of flows.

As described in Appendix A, in turbulent flows all variables at a point are considered as a sum of the mean (time-averaged) and fluctuating components. For velocity we will have:

$$u_i = \overline{u}_i + u'_i$$

As described in Appendix A, three turbulence models are available in FLUENT software. The Renormalization Group (RNG) model was implemented to solve the problem in hand. It has many of the characteristics of a good engineering turbulence model. These characteristics are universality, economy, and robustness. The domain of applicability is considerably broader than the standard k-ε model, and yet the computer resources required are only marginally increased. The improved results from the RNG model have been documented for a broad range of turbulent flows including separated flows, flow with curvature, and swirling like we have in the problem in hand.

In this model the conservation equations of turbulent kinetic energy and dissipation are solved at every point in the domain. Because this model is isotropic, there are no preferred directions for the fluctuations, and the intensity of fluctuations in the x, y, and z coordinate system directions are equal, i.e.,

$$\overline{u'^2} = \overline{v'^2} = \overline{w'^2}$$

and k which is the turbulent kinetic energy is defined as :

$$k = \frac{1}{2} * \left(\overline{u'^2} + \overline{v'^2} + \overline{w'^2} \right)$$

Then, the fluctuating component in the direction of flow can be calculated as follows:

$$u' = \sqrt{\frac{2}{3}k}$$

A subroutine was written and linked to the main program of Fluent to generate the values of the fluctuating component at every grid point in the domain of calculation. Contour plots of these values are shown in Figures 3-6, 3-8, 3-10, 3-12, 3-14 and 3-16.

APPENDIX F

LIST OF STATIONS ON THE NORTHEAST CORRIDOR AND OTHER INFORMATION

Railroads Serving Stations, Washington, DC to Boston, MA

Service Provider Acronym	Service Provider Name	Service Owner	Service Operator
AMTRAK	National Railroad Passenger Corporation	National Railroad Passenger Corporation	National Railroad Passenger Corporation
VRE	Virginia Railway Express	Virginia Department of Transportation	National Railroad Passenger Corporation
MARC	Maryland Rail Commuter	Maryland Mass Transit Administration	National Railroad Passenger Corporation
SEPTA	Southeastern Pennsylvania Transportation Authority	Southeastern Pennsylvania Transportation Authority*	Southeastern Pennsylvania Transportation Authority
NJT	New Jersey Transit Rail Operations, Inc.	New Jersey Transit Rail Operations, Inc.	New Jersey Transit Rail Operations, Inc.
LIRR	Long Island Rail Road Co.	New York Metropolitan Transportation Authority	Long Island Rail Road Co.
MNR	Metro North Railroad	New York Metropolitan Transportation Authority	Metro North Railroad
CCR	Connecticut Commuter Rail, Shore Line East	Connecticut Department of Transportation	National Railroad Passenger Corporation
MBTA	Massachusetts Bay Transportation Authority	Massachusetts Bay Transportation Authority	National Railroad Passenger Corporation

***** Within the State of Delaware, SEPTA provides commuter rail service for the Delaware Department of Transportation.

Ownership of Right-of-Way and Dispatchment of Trains, Washington - Boston

Territory	Ownership	Dispatchment
Washington, DC to New Rochelle, NY	AMTRAK	AMTRAK
New Rochelle, NY to Connecticut Border	State of New York	MNR
Connecticut Border to New Haven	State of Connecticut	MNR
New Haven, CT to Massachusetts Border	AMTRAK	AMTRAK
Massachusetts Border to Boston South Stn.	Commonwealth of Massachusetts	AMTRAK

Explanation of Types of Amtrak and Commuter Service and Other Column Headers for the Following Tables

Type of Service	Explanation
HST (High-Speed Trainset)	Trains making a limited number of stops and operating at speeds up to 150 mph. Begins in 1999.
NE Dir. (NortheastDirect)	Metroliners, and trains identified in the public timetable as “Northeast Direct” plus a train name.
Other	Named trains (e.g., “Silver Palm”), and special services, e.g., Keystone and “Clockers”.
Commuter	Local train service provided by public transportation agencies within designated service areas.
MAS	Maximum Authorized Speed through the stations.
Cur	Current MAS.
Pro	Proposed MAS with HST trains.

Station Name	Location	MAS		Serviced By	Atk. HST	Atk. NE Dir.	Atk. Other	Commuter Rail
		Cur	Pro					
Union Station	Washington, DC	15	15	ATK/MARC/VRE	x	x	x	x
New Carrolton	New Carrolton, MD	125	125	ATK/MARC	x	x	x	x
Seabrook	Seabrook, MD	125	125	MARC				x
Bowie State	Bowie, MD	125	125	MARC				x
Odenton	Odenton, MD	125	125	MARC				x
BWI Rail Station	MD	110	125	ATK/MARC	x	x	x	x
Halethorpe	Halethorpe, MD	110	125	MARC				x
West Baltimore	Baltimore, MD	50	60	MARC				x
Pennsylvania Station	Baltimore, MD	30	30	ATK/MARC	x	x	x	x
Martin Airport	Middle River, MD	125	125	MARC				x
Edgewood	Edgewood, MD	125	125	MARC				x
Aberdeen	Aberdeen, MD	125	125	ATK/MARC		x		x
Perryville	Perryville, MD	125	125	ATK/MARC		x		x
Newark [**See Note 1.**]	Newark, DE	125	135	ATK/SEPTA		x		x
[Churchman's Crossing] **TBC**	MP 34.2 (South of Stanton, DE)	125	135	SEPTA				[x]
Wilmington	Wilmington, DE	30	30	ATK/SEPTA	x	x	x	x
Claymont	Claymont, DE	110	125	SEPTA				x
Marcus Hook	Marcus Hook, PA	110	125	SEPTA				x
Highland Avenue	Chester, PA	90	90	SEPTA				x
Lamokin Street	Chester, PA	90	90	SEPTA				x
Chester	Chester, PA	90	90	SEPTA				x
Eddystone	Eddystone, PA	90	90	SEPTA				x
Crum Lynne	Crum Lynne, PA	100	100	SEPTA				x
Ridley Park	Ridley Park, PA	100	100	SEPTA				x
Prospect Park-Moore	Prospect Park, PA	100	100	SEPTA				x
Norwood	Norwood, PA	100	100	SEPTA				x
Glenolden	Glenolden, PA	100	100	SEPTA				x
Folcroft	Folcroft, PA	100	100	SEPTA				x

Station Name	Location	MAS		Serviced By	Atk. HST	Atk. NE Dir.	Atk. Other	Commuter Rail
		Cur	Pro					
Sharon Hill	Sharon Hill, PA	100	100	SEPTA				x
Curtis Park	Curtis Park, PA	100	100	SEPTA				x
Darby	Darby, PA	100	100	SEPTA				x
30th Street Station	Philadelphia, PA	30	40	ATK/SEPTA/NJT	x	x	x	x
North Philadelphia	Philadelphia, PA	60	65	ATK/SEPTA		x	x	x
Bridesburg	Philadelphia, PA	100	125	SEPTA				x
Wissinoming	Philadelphia, PA	100	125	SEPTA				x
Tacony	Philadelphia, PA	100	125	SEPTA				x
Holmesburg Junction	Philadelphia, PA	100	125	SEPTA				x
Torresdale	Torresdale, PA	90	105	SEPTA				x
Cornwells Heights	Cornwells Heights, PA	125	135	ATK/SEPTA			x	x
Eddington	Eddington, PA	125	135	SEPTA				x
Croydon	Croydon, PA	125	135	SEPTA				x
Bristol	Bristol, PA	125	135	SEPTA				x
Levittown	Levittown, PA	125	135	SEPTA				x
Trenton	Trenton, NJ	110	125	ATK/SEPTA/NJT	[?]	x	x	x
[Hamilton Twp.] **U.C.**	Hamilton Twp, NJ	125	135	ATK(?)/NJT				[x]
Princeton Junction	West Windsor, NJ	125	135	ATK/NJT	[?]	x	x	x
Jersey Avenue	New Brunswick, NJ	125	135	NJT				x
New Brunswick	New Brunswick, NJ	125	125	ATK/NJT		x	x	x
Edison	Edison, NJ	125	125	NJT				x
Metuchen	Metuchen, NJ	110	125	NJT				x
Metropark	Iselin, NJ	90	125	ATK/NJT	x	x	x	x
Rahway	Rahway, NJ	125	125	NJT				x

Station Name	Location	MAS		Serviced By	Atk. HST	Atk. NE Dir.	Atk. Other	Commuter Rail
		Cur	Pro					
Linden	Linden, NJ	125	125	NJT				x
Elizabeth	Elizabeth, NJ	65	80	NJT				x
North Elizabeth	North Elizabeth, NJ	110	110	NJT				x
[Newark Airport] **U.C.**	Newark, NJ	110	110	ATK(?)/NJT				[x]
Penn Station	Newark, NJ	35	35	ATK/NJT	x	x	x	x
[Allied Junction] **U.C.**	Secaucus, NJ	60	90	NJT				[x]
Pennsylvania Station	New York City, NY	15	15	ATK/LIRR/NJT	x	x	x	x
New Rochelle	New Rochelle, NY	70	100	ATK/MNR		x		x
Larchmont	Larchmont, NY	90	100	MNR				x
Mamaroneck	Mamaroneck, NY	90	100	MNR				x
Harrison	Harrison, NY	70	80	MNR				x
Rye	Rye, NY	60	65	MNR				x
Port Chester	Port Chester, NY	45	80	MNR				x
Greenwich	Greenwich, CT	70	75	MNR				x
Cos Cob	Cos Cob, CT	70	75	MNR				x
Riverside	Riverside, CT	75	75	MNR				x
Old Greenwich	Old Greenwich, CT	75	75	MNR				x
Stamford	Stamford, CT	50	65	ATK/MNR	x	x		x
Noroton Heights	Noroton Heights, CT	70	75	MNR				x
Darien	Darien, CT	70	75	MNR				x
Rowayton	Rowayton, CT	70	75	MNR				x
South Norwalk	South Norwalk, CT	70	75	MNR				x
East Norwalk	East Norwalk, CT	75	75	MNR				x
Westport	Westport, CT	75	75	MNR				x

Station Name	Location	MAS Cur	MAS Pro	Serviced By	Atk. HST	Atk. NE Dir.	Atk. Other	Commuter Rail
Green's Farms	Green's Farm, CT	75	75	MNR				x
Southport	Southport, CT	75	75	MNR				x
Fairfield	Fairfield, CT	75	75	MNR				x
Bridgeport	Bridgeport, CT	45	45	ATK/MNR		x		x
Stratford	Stratford, CT	70	75	MNR				x
Milford	Milford, CT	60	75	MNR				x
New Haven	New Haven, CT	15	50	ATK/MNR/CCR	x	x	x	x
Branford	Branford, CT	55	70	CCR				x
Guilford	Guilford, CT	90	125	CCR				x
Madison	Madison, CT	85	105	CCR				x
Clinton	Clinton, CT	85	115	CCR				x
Westbrook	Westbrook, CT	90	95	CCR				x
Old Saybrook	Old Saybrook, CT	90	110	ATK/CCR		x		x
New London (Foxwoods)	New London, CT	25	30	ATK/CCR	x	x		x
Mystic	Mystic, CT	60	65	ATK		x		
Westerly	Westerly, RI	75	95	ATK		x		
Kingston	West Kingston, RI	110	150	ATK		x		
[Wickford] **TBC**	MP 165.8 (Near Wickford Jct., RI.)	110	150	Undetermined.				[x]
[Warwick] **TBC**	MP 176.2 (Near T. F. Green Airport, Warwick, RI.)	110	135	Undetermined.		[x]		[x]
Providence	Providence, RI	30	30	ATK/MBTA	x	x		x
South Attleboro	South Attleboro, MA	100	115	MBTA				x
Attleboro	Attleboro, MA	100	150	MBTA				x
Mansfield	Mansfield, MA	100	150	MBTA				x
Sharon	Sharon, MA	100	130	MBTA				x
Canton Junction	Canton, MA	80	135	MBTA				x

Station Name	Location	MAS Cur	MAS Pro	Serviced By	Atk. HST	Atk. NE Dir.	Atk. Other	Commuter Rail
Route 128	Westwood, MA	60	135	ATK/MBTA	x	x		x
Readville	Boston, MA	100	125	MBTA				x
Hyde Park	Boston, MA	100	125	MBTA				x
Forest Hills	Boston, MA	100	125					
Ruggles	Boston, MA	100	120	MBTA				x
Back Bay	Boston, MA	30	30	ATK/MBTA		x	x	x
South Station	Boston, MA	15	15	ATK/MBTA	x	x	x	x

TBC = To Be Constructed.

U.C. = Under Construction.

x = Station stop for the type of service indicated by the column heading.

Note 1: There are two passenger stations in Newark, DE. The original passenger station on the west side of the tracks is now owned by the City of Newark, DE. The station building on the west side is not in use for passengers; the platform is. The platform, adjacent to Track 3, is maintained by Amtrak, and is used by its passengers. On the east side of the tracks is a new commuter rail passenger station. It is adjacent to Track A, the lead to the Chrysler Motor Car assembly plant. It was purposely located adjacent to Track A because of the 35 mph MAS on that track. The commuter rail station is owned and maintained by the Delaware Department of Transportation.

Note 2: Amtrak provided the information for the MAS of the HSTs.

APPENDIX G

NORTHEAST CORRIDOR CHARACTERISTICS, BY STATE

State/Jurisdiction	Number & Owned By	Maintained By	Safety Systems/ADA	Landmark Status	Other
District of Columbia	1; Amtrak (Atk.)	Atk.	Not Applicable/Yes	Union Station is in the National Register of Historic Places.	High-Speed Aclea Trainset stop.
Maryland	12. Atk. owns 5: New Carrolton, BWI, Penn Stn. (Baltimore), Aberdeen, Perryville. MARC owns the other 7.	Atk. maintains the stations it owns. MARC maintains the stations it owns, **plus** Aberdeen and Perryville which are leased from Atk.	All Atk. and MARC stations are equipped with PAs. All Atk. stns. are ADA-compliant and have LED message boards. MARC stations at Perryville, Aberdeen, Odenton, Bowie State, and Seabrook are ADA-compliant and have LED message boards. PA announcements at the Atk.-owned stations are made by Atk. MARC-owned/leased stations are tied into a common PA system. Announcements are made from the MARC Operations Center at BWI. PA system was also designed for local operation, but for the most part it doesn't work. Overall, the	Pennsylvania Station, Baltimore, is in the National Register of Historic Places.	Acela trains will stop at New Carrolton, BWI, and Baltimore. MARC plans no new stations within the next 5 - 10 years. MARC staffs (ticket agents) all its stations for all except the last train in the evenings. At Martin Airport, MARC has its platform adjacent to Track A. There is planking in the track area, so that passengers can load/unload from tracks 1 and 2 as well (Track 2 loading is the exception, not the norm).

State/Jurisdiction	Number & Owned By	Maintained By	Safety Systems/ADA	Landmark Status	Other
Maryland (con't.)			MARC PA system is about 85% reliable. It is used solely for, passenger information, not safety. MARC plans no additional safety systems or special safety precautions for Acelas.		
Delaware	4, including one under construction. Atk. owns 1 (Wilmington). Del. DOT owns 3: Newark Commuter Rail, Churchman's Crossing (under const.; due to open in 1999), and Claymont.	Atk. maintains Wilmington Station. It also maintains the station platform at the old Newark Station (located across the tracks from the new Del. DOT commuter rail station) at which its trains stop. Del. DOT maintains its stations.	Atk.'s Wilmington Station has a PA system, and is ADA-compliant; the Newark Station is not, and has no PA.. Del. DOT employs full-time security guards at its Newark and Claymont stations. There is no PA or other device at either station. Part of the guard's job at Newark is to keep people from crossing the tracks. The guard's booth is on the Claymont Station platform; it's within 20 - 30 feet of the tracks at Newark.	The city-owned old Newark Station building is in the National Register of Historic Places. The Atk.-owned Wilmington Station has received a Determination of Eligibility for inclusion in the National Register of Historic Places.	Acela trains will stop at Wilmington. The city of Newark, DE, owns the old Newark Station building. It is leased and **not** used in connection with train service. Del. DOT provides a ticket agent at its Newark Station during the AM peak hours. Del. DOT owns a large tract of land near the Maryland border (Sandy Brae) for a future park/ride station. Del. DOT trains use Track A at Newark.

State/Jurisdiction	Number & Owned By	Maintained By	Safety Systems/ADA	Landmark Status	Other
Pennsylvania	26. Atk. owns them all. SEPTA leases the commuter rail stations from Atk.	Atk. maintains the 30th Street and North Philadelphia Stations. SEPTA maintains the stations it leases from Atk.	The Newark Del. DOT Station is ADA-compliant; Claymont Station is not. Some of the SEPTA commuter rail stations are equipped with a PA system linked to the SEPTA Operations Control Center. Plans are to install PAs at all stations. However, the PAs are for passenger information purposes only, not safety. SEPTA has no plans for any safety systems or measures for Acela. Amtrak's 30th Street, North Philadelphia, and Cornwells Heights Stations are ADA-compliant. None of the stations served solely by SEPTA commuter trains are ADA-compliant.	30th Street and North Philadelphia Stations, in Philadelphia, are both in the National Register of Historic places. The old Bristol Station (adjacent to the current facility but no longer in use) has received a Determination of Eligibility for inclusion in the National Register. The Chester Station has received a Determination of Eligibility for inclusion in the National Register. The Ridley Park Station is part of a district that has received a Determination of Eligibility for inclusion in the National Register.	Acela trains will stop at 30th Street Station. SEPTA has no definite plans for any new commuter rail stations. There has been discussion, only, about the possibility of new stations at Baldwin and Zoo. SEPTA staffs some of its stations with ticket agents, typically during the morning commute and early afternoon hours, weekdays-only.

State/Jurisdiction	Number & Owned By	Maintained By	Safety Systems/ADA	Landmark Status	Other
New Jersey	12 (plus three under construction). NJT owns all the stations	NJT maintains all stations, **except** the Newark Station platforms are maintained by Atk.	Local station announcements are made at Newark Penn Station and Trenton. All other stations are equipped with a NJT PA system that's normally operated out of the Penn Station, New York, 40 Office. PA announcements can also be made through the Hoboken NJT Train Dispatcher's Office. PA announcements are made 24 hours per day. The Princeton Jct. Station is equipped with audible and visual alerters for trains that are approaching on the near track to make a station stop. All station platforms on the corridor, except Edison and Jersey Ave., are ADA-compliant. Access between the platform and the train is by a bridge plate that is kept on the station platform.	The following are in the National Register of Historic Places: Penn Station, Newark; and the New Brunswick Station. The Elizabeth Station is located within the Mid-Town Elizabeth Historic District, although the station building itself has been demolished. The Metuchen Station has received a Determination of Eligibility for inclusion in the National Register. The Linden Station is possibly eligible, but it needs an evaluation.	Acela trains will stop at Metropark and Newark Penn Station. They may also stop at Trenton and Princeton Jct. Hamilton Station is scheduled to be opened in the Fall of 1998. Allied Junction Transfer Station (Secaucus) is due to open in 2002. Newark Airport Station is under construction. Additional station improvements include: Elizabeth - new office building; Rahway - station rehabilitation and new platform-level ticket office. Metro Park - new platform-level ticket office.

State/Jurisdiction	Number & Owned By	Maintained By	Safety Systems/ADA	Landmark Status	Other
New Jersey (con't.)					Edison - New waiting room and extended platforms; Jersey Ave. - Two new high-level platforms. Most stations are staffed with ticket agents at least part of a day. All stations are equipped with ticket-vending machines (TVMs).
New York	7. Atk. owns Penn Station, NY. MNR owns all other stations, except New Rochelle. The New Rochelle Station building and parking lot are owned by the City of New Rochelle. The Station's platforms, overpasses, elevators, and stairs are owned by MNR.	Atk. maintains Penn Station. In the future, when the East End Concourse Project is completed, NJT will share maintenance. MNR maintains all other stations, except at New Rochelle. There, MNR maintains the platforms, overpasses, elevators, and stairs. The Station building and parking lot are maintained by the City of New Rochelle.	All stations are equipped with a PA system, used for passenger information purposes only. The announcements are made from MNR's Command and Control Center in New York City. "Key Stations" also have "Visual Information Systems," which are basically CCTV screens providing various types of non-safety-related train information. Only "Key Stations" are	The New Rochelle Station has received a Determination of Eligibility for inclusion in the National Register of Historic Places.	Acela trains will stop at New York City's Pennsylvania Station. All stations were rebuilt about 10 years ago. Penn Station is fully staffed. Only some of the MNR stations are staffed with ticket agents. The hours of those that are staffed are typically 6AM-6PM.

State/Jurisdiction	Number & Owned By	Maintained By	Safety Systems/ADA	Landmark Status	Other
New York (con't.)			accessible. Elevators to platforms. On-train bridge plates and/or ramps are used to provide access to the trains.		
Connecticut	26. State of Connecticut owns all stations from the New York State line to and including Hew Haven. Atk. owns the stations at Branford, Guilford, Madison, Clinton, and Westbrook. Connecticut leases these stations from Atk Atk. owns the Old Saybrook Station, and leases the New London Station from a private developer.	Connecticut maintains all station *buildings* from the New York border to and including New Haven. The stations north of New Haven leased from Atk. have had parking lots and station appurtenances built by the State. These stations are maintained by Atk.and the towns, with Atk. maintenance work funded by the State. The towns provide policing, trash removal, building cleaning, and landscaping. Atk. maintains the platforms and the cross-track walkways.Atk. maintains the station it owns and the one it leases.	All stations are equipped with a PA system. New Haven Station PA announcements are made locally. The PA systems at all other stations in Conn. north of New Haven are l inked to an automated system. Announcements can still be made locally at each station. New London has its own PA system, but it, too, is linked to the network. Conn. DOT is not committed to making any changes at its stations for Acela. The MNR stations south of New Haven are linked to the MNR PA system described above,	The following railroad stations are listed on the National Register of Historic Places: Cos Cob, Fairfield, New Haven, Guilford, New London, and Mystic. In addition, the following railroad stations are listed on the State Register of Historic Places: Darien, Rowayton, South Norwalk, East Norwalk, Westport, Southport, Stratford, Milford, and Old Saybrook.	Acela trains will stop at Stamford, New Haven, and New London. Conn. DOT does not have plans for any new stations. In the MNR territory south of New Haven, all stations were rebuilt about 10 years ago. Only some of the stations south of New Haven are staffed, with ticket agents. The hours of those that are staffed are typically 6AM-6PM. New Haven, Old Saybrook, and New London Stations are staffed with ticket

State/Jurisdiction	Number & Owned By	Maintained By	Safety Systems/ADA	Landmark Status	Other
Connecticut (con't.)		The platforms, overpasses, elevators, and stairs at the stations south of New Haven are maintained by MNR. In Connecticut, MNR or, in some cases, the local communities, contract for snow removal from the platforms. The system works well, with no problems in removal.	with no local announcements. South of New Haven, only the MNR "Key Stations" are handicapped-accessible, in the manner described above for New York State. North of New Haven, the physically challenged can access trains via portable lift devices, kept on the. platforms and operated by train crews.		agents from early morning to late evening seven days a week, including holidays.
Rhode Island	3. Atk. owns Providence Station. Rhode Island owns Kingston and Westerly, and the two new station that are planned. However, Atk. owns 22 feet in from the center line of the track, which includes the stations' platforms.	Atk. maintains Providence Station and the platforms of the other stations. RI DOT maintains the buildings and grounds of the stations it owns.	The stations at Kingston and Westerly are equipped with PAs. Announcements are made locally by the Atk. station agents. (Atk. rents space for the agents from RI DOT.) There are no other devices. There are no plans for additional safety systems at this time. Westerly and Kingston Stations currently have low-level platforms at	Kingston and Westerly Stations are both in the National Register of Historic Places. The old Providence Station (no longer in use for train service) is in the National Register; the new one is not. However, the new Providence Station is in an "extremely sensitive area"	Acela trains will stop at Providence Station. RI DOT plans two new stations. Warwick (T. F. Green Airport) is planned to open in the year 2000; nothing is yet under construction. Wickford Junction does not yet have a definite date for construction.

State/Jurisdiction	Number & Owned By	Maintained By	Safety Systems/ADA	Landmark Status	Other
Rhode Island (con't.)			ground level. Westerly Station's platform is directly accessible to the physically challenged. The Kingston Station platform is accessible by ramps. At both stations, portable wheelchair lifts provide access from platforms to trains. As in Connecticut, above, these lifts are kept chained on the platforms, and are operated by the train crews. Providence Station has high-level platforms that are accessible by elevator from the interior part of the Station. Persons in wheelchairs get from the platforms to or from the trains by means of bridge plates. For Atk. trains, the bridge plates are on kept on the Station platform; for MBTA commuter trains, the bridge plates are on the trains.	directly opposite the State Capitol.	RI DOT is currently building a layover facility in Pawtucket for MBTA commuter trains. It is planned to extend commuter rail service from Providence to the Warwick (T. F. Green) Station. No operator for the service has yet been selected. Atk is going to build new, high-level platforms at the Kingston and Westerly Stations prior to the advent of Acela service. The stations are staffed by ticket agents at Kingston and Westerly. At Providence, there is a staffed Baggage Room in addition to ticket agents.

State/Jurisdiction	Number & Owned By	Maintained By	Safety Systems/ADA	Landmark Status	Other
Massachusetts	12; all owned on behalf of the Commonwealth by the MBTA.	Atk. maintains all the stations for the MBTA, under contract.	Audible/visual safety devices were observed in use at several of the stations. They consist of loud bells and flashing amber lights. The devices are actuated by track circuit when an approaching train is approximately one quarter mile from the platform. They remain in operation until the train has passed beyond the platform by a similar distance, including during any station stop. The stations and platforms are, for the most part, accessible to the disadvantaged. Access between a low-level platform and the train is accomplished by a portable wheelchair lift kept on the platform, or from a mini high-level platform at one end of the low platform via a bridge plate carried on board each MBTA car. The mini	The Headhouse and the Waiting Room of the Boston South Station are each individually listed in the National Register of Historic Places. In Attleboro, both the northbound and the southbound Station buildings are in the National Register. In Canton, the Canton Jct. Station has received a determination of eligibility for inclusion in the National Register.	Acelas will stop at Route 128 and Boston's South Station. No new stations are planned. The Route 128 Station is going to be completely rebuilt with high-level platforms. MBTA stations are staffed from early morning until late evening, seven days a week, at South Station and Back Bay. Tickets are sold on varying schedules at all other stations except Ruggles, Forest Hills, Hyde Park, and Readville. At those stations, patrons purchase their tickets on board the train.

State/Jurisdiction	Number & Owned By	Maintained By	Safety Systems/ADA	Landmark Status	Other
Massachusetts (con't)			high-level platform is accessed by a ramp. Access between a high-level platform and the train is by means of a bridge plate.		

NOTE: Amtrak plans to install audible (PA) and visual (LED message boards) systems at all of its ADA "Key Stations" in the Northeast Corridor. They will be used to alert people that a train is approaching and to stand back. However, they are not truly a "safety system" in that there is no vital circuitry involved, i.e., they will not fail safe.

APPENDIX H

CHARACTERISTICS OF STATIONS SURVEYED

Station Name	No. of Trks	Platform Data										Mid-Track Fence		Speed on Track Next to Platform (in MPH)			
		Width (in Feet)		High		Low		High w/Low		Extends Across Tracks				Current		Proposed for HST	
		NB	SB	NB	SB	NB	SB	Yes	No	Yes	No	Yes	No	NB	SB	NB	SB
Seabrook, MD	3	12.3	12.3	X	X			X		X			X	80	125	80	125
Bowie State	3	12	12	X	X			X		X			X	80	125	80	125
Odenton	3	12.3	12.3	X	X			X		X			X	80	125	80	125
Halethorpe	4	6	6			X	X			X		X		80	110	80	125
Martin Airport	4	12	N/A			X	N/A			X			X	60	(125)	60	(125)
Newark, DE	4	11	5.7			X	X			X		X		35	125	35	135
Claymont	4	10	10			X	X			X		X		105	110	105	110
Marcus Hook, PA	4	10	18.5			X	X			X		X		105	110	105	110
Highland Ave.	4	18	8			X	X			X			X	90	90	90	90
Lamokin St.	4	10.5	10.5			X	X			X		X		90	90	90	90
Chester	4	32	32			X	X			X		X		90	90	90	90
Eddystone	4	6.5	8.8			X	X			X		X		90	90	90	90
Crum Lynne	4	7.8	9.5			X	X			X			X	90	90	90	90
Ridley Park	4	11	9.8			X	X			X		X		90	90	90	90
Prospect Park	4	15.2	10			X	X			X		X		90	90	90	90
Norwood	4	9.8	10			X	X			X		X		90	90	90	90
Glenolden	4	7	7			X	X			X			X	90	90	90	90
Darby	4	9	12.5			X	X			X		X		90	90	90	90
Bridesburg	5	9.5	15			X	X			X			X	Est. 15	90	Est. 15	90
Wissinoming	5	7.5	22			X	X			X			X	Est. 15	90	Est. 15	90
Tacony	5	7.5	18.5			X	X			X			X	Est. 15	90	Est. 15	90
Holmesburg Jct.	4	17.5	22			X	X			X		X		90	90	90	90
Torresdale	4	18.7	10.2			X	X			X		X		80	80	80	80
Cornwells Hts.	4	8.5	9.5			X	X			X		X		100	100	100	100
Eddington	5	12+	12.5			X	X			X			X	Est. 15	100	Est. 15	100

Station Name	No. of Trks	Platform Data										Mid-Track Fence		Speed on Track Next to Platform (in MPH)			
		Width (in Feet)		High		Low		High w/Low		Extends Across Tracks				Current		Proposed for HST	
		NB	SB	NB	SB	NB	SB	Yes	No	Yes	No	Yes	No	NB	SB	NB	SB
Croydon, PA	4	9.5	9.3			X	X			X		X		100	100	100	100
Bristol	4	11.8	14			X	X			X			X	100	100	100	100
Levittown	4	14.3	13			X	X			X		X		100	100	100	100
Trenton, NJ	8	33	31.5	X	X						X		X	80	80	80	80
Princeton Jct.	4	11.5	11.5	X	X			X		X		X		110	110	110	110
Jersey Ave.	4	N/A	11.2			N/A	X			X			X	N/A	110	N/A	110
New Brunswick	4	9.5	10.3	X	X			X		X		X		100	90	100	90
Edison	4	9.5	9.5	X	X			X		X		X		100	90	100	90
Metuchen	4	12.8	12.8	X	X			X		X			X	90	90	90	90
Metropark	4	10	10	X	X			X		X		X		45	45	45	45
Rahway	6	13	27.8	X	X			X		X		X		70	90	70	90
Linden	6	9.5	9.5	X	X			X		X		X		70	75	70	75
New Rochelle, NY	5	16.5	16+	X	X				X		X		X	70	50	70	50
Branford, CT	2	N/A	23			N/A	X			X			X	(55)	55	(70)	70
Guilford	2	20.8	N/A			X	N/A			X			X	90	(90)	125	(125)
Madison	2	22.7	N/A			X	N/A			X			X	85	(85)	105	(105)
Clinton	2	22	N/A			X	N/A			X			X	85	(85)	115	(115)
Westbrook	2	N/A	17			N/A	X			X			X	(90)	90	(95)	95
Old Saybrook	4	15.8	7			X	X			X			X	90	90	110	110
Mystic	2	11.5	11.5			X	X				X	X		60	60	65	65
Westerly, RI	2	17	7.5			X	X				X	X		75	75	95	95
Kingston	2	10.5	6.2			X	X			X			X	110	110	150	150
South Attleboro, MA	2	12.8	12.8			X	X				X	X		100	100	115	115

Station Name	No. of Trks	Platform Data										Mid-Track Fence		Speed on Track Next to Platform (in MPH)			
		Width (in Feet)		High		Low		High w/Low		Extends Across Tracks				Current		Proposed for HST	
		NB	SB	NB	SB	NB	SB	Yes	No	Yes	No	Yes	No	NB	SB	NB	SB
Attleboro, MA	3	16.8	12			X	X				X	X		60	100	60	150
Mansfield	2	12	10.2			X	X				X	X		100	100	150	150
Sharon	2	12+	7.5			X	X				X	X		100	100	130	130
Canton Jct.	2	10	11+			X	X				X	X		80/50	80/60	135	135
Route 128	2	12	12			X	X				X	X		60	60	(Stop)135	(Stop)135
Readville	3	14	14			X	X				X	X		100	60	125	60
Hyde Park	3	11	12			X	X				X	X		100	80	125	80
Forest Hills	4	N/A	22.3	N/A	X				X		X		X	(100)	100	(125)	100
Ruggles	3	N/A	21	N/A	X				X		X		X	(100)	100	(120)	100

NOTES

1. NB = The Northbound or Eastbound platform.
2. SB = The Southbound or Westbound platform.
3. Platform Width: A "+" after the number indicates considerably more available width.
4. N/A = Not Applicable. This indicates there is one platform, on the side of the right-of-way indicated. It may be served by trains in both directions. Where the N/A appears in the Current or Proposed speed columns, the platform is served by trains only in the direction indicated.
5. Estimated (Est.) speeds are shown for Conrail Running Tracks not used by passenger trains. These tracks lie between the station platform and the closest passenger track.
6. Speeds shown in parenthesis are on a track one or more tracks removed from the track next to the platform.
7. Where there are three (3) or more tracks, HSTs will operate at MAS only on those tracks currently designated for the highest speeds.
8. At Canton Jct., MA, there is currently a weekday morning and evening rush hours speed restriction for trains passing the station without stopping.
9. Route 128 is planned to be a stop for HSTs.
10. At Metropark, Iselin, NJ, current Metroliners and future HSTs that will make a station stop wil slow to 45 mph to cross from their high-speed track to the platform track. They will not operate on Tracks 1 and 4 for straight-through, non-stop movements.

APPENDIX I

Station Data From Representative Station Checklist Forms

Station Name: **Halethorpe**	Station Location: **Halethorpe, MD**		Owner: **MARC**	Operator: **MARC**				
National Landmark (Yes/No): **No**	No.of Tracks: **4**	HSR Stop (Y/N): **No**	Platform Length (ft): **130' (S/B); 150' (N/B)**	Platform Width (ft): **6'**	Proposed speed through station:	**125 mph**	Distance (ft) Platform Edge to Near Rail: **5'**	
Station Staffing (Y/N): **No**								
Platform Shelter: **Yes**	**Open Toward Track**	Other: **On S/B side, S. End only. Only cover on N/B Platform under overhead bridge.**						
Platform Type:	**Low**							
Platform Configuration:	**Both sides of track**							
Pedestrian Platform Access:	Overpass: **Via Hwy. with stairs @ N. End**							
Access to Platform for Physically Challenged People (Y/N): **No**	Access to train for Physically Challenged People: **No**							
Unauthorized Access Availability (Y/N): **Y**	Other: **R.O.W. wide open at both N. & S. ends.**			Barrier(s) Between Tracks (Y/N): **Yes**				
Station Appurtenances: **Lighting & shelter @ S/B Plat. See Platform shelter note above.**				Telephones/ Tel. Booths: **No**	Newspaper Stands: **No**	Fixed Lighting: **Yes**	Suspended Lighting: **No**	Wind Screens (Y/N): **No**
Maximum Distance People Can Stand from Near Rail Along Most of the Length of Platform: **11'**								
Existing Safety System(s):	**P.A. Not for safety use.**	Message Board(s): **No**	Signs: **No**	Flashing Lights: **No**	Audible Warning Devices (AWD): **No**	Handrails: **No**		
Proposed Safety System(s)-Advanced Waring Systems (AWS):								
Recommended Safety System(s):								

Potential Adverse Effect on Comfort and/or Safety:

1. **High Hazard Station! (High-Speed Track #3 is next to S/B station platform, which is 6-feet wide, and 5-feet from the nearest rail.)**
2. **Severe blast effect as S/B Amtrak train passed at full speed on #3 track next to the platform.**

Recommended Mitigating Measures: **Could be developed as part of an action plan for possible mitigation.**

Other Comments:

APPENDIX I

Station Data From Representative Station Checklist Forms

Station Name: **Newark (S/B)**	Station Location: **Newark, DE**		Owner (Platform Only): **Amtrak**			Operator: **Amtrak**	
National Landmark (Yes/No): **Yes**	No.of Tracks: **4**	HSR Stop (Y/N): **No**	Platform Length (ft): **172**	Platform Width (ft): **11'-3" S. End & 10' N. End**	Proposed speed through station: **135**	Platform Edge to Near Rail: **2'-6"**	
Station Staffing (Y/N): **No**							
Platform Shelter: **None**	Other: **Roof overhang extending out from side of building.**						
Platform Type:	**High & Low**	Other: **High in front of building, and low in front of that.**					
Platform Configuration:	**One side of track. Westside.**						
Pedestrian Platform Access:	Overpass: **S. College Rd.**	Stairs/Ramp from Station: **Directly from parking, accessed from adjacent dead-end street.**					
Access to Platform for the Physically Challenged (Y/N): **No**							
Unauthorized Access Availability (Y/N): **Yes**	Other: **Easy access to track anywhere along platform or its ends.**			Barrier(s) Between Tracks (Y/N): **Yes**			
Station Appurtenances: **None**							
Maximum Distance People Can Stand from Near Rail Along Most of the Length of Platform: **10'-8"**							
Existing Safety System(s): **None**	P.A.: **No**	Message Board(s): **No**	Signs: **Yes**		Flashing Lights: **No**		
Proposed Safety System(s)-Advanced Waring Systems (AWS):							
Recommended Safety System(s):							
Potential Adverse Effect on Comfort and/or Safety:							
1. No yellow/or any other warning striping on platform edge.							
2. Only signage is the small Amtrak "No Trespassing" signs on mid-track fence.							
3. As Amtrak train passed on track 3 at approximately 80+ mph, severe wind turbulance was felt.							
Recommended Mitigating Measures: **Could be developed as part of an action plan for possible mitigation.**							
Note: Platform is only 5'-8" wide between the bottom of the wall separating the high from the low platform. The wall is 76'-10" long.							

APPENDIX I
Station Data From Representative Station Checklist Forms

Station Name: **Sharon**	Station Location: **Sharon, MA**		Owner: **MBTA**	Operator: **MBTA**			
National Landmark (Yes/No): **No**	No.of Tracks: **2**	HSR Stop (Y/N): **No**	Platform Length (ft): **520'**	Platform Width (ft): **12'**	Proposed speed through station: **130**	Distance (ft) Platform Edge to Near Rail: **2'**	
Station Staffing (Y/N):	**AM Peak**						
Platform Shelter: **Yes**	**Open Toward Track (S/B)**	Canopy Only: **N/B**					
Platform Type:	**Low**						
Platform Configuration:	**Both sides of track**						
Pedestrian Platform Access:	**Overpass: See below**	**Access from parking lots on both sides and station building at the N/B side.**					
Access to Platform for Physically Challenged People (Y/N): **Yes, See Other**	Access to train for Physically Challenged People: **No**	Other: **Curb cuts at parking lot edge.**					
Unauthorized Access Availability (Y/N): **Yes**	Other: **Across mid-track fence at N. End**	Barrier(s) Between Tracks (Y/N): **Yes**					
Station Appurtenances:	**Benches**	**Fixed Signs**	**Fixed Trash Cans**	**Telephones**	**Newspaper Stands**	**Fixed Lighting**	Wind Screens (Y/N): **No**
Maximum Distance People Can Stand from Near Rail Along Most of the Length of Platform: **12 feet**							
Existing Safety System(s):	**Amber Flashing Lights and loud bells.**						
Proposed Safety System(s)-Advanced Waring Systems (AWS):							
Recommended Safety System(s):							

Potential Adverse Effect on Comfort and/or Safety:

1. Bench on S/B platform is too close to the platform edge.

Note: Two-unit S/B Amtrak train passed by at approximately 80 mph "rocking" the observer who sat at the bench, 6'-6" away from the platform edge.

Platform is approximately 8-feet wide at this point.

Recommended Mitigating Measures: **Could be developed as part of an action plan for possible mitigation.**

APPENDIX J

Field Measurement Reports

This Appendix contains the following three Field Reports:

Date:	**Location:**
1 Sept. 1998	1000 ft north of Princeton Junction, NJ railroad station, along tracks (equivalent to low-level platform condition)
8 Sept. 1998	Northbound high-level platform at Princeton Junction, NJ railroad station
17 Sept. 1998	Southbound low-level platform at Newark, DE railroad station

These are the field reports as submitted by PB field personnel. Please note that reference is made to **Metroliner** service, which at these station locations, is synonymous to use of the **Amfleet** trainset discussed in the main text of this report.

Field Measurement of Train-Induced Air Velocities 1 September 1998

1. Purpose

A series of tests were made to measure the air velocities caused by the passage of an Amtrak Metroliner. The purpose of the tests was to estimate the air velocities that would occur on a low-level platform as a Metroliner passed.

2. Description

Date and time: Tuesday, 1 September 1998 between 10:00 a.m. and 11:44 a.m.

Location: About 1000 feet north of the Princeton Junction, NJ, railroad station.

Conditions: The weather was clear. The ambient temperature varied from about 75°F to 85°F, and the relative humidity was about 60 percent.

Measuring equipment: The air velocity measuring instrumentation consisted of an Alnor 6006-P Velometer connected with Alnor tubing to an Alnor 6030-P Range Selector which had an Alnor 6060-P Pitot Tube mounted in it. The range selector was set to zero to 2500 feet per minute (fpm).

Other equipment: The assembled measuring equipment was taped to a six-foot aluminum household step ladder (UL listing number SA-3895, Issue D-816) with two-inch Nashua 398 duct tape.

Attendees:

Keith Bradley	(Amtrak Foreman - acted as Flagman)
William Kennedy	(Parsons Brinckerhoff Mechanical Engineer)
Harry A. McCall	(Amtrak Safety and Environmental Control Engineer)

3. Procedure and observations

Prior to the team entering the track area, H.A. McCall inspected everyone's safety gear including hard hat, glasses with side shields, bright-colored safety vests and boots. Although Track 4 was not in service, he asked us to assume its catenary was live. It was also pointed out the safety gear would not mitigate being hit by a train.

The Pitot tube inlet was about 75 inches above the track ballast or a little more than five feet above the top of rail. The instrument was centered over the outside rail of Track 4, which was not in service. The pitot tube opening faced north along this rail. All southbound Metroliners (the trains of interest) used Track 3. The distance between track centers is about 12 feet and width of a Metroliner car is about 10.5 feet. Therefore, the instrument was about 9 feet from the passing train. The instrument was located about 50 feet north of catanery pole 46/77, approximately 80 feet north of the Route 571 bridge as it crosses the Amtrak right of way. Track 4 is having its wooden ties changed over to concrete ones. The nearest Amtrak work train was about 750 feet north of the test site.

Prior to the beginning of the tests, W.D. Kennedy explained the purpose of the test program. During the tests, W.D. Kennedy read and recorded the air velocities. H.A. McCall held the step ladder to ensure it would not be deflected by the passing train. K. Bradley acted as flagman to ensure that all were aware of southbound and northbound train movements. After each southbound Metroliner passed, H.A. McCall contacted its engineer to determine its speed past the test site.

Amtrak Metroliner 109 passed the test site at about 10:42 AM. Prior to its passage there was a slight wind of about 200 fpm [2 mph]. Let X be the approximate distance the rear of the train moved past the test site:

$X < 100$,	V = 200 fpm [2 mph]
$100 < X < 300$,	V climbs to about 900 fpm [10 mph]
$300 < X < 400$,	V decreases to about 400 fpm [5 mph]
$400 < X < 600$,	V increases to 1500 fpm [17 mph], then rapidly falls off

A persistent air velocity decreasing from about 500 fpm [6 mph] to about 300 fpm [3 mph] was noticed for sometime after the train passed. The train speed was determined to be 125 mph (11000 fpm, 183 feet per second).

Amtrak Metroliner 111 passed the test site about 11:45 AM. There was no ambient wind as the train approached. A "bow wave" from the front of the train was felt, but no motion was detected by the Amenometer. This was probably because its pressure and velocity were transverse to the pitot tube. The velocities were similar to those recorded for Train 109.

During the test period a number of qualitative observations were made for Amtrak Northeast Direct Trains which have a configuration similar to the Metroliner Trains. One important and consistnet observation was that the perceived air velocity at about 4.5 feet away from the train was the same as that 9 feet away from the train.

Extrapolating the maximum measured air velocity to a train speed of 150 mph would predict a maximum air velocity of about 21 mph.

Therefore, these measurements conclude that the Amtrak high speed trains will not cause any air velocity problems at low level platforms, provided the people are 4.5 feet from the point of train passage.

Field Measurement of Train-Induced Air Velocities 8 September 1998

1. Purpose

A series of tests were made to measure the air velocities caused by the passage of an Amtrak Metroliner. The purpose of the tests was to estimate the air velocities that would occur on a high-level platform as a Metroliner passed.

2. Description

Date and time: Tuesday, September 8, 1998, between 2:12 p.m. and 5:15 p.m.

Location: Northbound high-level platform of NJT Princeton Junction railroad station. The tracks are numbered as follows: Stopping track (adjacent to platform) northbound - Track 1; non-stopping track northbound - Track 2.

Conditions: Air temperature estimated between 70°F to 75°F. Relative humidity estimated at about 40%. Gusty, variable wind which mostly came from the north west to the south west, either across the tracks or in the usual direction of trains observed from the south. Wind speed varied up to about 300 feet per minute (fpm).

Measuring equipment: Velometer manufactured by Alnor Instrument Corp., consisting of 6006AP meter, 6030CP Range Selector, and 6070P Pitot Tube. The Range Selector was set to 0-1250 fpm.

Other equipment: 5 foot stepladder to support the Velometer, wooden batten and "C" clamp to steady the ladder, duct tape to hold the Velometer components in place.

Attendees:

HA McCall, CSP	(Amtrak Safety and Environmental Control Engineer)
TJ Duffell	(PB Engineer)

3. Procedure and observations

Prior to starting work, a Job Briefing was performed by Mr. McCall as the Safety Officer. Safety training, safety equipment, and measuring equipment and activities were discussed.

The measuring setup was placed approximately 330 foot from the south end of the platform. The Velometer Pitot tube was located approximately 5'-6" above platform level, and approximately 5'-6" in from the platform edge. The head of the Pitot tube was aligned parallel to the edge of the platform, pointing toward oncoming northbound trains.

Observations of the air velocity on the platform caused by northbound trains was measured for one Metroliner traveling north on Track 2, two Metroliners traveling south on track 2, two non-Metroliners on Track 2, and five trains (Metroliners and others) on Track 1. As more trains had been expected to use Track 2, Mr. McCall called Amtrak Train Control for an explanation. He was advised that due to loss of traction power earlier that day, trains had been diverted to Track 1 and reverse operation was also taking place. The speed of the Metroliners was provided by Mr. McCall contacting Amtrak Train Control. The speed of other trains was estimated by Mr. McCall using his experience of train movements through the location. The distance of the center of Track 2 to the edge of the platform was provided by Mr. McCall from his knowledge of the geometry of the Princeton Junction station alignment. This was 15'-9".

The general form of the observations was as follows:

First train-induced change detected by the Velometer - Approximately as the end of the train passed the test setup. (Although a pressure pulse could be felt as the head of the train passed the observation point, no change was indicated by the Velometer).
Subsequent observation - A rapid climb lasting about two seconds to a peak velocity, followed by a slower decline to the ambient value of about three seconds. The highest peak value was about 700 fpm for a train on Track 2. The wind gusting gave an ambient air velocity of up to 300 fpm.

The observations are provided in Table 1.

Table 1 - Train-induced air velocities

Time, p.m.	Air velocity, fpm	Train speed, mph	Track	Comments
2:10	700	125	2	Metroliner, 6 cars
2:25	400	80	2	Non-Metroliner, "short set", 3 cars
3:00	600	80	2	Non-Metroliner, 5-6 cars
3:10	300	125	2	Metroliner southbound, 6 cars
3:15	900	110	1	Metroliner, 5-6 cars
3:30	300	125	2	Metroliner southbound, 6 cars
4:00	500	110	1	Non-Metroliner, 5-6 cars
4:15	800	110	1	Metroliner, 5-6 cars
4:35	900	110	1	Non-Metroliner, 5-6 cars
5:15	700	110	1	Metroliner, 5-6 cars

Estimated tolerance: +/- 150 fpm, mainly due to gusting

Extrapolating the maximum measured air velocity to a train speed of 150 mph would predict maximum air velocities of about 13 mph (Track 2) and 14 mph (Track 1).

Therefore, these measurements conclude that Amtrak high speed trains will not cause any air velocity problems at high level platforms, provided the people are 5.5 feet away from the point of train passage.

Field Measurement of Train-Induced Air Velocities 17 September 1998

1. Purpose

A series of tests were made to measure the air velocities caused by the passage of an Amtrak Metroliner. The purpose of the tests was to estimate the air velocities that would occur on a low-level platform as a Metroliner passed.

2. Description

Date and time: Thursday, September 17, 1998, between 8:30 a.m. and 10:00 a.m.

Location: Southbound low-level platform of Newark, Delaware railroad station, operated by the city of Newark. The tracks are identified as follows, starting nearest to the platform: Amtrak southbound (stopping and non-stopping) - Track 3; Amtrak northbound (non-stopping) - Track 2; Amtrak northbound (stopping) - Track 1; Delaware DOT (bi-directional) - Track A.

Conditions: Air temperature estimated between 70°F to 75°F. Relative humidity estimated at about 60%. Gusty, variable wind which mostly came from the north east to the south east. Wind speed varied up to about 350 feet per minute (fpm). The track direction was stated to be nearly due north-south.

Measuring equipment: Velometer manufactured by Alnor Instrument Corp., consisting of 6006AP meter, 6030CP Range Selector, and 6070P Pitot Tube.

Other equipment: Rigid cardboard tube to extend the Pitot tube to the appropriate location, 4' stepladder, duct tape and rubber hook-ended tie-downs to hold the Velometer components in place. Lightweight plastic film ribbon wind-vane attached to the end of the cardboard tube to indicate wind direction.

Attendees:

DL Andrus Jr.	(PB Engineer)
D Conlon	(Amtrak Safety Committee Member)
TJ Duffell	(PB Engineer)
CJ Palumbo	(Amtrak Division Road Foreman, Mid-Atlantic Division)

3. Procedure and observations

Prior to starting work, a Job Briefing was performed by Mr. Palumbo as the Safety Officer. Safety training, safety equipment, and measuring equipment and activities were discussed. As a result of this, the test setup was changed so that the supporting ladder was removed from the low-level area, with the cardboard tube supported from the high-level waiting area immediately behind.

The measuring setup was located adjacent to the station building, such that the base of the outside high-level waiting area (about 4' high) was behind the measuring equipment, with south end of the station about 8' away. The Velometer Pitot tube was located approximately 5'-6" above the low-level platform, and approximately 5'-6" in from the expected side of the train. The head of the Pitot tube was aligned parallel to the edge of the platform, pointing toward each oncoming train.

Observations of the air velocity on the platform caused by southbound trains was measured for two Metroliners traveling south on Track 3, and two Metroliners traveling north on track 2. The speed of the Metroliners was provided by Mr. Palumbo using an Amtrak-supplied speed gun. The distance of the center of Track 2 to the edge of the platform was provided by Mr. Palumbo from his knowledge of the geometry of the station alignment. This was about 17'. The use of an extending steel tape measure was not permitted.

The general form of all Velometer observations was as follows:

First train-induced change detected by the Velometer - Approximately as the tail end of the train passed the test setup. (Although a 'bow wave' could be felt as the head of the train passed the observation point, no change was indicated by the Velometer).
Subsequent observation - A rapid climb lasting about two seconds to a peak velocity, followed by a slower decline to the ambient value of about three seconds.

The general form of the wind-vane observations for trains passing on track 3 was as follows:

First train-induced movement caused by the train - Approximately as the head of the train passed the test setup. A rapid movement away from the side of the train and then toward it was observed (lasting about ¼ to ½ second), with no clear movement thereafter until the end of the train passed the test setup. The movement of the wind-vane was then variable and energetic, generally either normal to the track, or parallel to and toward the receding train.

No clear movement of the wind-vane was detected for trains passing on track 2.

Although Amtrak permitted no further observations after 10:00 a.m. which precluded observations away from the station, the PB Engineers remained on the high-level public waiting area as the 10:08 a.m. Metroliner no. 181 passed on track 3. The subjective experience of the passage of the train was felt to be about the same as that for Metroliners 103 and 105 that had passed on track 3.

The observations are tabulated on the next page.

Volpe Task Order 17
FIELD MEASUREMENT OF WIND SPEEDS OF PASSING TRAINS
Newark, Delaware, 9/17/98

Dir.	Trn. No.	Name	Sched. Time	Actual Time	No. of Cars	Type of Cars	On Trk. No.	Train Speed (mph)	Train-induced (fpm)	Extrapolated to 150 mph train speed (mph)
SB	103	Metro	845A	848A	7	Amfleet	3	122	2200	31
NB	104	Metro	913A	913A	7	Amfleet	2	114	200	3
NB	182	NE Dir	932A	931A	6	Amfleet	2	106	100	2
SB	105	Metro	945A	951A	7	Amfleet	3	123	2500	35
NB	84	NE Dir	959A	959A	6	Amfleet	2	Est. 106	100	2

NOTES

1. Sched. Time is +10 min. from scheduled time at Wilmington for SB trains and -10 min. from scheduled time at Wilmington for NB trains.
2. Metro = Metroliner.
3. NE Dir = Northeast Direct.
4. SB = Southbound.
5. NB = Northbound.

FIELD NOTES

1. Wind Direction: Northeast.
2. Weather: Cloudy.
3. Temp. & humidity: Estimated 70° & 60%.
4. Wind speed was measured with an Alnor 6006-P Velometer. The aperture of the Pitot Tube was positioned approximately 5'6" above the surface of the station platform and 5'6" away from the side of the trains passing on Track 3, and 17'2" from the side of trains on Track 2.
5. Measured air speed for Trains 182 and 84 was from the 0-1250 fpm setting on the Velometer's Range Selector. The 0-2500 fpm setting was used for the other trains.
6. Measured air speed in the wake from Train 105 ranged from 1000 to 2500 fpm.
7. Measured wind speed was about 0 for trains 103 and 104, 100 fpm for trains 182 and 84, 350 fpm for train 105.
8. The Amtrak Division Road Foreman measured the speed of passing trains with a speed (radar) gun that was plugged into the cigarette lighter on the dashboard of his company vehicle. The vehicle was parked adjacent to Track 3, about 13 feet from the near rail.
9. All measurements were taken from the southbound platform of the old Newark Station, located on the west side of the Amtrak right-of-way adjacent to southbound Track 3. A mid-track cyclone fence of about 4 - 4.5 ft in height separated Track 3 from the other tracks. They were (from west to east): Track 2, Track 1, and Track A (this lead to the Chrysler Corp. motor car assembly plant).

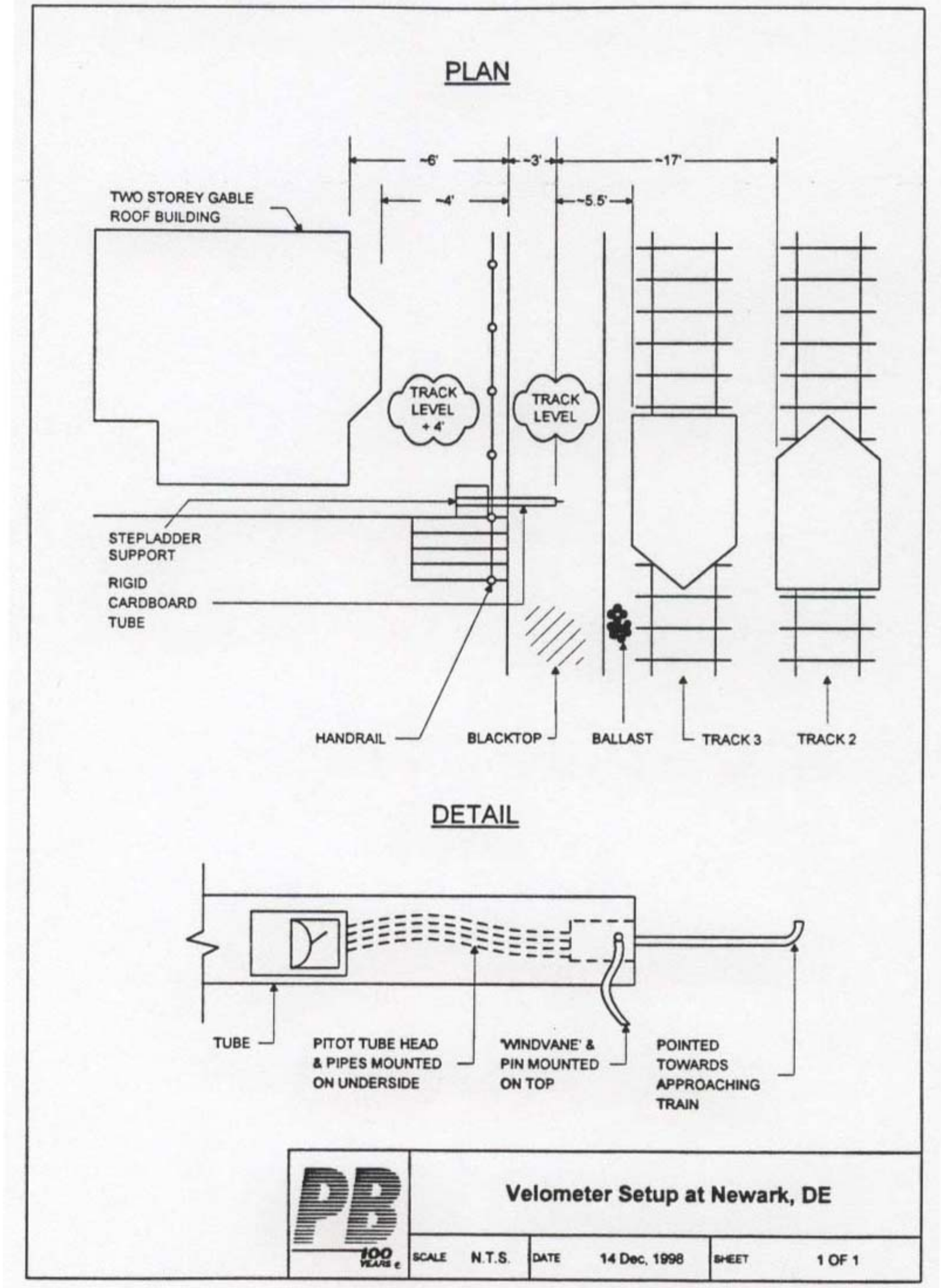
PLAN
~6'
~3'
~17'
~4'
~5.5'
TWO STOREY GABLE ROOF BUILDING
TRACK LEVEL + 4'
TRACK LEVEL
STEPLADDER SUPPORT
RIGID CARDBOARD TUBE
HANDRAIL
BLACKTOP
BALLAST
TRACK 3
TRACK 2
DETAIL
TUBE
PITOT TUBE HEAD & PIPES MOUNTED ON UNDERSIDE
'WINDVANE' & PIN MOUNTED ON TOP
POINTED TOWARDS APPROACHING TRAIN
PB
100 YEARS
Velometer Setup at Newark, DE
SCALE N.T.S.
DATE 14 Dec, 1998
SHEET 1 OF 1

REFERENCES AND BIBLIOGRAPHY

References

1. Associated Engineers (1976). Subway Environmental Design Handbook, Second Edition, NTIS No. 254-788, Transit Development Administration, Urban Mass Transit Administration, March, 1976. [Note: Associated Engineers was a Joint Venture of Parsons Brinckerhoff Quade and Douglas, Inc., Deleuw Cather & Company, and Kaiser Engineers.]

2. Baumeister, T., Avallone F.A., and Baumeister, T. III (1979). Mark's Standard Handbook for Mechanical Engineers, Eighth Edition, McGraw Hill, New York, 1979.

3. Bombardier (1998). Drawings for the Power Car and Coach Car, Bombardier Inc, 1998.

4. Chapman, C.F., (1970). Piloting, Seamanship and Small Boat Handling, Hearst Publishing, New York City, New York, 1970.

5. Fluent, Inc. (1996). FLUENT (Computational Fluid Dynamics Software), Release 4.4, Fluent Incorporated, Lebanon, NH, 1996.

6. Gawthorpe, R.G. (1972). "Aerodynamics of High-Speed Trains Running on Conventional Tracks," von Karmen Institute for Fluid Dynamics, Lecture Series 48, High Speed Ground Vehicles, Aprils 10-14, Rhode-Saint-Genese, Belgium, 1972.

7. Gawthorpe, R.G. (1998), Personal Communication between Roger Gawthorpe (British Rail) and William D. Kennedy (Parsons Brinckerhoff) concerning results of field measurements of train induced airflows, 1998.

8. Gielow, M. A., and Furlong, C. F. (1988). "Results of Wind Tunnel and Full-Scale Tests Conducted from 1983 to 1987 in Support of the Association of American Railroad's Train Energy Program", Final Report, Airflow Sciences Corporation, Livonia, MI, December 30, 1988.

9. Hammitt, A.G. (1973), The Aerodynamics of High Speed Transportation, North Hollywood, CA, 1973.

10. Hoerner, S.F., (1965). Fluid Dynamic Drag, Published by the Author, USA, 1965.

11. Laneville, A. (1998). "Amtrak High Speed Electric Locomotive & Trainset, Drag Coefficient Qualification Test Report", Groupe de recherche en Thermique et Aérodynamique de l'Université de Sherbrooke, Département de Génie Mécanique, Faculté des Sciences Appliquées, Sherbrooke (Québec), Canada, February 1998.

12. Lee, H.S. (1999). "Assessment of Potential Aerodynamic Hazards to Personnel and Equipment in Proximity to High-Speed Rail Operations", U.S. Department of Transportation, Federal Railroad Administration, Draft Final Report, Washington, D.C. April 1998.

13. Lee, H.S. (1988a). Personal Communication between Harvey Lee (USDOT - Volpe Center) and Sam Liao (Parsons Brinckerhoff) concerning data for airflow velocity as a function of lateral distance from the train, 1998.

14. Neppert , H. And Sanderson, R.(1977). “Aerodynamics of High-Speed Trains Based on a comparison of Results from Model Tests, Full Scale Measurements, and Theoretical Studies,” Glasers Annalen ZEV, 1997/04/04, 101(4), pp. 97-102 (30 Ref.). (German)

Bibliography

1. ASME (1979). “Aerodynamics of Transportation”, Proceedings of the Joint ASME-CSME Applied Mechanics, Fluids Engineering and Bioengineering Conference, June 1979, Niagara Falls, NY, USA, the Fluids Engineering Division of the American Society of Mechanical Engineers.

2. BHRA (1973). Proceedings of the 1st International Symposium on the Aerodynamic and Ventilation of Vehicle Tunnels, March 1973, Canterbury, England, British Hydromechanics Research Association, Cranfield, England.

3. BHRA (1976). Proceedings of the 2nd International Symposium on the Aerodynamic and Ventilation of Vehicle Tunnels, March 1976, Cambridge, England, British Hydromechanics Research Association, Cranfield, England.

4. BHRA (1979). Proceedings of the 3rd International Symposium on the Aerodynamic and Ventilation of Vehicle Tunnels, March 1979, Sheffield, England, British Hydromechanics Research Association, Cranfield, England.

5. BHRA (1982). Proceedings of the 4th International Symposium on the Aerodynamic and Ventilation of Vehicle Tunnels, March 1982, York, England, British Hydromechanics Research Association, Cranfield, England.

6. BHRA (1985). Proceedings of the 5th International Symposium on the Aerodynamic and Ventilation of Vehicle Tunnels, May 1985, Lille, France, British Hydromechanics Research Association, Cranfield, England.

7. BHRA (1988). Proceedings of the 6th International Symposium on the Aerodynamic and Ventilation of Vehicle Tunnels, September, 1988, Durham, England, British Hydromechanics Research Association, Cranfield, England.

8. BHRA (1991). Proceedings of the 7th International Symposium on the Aerodynamic and Ventilation of Vehicle Tunnels, November 1991, Brighton, England, British Hydromechanics Research Group, Cranfield, England.

9. BHRA (1994). Proceedings of the 8th International Symposium on the Aerodynamic and Ventilation of Vehicle Tunnels, July 1994, Liverpool, England, British Hydromechanics Research Group, Cranfield, England.

10. BHRA (1997). Proceedings of the 9th International Symposium on the Aerodynamic and Ventilation of Vehicle Tunnels, October 1997, Aosta, Italy, British Hydromechanics Research Group, Cranfield, England.

11. Dundee (1992). Proceedings of the First International Conference on Safety in Road and Rail Tunnels, Basel, Switzerland, November, 1992, University of Dundee and International Technical Conferences, Ltd.

12. Dundee (1995). Proceedings of the Second International Conference on Safety in Road and Rail Tunnels, Grenada, Spain, April, 1995, University of Dundee and International Technical Conferences, Ltd.

13. Dundee (1998). Proceedings of the Third International Conference on Safety in Road and Rail Tunnels, Nice, France, March, 1998, University of Dundee and International Technical Conferences, Ltd.

14. Engdahl, Roger (1984). "The State of the Art in Surface Vehicle Aerodynamics Research, a Summarized Bibliography", Association of American Railroads, Washington, DC, April 30, 1984.

15. JSME (1993). Proceedings of the International Conference on Speedup Technology for Railway and Maglev Vehicles, November 1993, Yokohama, Japan, the Japan Society of Mechanical Engineers.